ABSTRACT

Title of Document: INHIBITORS OF AUTOINDUCER-2 QUORUM SENSING AND THEIR EFFECT ON BACTERIAL BIOFILM FORMATION

Rebecca Melissa Lennen, Master of Science, 2007

Directed by: Dr. William Bentley, Professor
Department of Bioengineering

Bacteria utilize small signaling molecules, or autoinducers, to regulate their gene expression in tandem by a process termed quorum sensing. The gene encoding the synthase for autoinducer-2 (AI-2), *luxS*, is conserved in dozens of diverse bacteria. Behaviors controlled by AI-2 include virulence, motility, toxin production, and biofilm formation. The development of therapies that interfere with AI-2 quorum sensing are attractive for targeting biofilms, which exhibit inherent resistance to most antibiotics and biocidal agents. In this study, *in vitro* synthesized AI-2, LuxS inhibitors, and (5Z)-4-bromo-5-(bromomethylene)-3-butyl-2(5H)-furanone were screened for their effect on biofilm formation in *Escherichia coli*, *Bacillus cereus*, and *Listeria innocua*. The LuxS inhibitors were found to have no influence on biofilm formation in any of the screened species, but reduced exponential phase AI-2 production in *Listeria innocua*. The brominated furanone significantly inhibited growth in *B. cereus* and *L. innocua*, and under certain conditions preferentially inhibited biofilm formation independently from growth.

INHIBITORS OF AUTOINDUCER-2 QUORUM SENSING AND THEIR EFFECT ON BACTERIAL BIOFILM FORMATION

by

Rebecca Lennen

Thesis submitted to the Faculty of the Graduate School of the
University of Maryland, College Park in partial fulfillment
of the requirements for the degree of
Master of Science
2007

Advisory Committee:

Professor William Bentley, Chair
Professor F. Joseph Schork
Professor Srinivasa Raghavan
Professor John Fisher

Acknowledgements

I would like to thank my advisor, Dr. William Bentley, for his guidance and support on this project, and for providing me with the ability to pursue this thesis project part-time after my original source of funding fell through. I would also like to thank all of the members of the Bentley lab, including Rohan Fernandes for his assistance with initial trouble in the biofilm formation assay and for providing enzymes and 'good' AI-2, Angela Lewandowski for her help with HPLC, and Dr. Jun Li, Chen-Yu Tsao, Karen Carter, Chi-Wei Hung, Li Yang, Songhee Kim, and Hyunmin Yi for helpful discussions and general assistance in the lab. For providing samples of different inhibitors, I am indebted to the groups of Dr. Dehua Pei of Ohio State University, Dr. Thomas Wood at Texas A&M University, and Dr. Zhaohui Sunny Zhou of Northeastern University (formerly Washington State University).

Table of Contents

List of Tables

List of Figures

Chapter 1: Introduction

Bacterial biofilms are multicellular aggregations that occur at interfaces. The prevalence of biofilms and their negative role in chronic infectious diseases has been gaining significant attention in recent years. Biofilms readily develop on implanted medical devices, leading to ubiquitous infections from such common procedures as catheterization. Many industrial problems, such as the fouling of process equipment and corrosion, are caused or exacerbated by bacterial biofilms. Complicating the control of bacterial biofilms is their extraordinary resistance to most antibiotics and biocidal treatments. Quorum sensing inhibitors are a novel class of drugs that have great potential for selective activity against multicellular bacterial behaviors such as virulence and biofilm formation. Bacteria have been found to excrete and detect small signaling molecules (autoinducers) that accumulate extracellularly at high cell densities, in a process referred to as quorum sensing. Many types of quorum sensing systems with different classes of signaling molecules exist, typically with autoinducers unique to a certain organism. However, the production of a relatively newly discovered signaling molecule described as autoinducer-2 (AI-2) is conserved among large numbers of pathogenically relevant and phylogenetically diverse species. This makes AI-2 quorum sensing inhibitor development particularly attractive due to the possibility of a broad spectrum effect.

There were two major goals of this study. The first was to screen inhibitors of AI-2 quorum sensing for their effect on biofilm formation in diverse strains and species of bacteria. Although a handful of inhibitors of LuxS (the AI-2 synthase) have been developed to date, no data yet exists in the literature of their effect on bacteria. The

second goal was to further understand any observed effects of the quorum sensing inhibitors. For many organisms, the effect of AI-2 on biofilm formation is poorly understood, therefore this was investigated by the addition of *in vitro* synthesized AI-2.

The organization of this thesis is described as follows: Chapter 2 introduces the concept of bacterial biofilms, discusses their societal implications, and reviews a number of techniques developed to control biofilms; Chapter 3 discusses the different classes of known bacterial quorum sensing systems and introduces the AI-2 biosynthesis pathway and questions about its chemical identity and interrelationship with metabolism; Chapter 4 presents a complete review of the literature on AI-2 quorum sensing inhibitors. Chapter 5 details the experimental methods; Chapter 6 presents the results of screening *in vitro* synthesized AI-2, LuxS inhibitors, and a brominated furanone against three different organisms and discusses implications of the results; and Chapter 7 presents conclusions and suggestions for future research.

Chapter 2: Bacterial biofilms

2.1. Introduction

Bacteria have long been considered to be independent unicellular organisms, and this view remains the perception in most basic biology education today. Although observations in the 1930s-40s were documented in which bacteria were found to associate with surfaces, it was thought that these were isolated examples[1]. Beginning in the 1970s, studies were conducted which showed that the vast majority of bacteria in oligotrophic environments were surface-associated[1]. Today the predominance of biofilms as the primary state of bacteria in a wide variety of environments, including the human body, is now recognized[1].

Bacterial biofilms consist of live and dead cells immobilized on a surface, usually embedded in an extracellular polysaccharide matrix ('slime') that is excreted by the bacteria. The extracellular polysaccharide substance (EPS) often accounts for more of the biofilm volume than the cells themselves. The thickness of biofilms can range anywhere from a sub-monolayer of cells to hundreds of millimeters. A cross-sectional schematic of a typical mature biofilm is shown in Figure 1, however the structure of biofilms of individual species and in different environmental conditions can vary significantly.

2.2. Societal implications

In medicine, biofilms play a prominent role as being a major source of infections in the human body. The National Institutes of Health proclaimed in a public announcement that biofilms account for over 80% of microbial infections in the body[2]. Biofilms in the

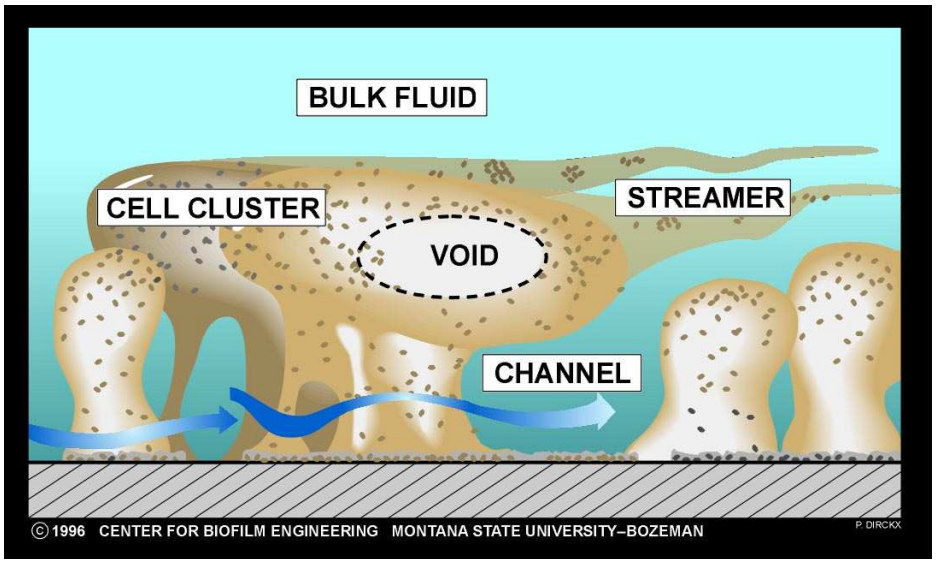

Figure 1: Cross-sectional schematic depicting a typical mature biofilm. A layer of cells covers the substrate, and pillars supporting cell clusters encased in extracellular polysaccharide allow the formation of channels for convective and diffusive flow of nutrients through the film. Streamers allow maximal contact of biofilm cells with the bulk fluid and are common in *Pseudomonas* biofilms. (from http://www.erc.montana.edu/ CBEssentials-SW/research/Structure_function/ default.htm)

body can either occur directly on host tissues, or in association with implanted devices, such as catheters, stents, mechanical heart valves, and pacemakers[3,4]. Examples of infections frequently caused by biofilms on host tissues include colitis, vaginitis, urinary tract infections, conjunctivitis, otitis, and gingivitis[3]. Chronic lung infections caused by biofilms of *Pseudomonas aeruginosa* are the main cause of loss of lung function and mortality in patients with cystic fibrosis[5].

Biofilms also have many negative industrial and engineering impacts. The fouling of process equipment results in increased fluid frictional resistance due to biofilm-induced drag, an increased overall heat transfer coefficient (in the case of heat transfer surfaces), and often accelerated rates of corrosion. The cumulative economic effect includes energy losses, increased capital costs for excess equipment capacity and equipment replacement, unscheduled downtime due to equipment failures, and scheduled downtime to

accommodate fouling removal[6]. Estimates on the cost of fouling (including but not limited to bacterial fouling) of heat exchangers in the U.S. alone range in the billions of dollars[6]. It has been approximated that at least 10% of the fuel consumed by Naval vessels is used to overcome the increased viscous drag as a result of fouling organisms[7]. Bacterial colonization is generally recognized to render a surface more conducive to the settlement of higher organisms, including algae, diatoms, fungi, protozoa, and eventually invertebrates such as tubeworms, barnacles, and zebra mussels[8]. Furthermore, biofilms can either accelerate or decelerate rates of corrosion. This is dependent on whether the microenvironment they create as a result of their metabolism creates conditions conducive to corrosion processes, or passivates a metal surface to protect from further corrosion. Localized potential differences can be caused by oxygen depletion in non-uniform biofilms, resulting in the flow of corrosion currents[9]. Many bacteria secrete organic acids such as acetic acid, lactic acid, and succinic acid, which are capable of removing some oxide passivation films and therefore promote increased corrosion[9]. Sulfate-reducing bacteria produce metabolic byproducts including iron sulfide, hydrogen sulfide, and sulfuric acid, which can also increase rates of corrosion by various mechanisms[9].

Complicating the control of biofilms for either medical or industrial purposes is their inherent resistance to antimicrobial agents, including both antibiotics and biocidal agents. Inherent diffusional limitations, particularly of larger molecules such as antibiotics, obviously play a role in resistance. Certain physical properties of the EPS, such as its positive charge serving as an adsorbent, may also be a factor[10]. Another postulated explanation is that the high level of differentiation of cells in biofilms creates many

"layers of defense" against antibiotics. For example, an antibiotic that acts by inhibiting growth would not affect non-proliferating regions of the biofilm and thus ensure its survival[11]. The high level of differentiation also results in alterations to the local environment within the biofilm, including reduced pH, which can render many antimicrobial agents ineffective[10,12]. Genomic and proteomic studies comparing biofilms with planktonic cells typically show hundreds of major deviations that would translate to significant physiological differences, making a full understanding of all the reasons behind biofilm resistance an extremely complex task. Thus the prevention of the onset of biofilm formation would, in many situations, be a more desirable outcome.

2.3 Control of biofilms

2.3.1. Strategies for non-medical applications

In industrial processes, including drinking water treatment, the most common means of controlling biofilms is chlorination[13]. Other oxidizing biocides such as ozone, hypochlorite (bleach), hypobromite, chloramine, chlorine dioxide, and hydrogen peroxide can similarly be used[13]. Non-chemical methods include mechanical cleaning and the use of pulsed acoustic devices[14].

Many biocidal paints have been developed that are used to prevent fouling of surfaces by macroscopic organisms in seawater. These include paints containing organotin compounds (eg. tributyltin) and copper ablative coatings designed to slowly release copper as the coating erodes. However, organotins have been found to accumulate in the environment and have adverse effects on biological processes, leading to their strict control by many international governments and a proposed international ban by 2008[15,16].

Copper has also been found to accumulate in aquatic ecosystems, leading to control by some governments[16].

Numerous treatments that directly attack the extracellular polysaccharide substance (EPS) have been attempted to varying degrees of success, including the use of chelating agents and various enzymes, as tabulated by Xavier et al[17].

2.3.2. Strategies for medical implants

Modification of surface properties is the primary strategy for reducing biofilm growth on medical implants. Surfactants containing a cationic quaternary ammonium head group and a long alkyl chain tail have long been used as bactericidal agents. Covalently-coupled coatings developed based on these surfactants greatly reduce the viability of numerous bacteria and mixed biofilms of bacteria and yeasts[18,19]. Similarly, poly(4-vinyl-N-alkylpyridinium bromide) functionalized surfaces are also effective at killing bacteria on contact, with N-hexylated PVP resulting in the largest drop in viable cell numbers[20]. These coatings have the common feature of preserving the flexibility and accessibility of the alkyl chain group for penetrating the bacterial cell wall, thereby allowing the cationic nitrogen to disrupt the underlying membrane.

Other approaches have focused on preventing the initial adhesion of bacteria to a surface, or lowering the force of adhesion between bacteria and a surface to facilitate removal. Many physical properties are involved, including surface energy (hydrophobicity or hydrophilicity), surface roughness, steric hindrance of surface groups, and electrostatic interactions. Due to speculation that the initial attachment of bacteria may be promoted by the detection of certain adsorbed proteins or carbohydrates, the adsorption of these biomolecules may also need to be controlled. Poly(ethylene glycol)-

modified surfaces have been shown to greatly reduce bacterial adhesion and protein adsorption by providing a steric repulsive barrier[21,22]. A covalently-attached hyperbranched fluoropolymer-poly(ethylene glycol) (PEG) composite coating was developed to combine both the steric repulsive properties of PEG and the low surface energy of fluoropolymers[23]. This coating was found to reduce the adsorption of various proteins and lipopolysaccharides, as well as facilitate the removal of algal sporelings. A novel discovery was the strong biofilm inhibitory activity of a group II polysaccharide capsule secreted by a uropathogenic strain of *E. coli*[24]. It was found to strongly quench biofilm formation in *E. coli*, *P. aeruginosa*, *Klebsiella pneumoniae*, *Staphylococcus aureus*, *Staphylococcus epidermis,* and *Enterococcus faecalis*. The polysaccharide capsules were found to act by electrostatically modifying surfaces and reducing cell aggregation.

2.3.3. Strategies for therapeutic drug development

The methods thus far described would only be useful in eliminating biofilms from industrial and medical implant surfaces. Specific therapeutic treatments against disease-causing biofilms in the body are presently virtually non-existent. Excess iron (Fe^{3+}) salts greatly decrease biofilm formation in *Pseudomonas aeruginosa* and *Staphylococcus aureus*, and disrupt pre-formed biofilms of *P. aeruginosa*[25,26]. Some antibiotics have recently been discovered to have anti-biofilm activity, possibly by inhibiting exopolysaccharide production. Azithromycin, a macrolide antibiotic, was found to delay biofilm formation in *P. aeruginosa* at concentrations below its minimum inhibitory concentration (MIC), but to have no effect when applied to established biofilms[27]. Similarly, clarithromycin, which is structurally related to azithromycin, inhibited biofilm

formation of *Mycobacterium avium* at a sub-MIC concentration but had no effect against established biofilms[28]. The screening of a plant compound library resulted in the discovery of ursolic acid from *Diospyros dendo* (an African ebony) as a new class of biofilm inhibitor[29]. It was shown to inhibit the formation of *P. aeruginosa, Vibrio harveyi*, and *E. coli* biofilms, and to disperse established biofilms of *E. coli*. Ursolic acid was proposed to act as a signal to cells to remain motile, based on the upregulation of genes related to chemotaxis and motility in *E. coli*. Other ursene triterpene compounds extracted from *Diospyros dendo* inhibit biofilm formation in *P. aeruginosa* by 32 to 62 percent[30]. N-acetyl-L-cysteine has been found to reduce EPS production in many bacteria and to reduce adhesion to stainless steel plates, and is already used in the treatment of patients with chronic bronchitis[31]. A novel class of therapeutic drugs being considered for the treatment of biofilms are quorum sensing inhibitors, which are discussed in detail in Chapter 4.

Chapter 3: Bacterial Quorum Sensing

3.1. Introduction

Quorum sensing is the process in which bacteria release and detect signaling molecules and thereby coordinate their behavior in a multicellular manner. The signaling molecules, or autoinducers, are observed to modulate behavior only above a certain threshold concentration corresponding to a certain cell population density, or 'quorum'. Three distinct types of quorum sensing have been discovered: acyl-homoserine lactone (AHL) signaling, which is unique to various species of Gram-negative bacteria; autoinducing oligopeptide signaling, which is unique to various species of Gram-positive bacteria; and autoinducer-2 signaling, which occurs over a broad range of Gram-positive and Gram-negative bacteria. Other more limited extracellular signaling systems have also been found.

3.2. Classes of quorum sensing systems

3.2.1. Acyl-homoserine lactone signaling

AHL signaling was first described in the bioluminescent marine bacteria *Vibrio fischeri*, where it was found that the synthesis of luciferase (an enzyme responsible for light production) was transcriptionally controlled by a phenomenon called "autoinduction[32]." It was observed that luciferase expression increased during exponential growth, although the signaling mechanism by which this occurred was not yet understood. Over a decade later, the autoinducer was definitively isolated and identified as N-3-oxo-hexanoyl-L-homoserine lactone (AI-1)[33]. In *V. fischeri*, AI-1 is synthesized by LuxI and can freely diffuse across the cell membrane. The signal receptor

protein, LuxR, resides within the cytoplasm and binds with AI-1 to form a multimer complex that can bind to a '*lux* box' located upstream from the target gene on an operon (Figure 2). RNA polymerase then interacts to stimulate transcription of the target gene[34]. Over 50 species of Gram-negative Proteobacteria have since been found to produce AHLs, with most species producing unique molecules that differ in acyl chain length and the functional group on the β-carbon of the acyl chain[35]. Most regulatory proteins are homologues of LuxI and LuxR, although *V. fischeri* has been found to produce a second AHL regulated by a novel AinS-AinR system[36]. AinS is similar to LuxM in *Vibrio harveyi* and is also present in *Escherichia coli*[35]. *Pseudomonas fluorescens* possesses an AHL synthase, HdtS, which is also not related to LuxI[37]. Although AHLs were originally discovered due to their regulation of bioluminescence in *Vibrio* spp., many different target functions are affected in other species. AHL-mediated target functions in *Pseudomonas* spp. include biofilm formation, protease production, cell aggregation, rhamnolipid synthesis, swarming, twitching, and virulence[38]. Other regulatory functions of AHLs include regulation of exopolysaccharide production by *Sinorhizobium meliloti* and *Pantoea stewartii*[39,40], virulence and exoenzyme production in *Erwinia carotovora*[41], and conjugation of the Ti plasmid in *Agrobacterium tumefaciens*[42].

3.2.2. Autoinducing oligopeptide signaling

Gram-positive bacteria lack AHL quorum sensing systems, but instead synthesize autoinducing oligopeptides consisting of between five to seventeen amino acids, sometimes with post-translational modifications[43]. These oligopeptides are actively transported out of the cell via an ATP-binding cassette (ABC) transporter complex, and

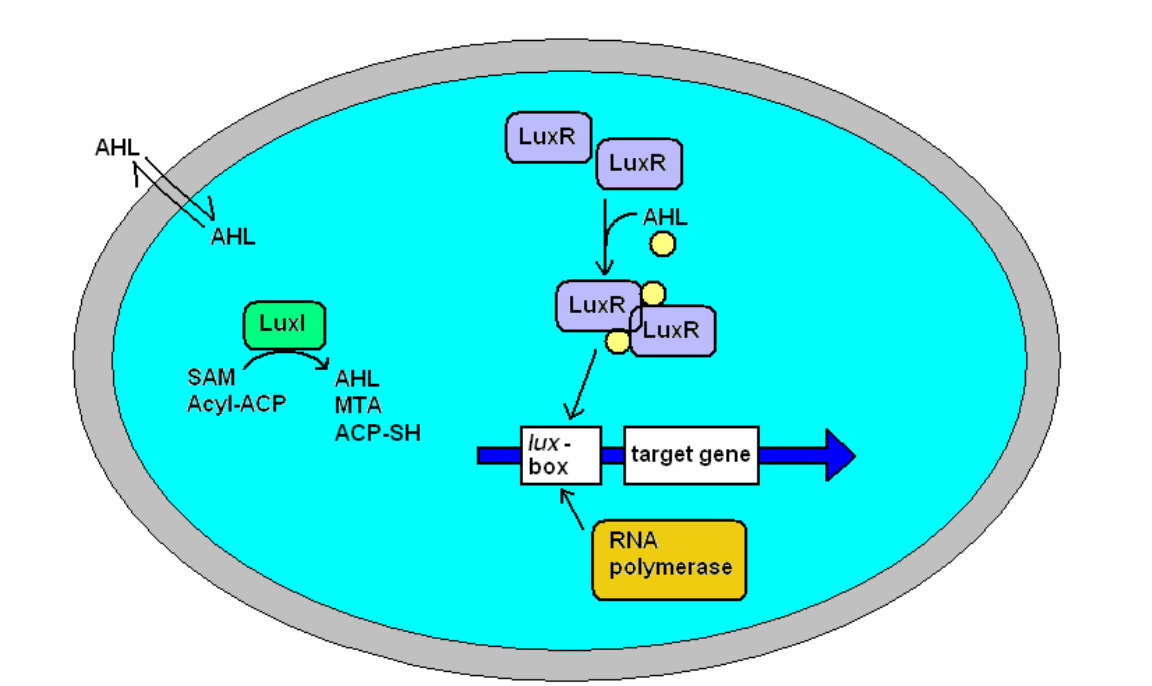

Figure 2: Schematic of the LuxI-LuxR acyl-homoserine lactone signaling system[35]. AHLs are synthesized by LuxI from S-adenosyl-L-methionine (SAM) and fatty acid precursors conjugated to an acyl carrier protein (acyl-ACP). AHLs can freely diffuse across the cell wall and membrane. The cytoplasmic receptor protein, LuxR, forms a multimer after binding to the AHL, which interacts with one or more *lux* boxes upstream from the regulated target gene. RNA polymerase interacts to stimulate transcription of the operon.

are detected extracellularly by a sensor kinase, which phosphorylates a downstream response regulator protein[44]. The phosphorylated response regulator binds to DNA to promote the expression of target genes. Each oligopeptide is unique to a particular species, with some species producing several different sequences. In *Staphylococcus aureus*, various oligopeptides modified with thiolactone rings control the production of virulence factors and surface attachment during late exponential growth, presumably to allow host invasion[43]. In *Enterococcus faecalis*, the synthesis of gelatinase, a virulence factor, is activated by an eleven-residue cyclic peptide containing a lactone ring[45]. *Bacillus subtilis* secretes several diverse peptide signaling molecules, including ComX, a peptide consisting of ten residues with a post-translational isoprenylation of a tryptophan

residue, which modulates the control of genetic competence and several other genes as a function of cell density[43,46]. Sporulation of numerous Gram-positive species, including *Bacillus subtilis* and *Streptomyces coelicolor*, and the production of bacteriocins (antimicrobial peptides) are also controlled by various autoinducing oligopeptide mediated quorum sensing systems[44,46].

3.2.3. Autoinducer-2 signaling

In experiments investigating the expression of luminescence by *Vibrio harveyi*, Bassler et al. found that in addition to the AHL signal response system, an additional unidentified density-sensing system was present[47]. This second system was later identified to involve LuxP and LuxQ, which served as detectors of this new, but still unidentified, autoinducer named autoinducer-2 due to it being the second autoinducer discovered in *V. harveyi*[48]. Surette and Bassler collected cell-free supernatants from *Salmonella typhimurium* and *Escherichia coli* and found that in the mid-exponential growth phase, a substance was produced by *S. typhimurium* and one strain of *E. coli* that induced bioluminescence in *Vibrio harveyi* BB170, a reporter strain that lacks the AI-1 sensor but retains the AI-2 sensor[49]. One strain, *E. coli* DH5α, was found to not produce the signaling molecule, therefore in a subsequent study, a library of *V. harveyi* BB120 (wild-type) genomic DNA was transformed into *E. coli* DH5α to screen for AI-2 activity using *V. harveyi* BB170[50]. An open reading frame, named *luxS*, was ultimately discovered that was essential for the production of AI-2 by *E. coli* DH5α. The open reading frame encoding LuxS was found to closely correspond to YgaG in *S. typhimurium* and *E. coli*. Use of the BLAST search algorithm (National Center for Biotechnology Information, http://www.ncbi.nlm.nih.gov/BLAST/) on fully-sequenced

bacteria in the database currently identifies homologues of *luxS* in well over 80 species spanning a wide variety of both Gram-negative and Gram-positive bacteria. Furthermore, AI-2 production has been observed in many species using the *V. harveyi* BB170 reporter strain, proving that *luxS* is translated to a functional protein. These include *Bacillus subtilis*[51], *Bacillus cereus*[52], *Bacillus anthracis*[53], *Listeria monocytogenes*[54.55], *Listeria innocua*[56], *Streptococcus mutans*[57], *Actinobacillus actinomycetemcomitans*[58], *Streptococcus gordonii*[59], various human oral bacteria[60], and even several species of hyperthermophilic bacteria[61].

3.2.3.1. Autoinducer-2 biosynthesis pathway

Schauder et al. utilized a genomics approach to deduce the function of LuxS[62]. They realized that *luxS* occurs in a three-gene operon in *Borrelia burgdorferi*, together with *metK* and *pfs*. MetK converts methionine to S-adenosylmethionine (SAM), and Pfs (methylthioadenosine/S-adenosylhomocysteine nucleosidase) hydrolytically cleaves methylthioadenosine (MTA) and S-adenosylhomocysteine (SAH) into either methylthioribose (MTR) or S-ribosylhomocysteine (SRH)[63]. SAM is used as a methyl donor by various methyltransferases, producing SAH as a byproduct. Because SAH potently inhibits the methyltransferases, it is quickly degraded by Pfs to SRH. An enzyme from *E. coli*, S-ribosylhomocysteinase, had long been known to convert SRH to homocysteine and 4,5-dihydroxy-2,3-pentanedione (DPD), however it had only been partially purified and its sequence was unknown[64]. Schauder et al. were able to prove that LuxS is S-ribosylhomocysteinase by comparing dialysed cell-free extracts from a *luxS*$^{+}$ strain and a *luxS*$^{-}$ strain of *Salmonella typhimurium*[62]. SAM, SAH, SRH, and/or MTA were added as substrates and AI-2 activity was tested using *Vibrio harveyi* BB170.

Only the addition of SRH resulted in AI-2 activity. The full AI-2 biosynthesis pathway, as a part of the activated methyl cycle, is shown in Figure 3. Homocysteine produced by LuxS as a degradation product of SRH can be recycled back to methionine through either MetE or MetH (conserved in nearly all bacteria possessing LuxS[65]) by transferring a methyl group from tetrahydrofolate[66]. Methionine can then be utilized in protein synthesis or can be used to reconstruct SAM via a SAM synthase. In this manner, LuxS is an important part of the sulfur recycling pathway.

3.2.3.2. Chemical identity of autoinducer-2

Schauder et al. argued that DPD is not the final identity of AI-2, due to it not being observed in MS or NMR analyses after *in vitro* synthesis, and because it is a highly reactive molecule that undergoes nucleophilic attack[62]. They suggested that the true identity of AI-2 was a furanone formed by a spontaneous cyclization reaction, based on DPD having been shown in a prior study to be an unstable intermediate in the formation of 4-hydroxy-5-methyl-3(2H)-furanone (MHF) from pentoses[69]. Various furanones, including MHF, 4-hydroxy-2,5-dimethylfuranone, homofuraneol, and 4,5-dyhydroxy-2-cyclopentan-1-one were all found to induce AI-2-like activity, but only at several fold higher concentrations than DPD. The structural identity of enzyme-bound AI-2 was first determined by crystallization of *V. harveyi* LuxP[70]. The resulting structure was determined to be a furanosyl borate diester (Figure 4). However in another study, structures of compounds produced by *in vitro* reaction of SAH with cell-free extracts of *E. coli* K-12 MG1655, and exhibiting AI-2 activity with the *V. harveyi* BB170 bioassay, were determined by GC/MS (after methanol extraction) to be MHF[71]. Similar to results

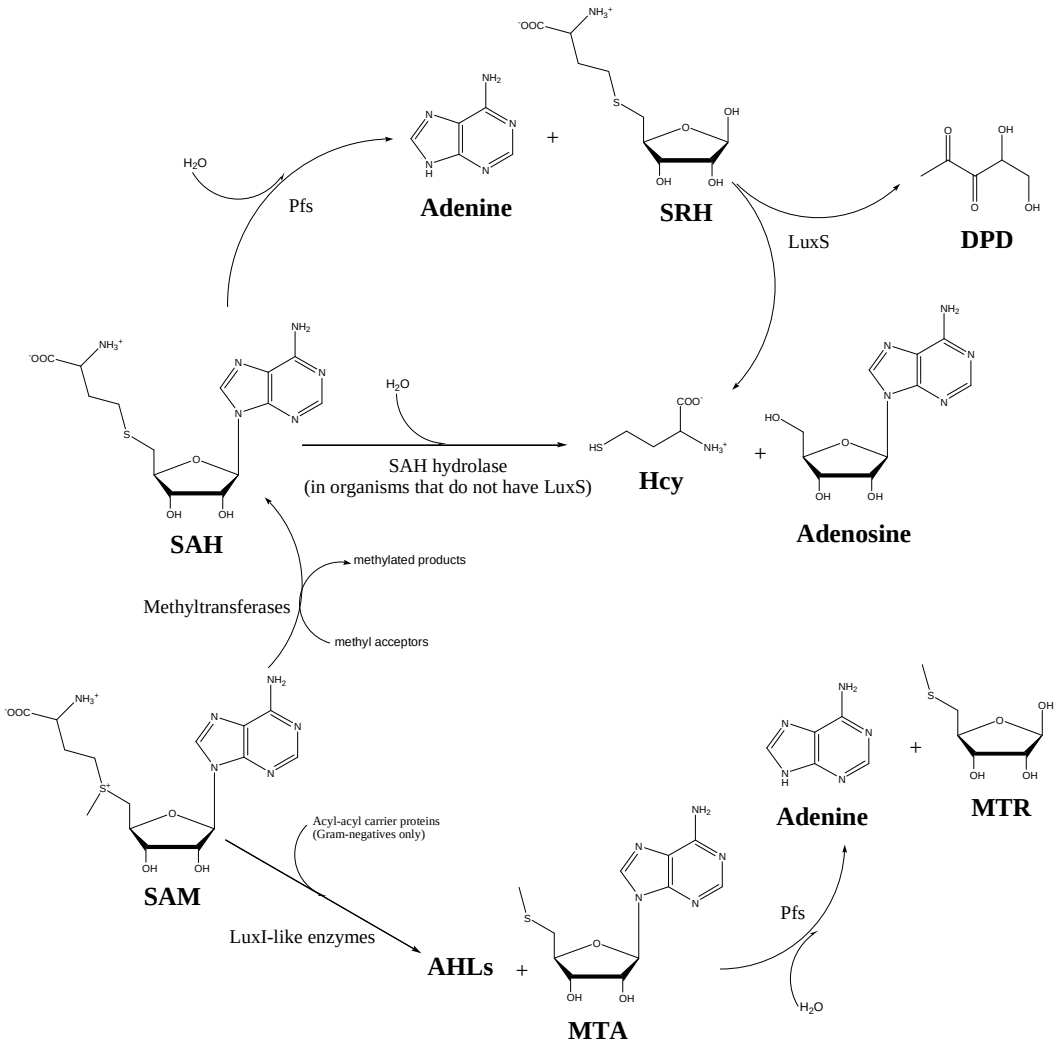

Figure 3: AI-2 biosynthesis pathway as part of the activated methyl cycle. SAM (S-adenosylmethionine) is used as a methyl donor and its byproduct is SAH (S-adenosylhomocysteine). SAH is converted to Hcy (L-homocysteine) and adenosine in organisms that do not have LuxS. In organisms that have LuxS, SAH is hydrolyzed by Pfs to SRH (S-ribosylhomocysteine) and adenine. SRH is then converted by LuxS to Hcy and DPD (4,5-dihydroxy-2,3-pentadione), the precursor of AI-2. In organisms with AHL quorum sensing, SAM is acylated by LuxI to produce AHLs and MTA (methylthioadenosine). MTA is a second substrate of Pfs, producing adenine and MTR (methylthioribose). This figure is adapted from Xavier and Bassler[67] and Vendeville et al.[68].

shown by Schauder et al., synthetic MHF was found to induce equivalent luminescence in *V. harveyi* BB170 at a concentration 1000-fold higher than their *in vitro* synthesized AI-2, leading to the conclusion that AI-2 may be a precursor to MHF formation. In a

later report, LsrB, a protein that binds to AI-2 directly in *Salmonella typhimurium*, was crystallized and found to bind a non-borated furanone, (2R,4S)-2-methyl-2,3,3,4-tetrahydroxytetrahydrofuran (R-THMF, Figure 4)[72]. These results have led to the currently accepted idea that "AI-2" is in actuality no single molecule, but is manifested under varying environmental conditions by different equilibrium forms of DPD. It is likely no coincidence *V. harveyi* detects a borated furanone, and that boron is relatively plentiful in seawater, the natural habitat for this bacterial species. Figure 4 shows proposed equilibrium interconversions between AI-2 signaling molecules that are recognized by *Vibrio harveyi*[72]. Additionally, dehydration of R-DHMF and S-DHMF result in the formation of MHF (not shown in Figure 4). It is possible that the MHF detected by Winzer et al. was ultimately a product of R-THMF dehydration in methanol.

Although there is evidence supporting the non-enzymatic, spontaneous conversion of DPD to various equilibrium forms of AI-2, a recent study has indicated the presence of alternative synthesis pathways[73]. A stochastic petri net simulation of metabolic fluxes in *Escherichia coli* revealed that the increased AI-2 activity due to glucose supplementation could not be explained by the existing known pathways. It was concluded that adenosine is converted by an unidentified enzyme to a *V. harveyi* BB170-responsive autoinducer, possibly by salvaging a ribose phosphate from adenosine. DPD isolated from tomato plants, which lack LuxS, has been attributed to spontaneous non-enzymatic rearrangements and dephosphorylation of D-ribose-5-phosphate and D-ribulose-5-phosphate[74]. DPD was found to be a precursor for MHF production in these plants.

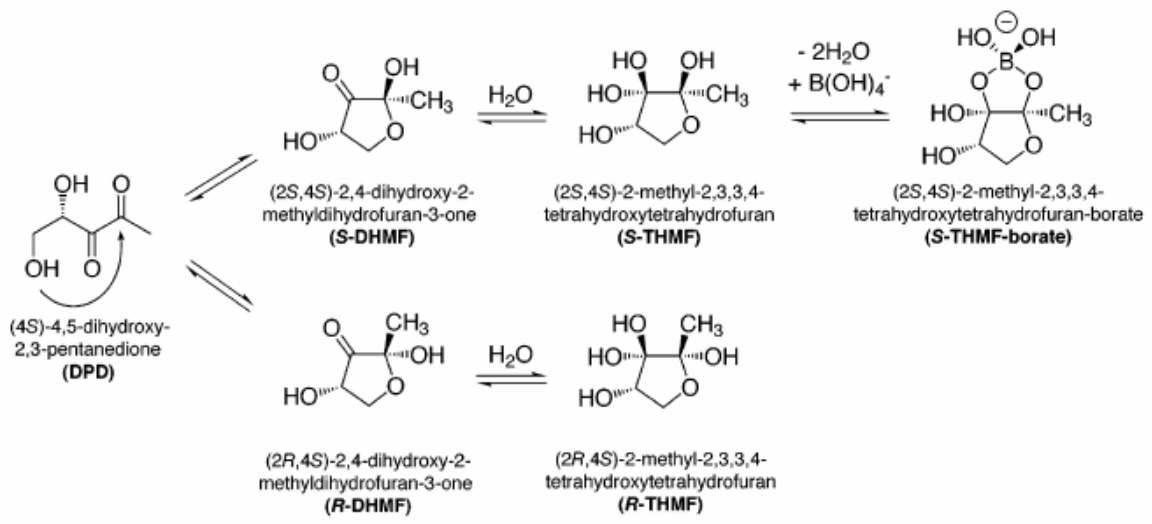

Figure 4: Equilibrium forms of DPD. *R*-DHMF and *S*-DHMF can also be hydrolyzed to 4-hydroxy-5-methyl-3(2H)-furanone (MHF), a toxic metabolite. The furanosyl borate diester (*S*-TMHF-borate) was the form of AI-2 first found by crystallization of LuxP in *Vibrio harveyi*. Figure taken from Miller et al.[72].

3.2.3.3. Behaviors regulated by AI-2 quorum sensing

The most comprehensive way to investigate regulation of gene expression, although not necessarily phenotype, is through the use of DNA microarrays. DeLisa et al. extracted RNA from an *E. coli luxS* mutant (MDAI2) grown in two different conditioned media exhibiting a 300-fold differential in AI-2 activity[75]. A total of 242 different genes were either induced or repressed, representing 5.6% of the genome of *E. coli*. Among the functional categories of genes that were affected were those involved in DNA replication and cell division, virulence, biofilm formation, exopolysaccharide formation, cell motility, signal transduction, and small molecule metabolism. In another study, gene expression of an AI-2 positive strain (*E. coli* K-12) and an AI-2 negative strain (*E. coli* DH5α) were compared[76]. Genes for chemotaxis, flagella synthesis, and motility were found to be induced by AI-2, and genes for central intermediary metabolism, biosynthesis, and transposons were repressed. In many other species, there exists a lack

of concerted genome regulation by AI-2. Differential gene expression of *Porphyromonas gingivalis* and its *luxS* mutant indicated that only 1% of its genome is regulated by AI-2, suggesting it is not a global regulator in this organism[77]. AI-2 mostly repressed genes related to stress response. In a *luxS* mutant of *Salmonella typhimurium*, differential gene expression in the absence and presence of *in vitro* synthesized AI-2 indicated that only 23 genes (out of 1136 open reading frames) were induced or repressed by AI-2[78]. AI-2 repressed genes encoding a Fur regulated iron transporter and several virulence-related genes. AI-2 induced several genes that encoded putative cytoplasmic or outer membrane proteins. In a differential gene expression study between *Neisseria meningitidis* and its *luxS* mutant, only one gene encoding a possible iron siderophore receptor was found to be significantly overexpressed by AI-2[79]. This led to the conclusion that in this species AI-2 may only be a metabolic byproduct rather than a signaling molecule. Further evidence supporting this conclusion was obtained with a proteomics analysis, where only three out of 1300 protein spots were differentially regulated by *in vitro* synthesized AI-2[80]. Regulation of two of the proteins, identified as MetE and MetF (involved in methionine biosynthesis), was attributed to the presence of L-homocysteine with *in vitro* synthesized AI-2. The third protein was not able to be identified.

Many other studies have directly investigated phenotypic or behavioral changes by constructing *luxS* mutants or by directly adding *in vitro* synthesized AI-2. The addition of 11 μM of *in vitro* synthesized AI-2 to *E. coli* K-12 (ATCC 25404), DH5α, and K-12 MG1655 resulted in 26-fold, 29-fold, and 4-fold increases in biofilm formation relative to the negative controls[81]. Additionally, *E. coli* DH5α was found to form less biofilm than the strains retaining *luxS*. In *Actinobacillus actinomycetemcomitans*, a periodontal

pathogen, leukotoxic activity was induced three-fold by conditioned media exhibiting AI-2 activity from both *A. actinomycetemcomitans* and *E. coli* relative to control media containing no AI-2[58]. The induction of leukotoxin protein was also increased nearly two-fold by AI-2, and the expression of *afuA*, a gene encoding a periplasmic iron transport protein, was induced eight-fold by AI-2. Regulation of toxin production by AI-2 has also been shown in *Clostridium perfringens*, with *luxS* mutants producing greatly reduced levels of three different toxins[82]. In two *Serratia* strains, *luxS* mutants were found to be less virulent, with one strain having decreased production of carbapenem (an antibiotic), and the other strain having decreased production of prodigiosin (an antibiotic) and reduced secretion of haemolysin[83]. In *Streptococcus mutans* biofilms, *luxS* mutants exhibited phenotypic differences, with a granular structure as opposed to the usual smooth confluent film in wild types[57]. Phenotypic differences in biofilm formation by *luxS* mutants of *Streptococcus gordonii* were found to be absent in five different media, but present in 25% human saliva as less confluent films with tall microcolony projections[84]. LuxS deficient *Bacillus subtilis* exhibited delayed biofilm formation, with defective pellicle formation and maturation, as well as greatly reduced swarming motility[51]. LuxS was also found to be critical for the development of aerial colony architecture leading to the formation of fruiting bodies in *B. subtilis*.

While the promotion of increased biofilm formation and increased virulence by AI-2 are common themes, much recent work has shown that these traits are inversely regulated by AI-2 in other species. A *luxS* mutant of *Helicobacter pylori* formed twice as much biofilm as the wild-type[85], and the addition of *in vitro* synthesized AI-2 greatly decreased early biofilm formation by *Bacillus cereus*[52]. Similarly, *luxS* mutants of *Listeria*

monocytogenes EGD-e have also been found to form increased quantities of biofilm[54,55]. The biofilms of *luxS* mutants were observed to be thicker but less confluent than those of EGD-e. Complementation with *in vitro* synthesized AI-2 in the *luxS* mutant failed to restore the parental strain phenotype, and addition of AI-2 had no effect on biofilm formation of the parental strain[54]. The addition of SRH increased biofilm formation. Because a *luxS* mutant would not be able to degrade SRH, it would experience an intracellular accumulation of SRH. This result is interesting because most investigations on *luxS* mutants did not attempt complementation with *in vitro* synthesized AI-2, making it impossible to distinguish between a depletion of AI-2 or an accumulation of SRH.

Despite AI-2 often being referred to as a putative interspecies signaling molecule, very few studies have directly investigated the effect of AI-2 or LuxS on cocultures of two or more species. In non-laboratory environments, such as in human dental plaque, hundreds of different bacterial species co-exist in complex biofilms. One study has shown that the presence of LuxS in at least one species is required for the formation of mixed biofilms of *Porphyromonas gingivalis* and *Streptococcus gordonii*, despite unimpaired biofilm formation by *luxS* mutants of either bacteria individually[59]. In coculture biofilms of *S. gordonii* and *Veillonella atypica*, expression of *amyB*, a gene encoding an α-amylase, was increased in *S. gordonii*[86]. Because *V. atypica* did not produce detectable AI-2, this was attributed to a different diffusible signaling molecule. However, the possibility that *V. atypica* may be able to detect and uptake AI-2, thereby modulating its gene expression, was not considered.

In summary, many of the more commonly investigated bacterial behaviors, including toxin production, biofilm formation, sporulation, swarming motility, and virulence, are

directly affected by either AI-2 or LuxS. The formation of confluent and/or thick biofilms can be regulated in opposite directions by AI-2 or LuxS, often with a strong dependence on the growth medium. Global gene or protein expression may be strongly regulated by AI-2 or LuxS, or only a handful of genes may be involved. Further complicating the situation, different bacterial species can interact through AI-2 signaling, resulting in unexpected phenotypes in co-cultures.

3.2.3.4. Metabolism and AI-2 quorum sensing

In *Vibrio harveyi*, the absence of AI-2 bound to LuxP in the membrane periplasm causes the phosphorylation of LuxU by an associated protein, LuxQ[48,87]. LuxU then passes its phosphate to LuxO, and the phosphorylated LuxO interacts with σ^{54} (the nitrogen-limitation sigma factor) to activate expression of small RNA[88]. These small RNA destabilize the mRNA that encodes LuxR with the assistance of the Hfq chaperone protein[89]. LuxR controls the transcription of luciferase, responsible for bioluminescence in *V. harveyi*. This phosphorelay signal transduction pathway has been suggested to indicate a true quorum sensing role for AI-2 in *Vibrio* spp. and other marine bacteria possessing LuxP, however this does not appear to be the case in most terrestrial bacteria[68].

The up-regulation of extracellular AI-2 production in *Escherichia coli* by glucose and other phosphotransferase system sugars (including fructose, mannose, and mannitol) was recognized even before the identity of AI-2 was revealed[49]. In chemostat cultures, the production of AI-2 by *E. coli* was found to depend on oxygenation, temperature, glucose concentration, and the addition of various nutrients and substrates[90]. It was postulated that AI-2 signaling was proportional to the overall metabolic rate, due to AI-2 production

per cell being linearly proportional to the growth rate. The level of AI-2 production and uptake in *Salmonella typhimurium* and *Escherichia coli* is intricately linked to growth conditions through regulation of the *lsr* operon[91,92]. The *lsr* operon consists of seven genes, *lsrACDBFGE*. They are analogous to many proteins encoded by the *rbs* operon, responsible for the transport and phosphorylation of ribose[93]. The *lsrACDB* genes encode an AI-2 importer complex, and *lsrF* and *lsrG* encode proteins for processing of internalized AI-2. The genes *lsrR* and *lsrK* are found adjacent to the *lsr* operon but are transcribed separately. LsrK phosphorylates AI-2 internalized by the Lsr ABC-type transporter. LsrR is a repressor of the *lsr* operon, preventing its transcription until it binds with phosphorylated AI-2[91,92]. In addition to transcriptional regulation by LsrR, the *lsr* operon was also found to be transcriptionally repressed by glyceraldehyde 3-phosphate and partially repressed by glycerol, as well as an unidentified metabolite (believed to be dihydroxyacetone phosphate). The mechanism of repression is through the cyclic adenosine monophosphate (cAMP)-cAMP receptor protein (CRP) complex[94]. Deletion of the entire *lsr* operon in *E. coli* does not completely stop the import of AI-2 into the cell (indicating the existence of a low-affinity transporter), nor does it stop transcription from the *lsr* promoter despite greatly reduced AI-2 importation[92,95]. It was also found that mutation of *rpoS* encoding the stationary-phase-specific sigma factor σ^s greatly increases transcription of the *lsr* operon, indicating that several regulators influence transcription of *lsrACDBFGE*[95]. While cAMP-CRP represses the expression of the *lsr* operon in the presence of glucose, it has been found that *luxS* is indirectly upregulated under these conditions[95]. Therefore a general picture emerges, as depicted in Figure 5, where in the presence of glucose production of AI-2 increases, and in the

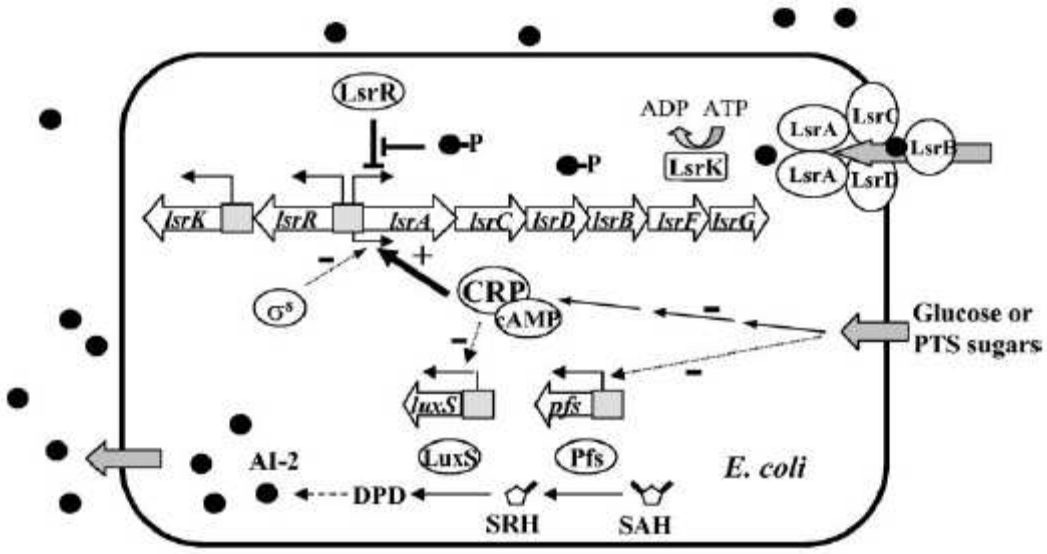

Figure 5: Schematic of AI-2 synthesis and uptake in *E. coli*[95]. LsrA, LsrC, LsrD, and LsrB form a transporter complex responsible for uptaking most AI-2 into the cell. Intercellular AI-2 is phosphorylated by LsrK. Phospho-AI-2, when bound to LsrR, derepresses expression of *lsrACDBFG*. In the absence of glucose or other PTS sugars, cAMP-CRP stimulates expression of *lsrACDBFG*. In the presence of glucose or other PTS sugars, expression of *luxS* is indirectly upregulated.

absence of glucose AI-2 is uptaken. The similarity of the *lsr* AI-2 uptake system to the *rbs* system has led to the suggestion that AI-2 has a metabolic function in these species[68]. However, Taga et al. point out that there would be no net energy gain from synthesizing and metabolizing the same molecule[91].

A BLAST search for the protein sequence of LsrR from *E. coli* K-12 MG1655 in all available bacterial genomes reveals homologous sequences not only in *Salmonella typhimurium*, but also in *Yersinia* spp. (transcriptional regulators), *Photorhabdus luminescens, Pasteurella multocida, Haemophilus somnus, Sinorhizobium spp., Rhizobium* spp., *Rhodobacter sphaeroides*, *Desulfovibrio* spp., and *Brucella* spp., which are all Gram-negative bacteria. Interestingly, a BLAST search reveals many *Bacillus* spp. that also have LsrR homologues denoted as transcriptional regulators. Sun et al. tabulate many other Gram-positive Firmicutes with low expectation values for

homologues of *lsrR* from *S. typhimurium*[66]. A BLAST search for the protein sequence of LsrK from *E. coli* K-12 MG1655 also reveals highly conserved homologous sequences in most species above, as well as *Serratia proteamaculans*, an *Enterobacter* species, *Shigella dysenteriae*, *Shewanella woodyi*, *Thiomicrospira denitrificans*, *Thermosinus carboxydivorans*, and many other Gram-negative species with very low expectation values. *Bacillus* spp. also exhibit LsrK homologues, as well as *Clostridium* spp., another genus of Gram-positive bacteria. The possibility that many organisms internally process AI-2 similarly to *E. coli* and *S. typhimurium* remains open. Conservation of *lsrACDB* is less widespread[66]. Notably, *Bacillus* spp. and *Streptomyces* spp. appear to be among very few Gram-positives having these open reading frames. Among selected Gram-negative species, *lsrACDB* is largely conserved in *Yersinia pestis*, *Shigella flexneri*, *Pasteurella multicida*, *Sinorhizobium meliloti*, and *Agrobacterium tumefaciens*.

Transcription of *lsr* is controlled by catabolite repression through cAMP-CRP in *E. coli* and *S. typhimurium*, raising the question of how the putative *lsr* operon in *Bacillus* and *Streptomyces* is controlled. Gram-positive bacteria do not possess cAMP-CRP, with catabolite repression occurring through the unrelated CcpA regulator[96]. In *Bacillus subtilis*, fructose-1,6-phosphate is produced from phosphorylated glucose. Fructose-1,6-phosphate then activates HPrK, which phosphorylates HPr at a serine site. HPr-Ser-P then binds to CcpA, resulting in a complex analogous to cAMP-CRP that inhibits the transcription of target genes[96]. No work is known that studies the interplay between LsrR and LsrK homologues, nor CcpA-dependent catabolite repression on AI-2 quorum sensing in Gram-positive bacteria. There have been studies that investigate the effect of CcpA on biofilm formation in Gram-positive bacteria, a behavior that is usually AI-2

regulated. A *ccpA*-deficient mutant of *Streptococcus mutans* was found to exhibit greatly decreased biofilm formation over the wild-type, whereas a *luxS*-deficient mutant had a similar level of biofilm formation to the wild-type.[39] A *ccpA* mutant of *Bacillus subtilis* grown in medium supplemented with 1.0% glucose exhibited greatly increased biofilm formation than the wild-type, indicating that CcpA inhibits a gene involved in biofilm formation in the presence of glucose[97]. If CcpA regulates transcription of the *lsr* operon in a manner similar to cAMP-CRP, then the presence of glucose would repress transcription of the transporter genes. This would prevent the importation of AI-2, consistent with *luxS* mutants of *B. subtilis* exhibiting delayed and defective biofilm formation[51].

3.2.4. Other extracellular signaling systems

Additional extracellular chemical signals used by bacteria include 2-alkyl-4(1*H*)-quinolones in *Pseudomonas* and *Burkholderia* spp.[40,41], and indole in *Escherichia coli*.[42] A newly discovered signaling molecule called autoinducer-3 has been proposed to mediate bacteria-host communication in enteric bacteria.[39] The mammalian hormones epinephrine and norepinephrine can both bind to the AI-3 receptor and stimulate similar responses.[43] Furthermore, AI-3 synthesis is downregulated by inactivation of *luxS*, although this is believed to be due to increased flux through an alternative pathway for homocysteine production that alters amino acid content and metabolism.[44]

Chapter 4: Quorum sensing inhibitors

4.1 Introduction

Bacterial antibiotics typically function by interfering with DNA transcription, RNA translation, or with the synthesis or crosslinking of peptidoglycan in the cell wall. Overuse and improper use of antibiotics has led to a prevalence of bacterial resistance to these chemicals. This can take the form of increased ability to degrade antibiotics, decreased membrane permeability, decreased affinity, or increased efflux[103]. As bacterial multiresistance increases, new antibiotics need to constantly be developed to meet medical needs. Because quorum sensing modulates the expression of many genes necessary for coordinated behaviors related to virulence and pathogenicity, quorum sensing inhibitors (QSIs) have been suggested as a new route for antibacterial drug development. QSIs would attenuate gene expression that leads to pathogenic phenotypes, rather than having inherent toxic or growth inhibitory properties. Therefore it would be expected that QSIs would exert less evolutionary pressure that could lead to resistance.

Much research has been carried out on inhibitors of AHL-based quorum sensing in Gram-negative bacteria, particularly *Pseudomonas aeruginosa*. These inhibitors are typically analogues of AHLs that either competitively bind to LuxR-like receptor proteins, or noncompetitive inhibitors that bind to other regions of the receptor protein, and are not AHL analogues. Smith et al. synthesized and tested analogues of an AHL produced by *P. aeruginosa*, 3-oxo-dodecylhomoserine lactone[104]. Two analogues, N-(trans-2-hydroxycyclopentyl)-3-oxododecanamide and N-(2-oxocyclohexyl)-3-oxodo-decanamide, acted as quorum sensing antagonists, reducing biofilm formation and the expression of certain virulence factors. Geske et al. also synthesized AHL analogues and

found three with activity against TraR, the quorum sensing transcriptional regulator in *Agrobacterium tumefaciens*[105]. Two of these analogues, containing an indol and a bromophenyl group on the acyl chain, significantly reduced biofilm density and organization in *Pseudomonas aeruginosa*.

4.2. Inhibitors of autoinducer-2 quorum sensing

Inhibitors of AI-2 quorum sensing are of particular interest due to the broad range of species that could potentially be affected by a single compound. These inhibitors could target enzymes involved in either the production or uptake of AI-2. However, it appears that different bacteria detect and uptake different equilibrium forms of AI-2 through a variety of largely unidentified enzymes (although an Lsr transporter complex may be relatively widely conserved[66]). Therefore, emphasis has so far been placed on inhibitors of enzymes in the production pathway.

4.2.1. Inhibitors of SAH/MTA nucleosidase

SAH/MTA nucleosidase (Pfs) has been considered a target for the design of antibacterial agents long before the discovery of AI-2 and knowledge of its role in this quorum sensing pathway. Inhibition of this enzyme results in a build-up of MTA and SAH, which at elevated levels are toxic to the cell. MTA is known to be a potent inhibitor of spermidine synthase, which is involved in the synthesis of polyamines[106]. Polyamines are in turn believed to be involved in growth processes and DNA synthesis[107]. Pfs also plays a part in sulfur metabolism pathways, with MTR eventually being recycled back to methionine, an essential amino acid that requires a large expenditure of energy to synthesize[107,108]. Finally, SAH buildup results in feedback

inhibition of SAM trans-methylation reactions[107]. Mammals lack Pfs, and instead metabolize MTA with MTA phorphorylase, and SAH with SAH hydrolase[109], therefore Pfs inhibitors would be expected to specifically target microbes. Pfs inhibition now has added attractiveness due to the reduction of downstream synthesis of AI-2, although it is unlikely that attenuation of quorum sensing would be a primary outcome of their usage.

Guillerm et al. published the earliest paper in the literature concerning the synthesis of proposed inhibitors of Pfs, however no results were published concerning their biological activity[110]. These compounds were hydroxylated pyrrolidines speculated to be transition state analogues (Figure 6A). Later work turned to analogues of MTA. Cornell et al. synthesized and tested enzyme activity of several alkyl-substituted and aryl-substituted MTA analogues, and also screened other MTA-like compounds, various nucleosides, MTR, and two MTR analogues[111]. They found that various aryl substitutions on the sulfur atom of MTA resulted in enzyme inhibition, with the most potent inhibitor being 5'-(p-nitrophenyl)thioadenosine (Figure 6B), exhibiting a K_i of 0.02 μM. MTA analogues with fluorinated methyl groups on the sulfur atom were also synthesized and tested by, however these had higher inhibition constants than compounds found in the Cornell study[112]. Detailed crystallographic information in recent years has elucidated the complete structure and geometry of the binding site of SAH/MTA nucleosidase in *Escherichia coli*, allowing for more rational inhibitor design[113]. In one study, hundreds of thousands of commercially available compounds were screened against certain binding site properties, leading to the discovery of a purine benzylamine derivative having K_i = 1 μM[114]. This molecule adopts an unexpected bound conformation in the binding site, with hydrogen bonding between purine nitrogens and binding site protein residues, and π-π

stacking with a phenylalanine residue. This led to ligand studies on a non-optimal portion of this molecule, resulting in the discovery of two compounds with nanomolar K_i values (Figure 6C). In another study, screening of commercially available compounds led to the consideration of 5-nitroindazole[115]. With this starting point, numerous 3,5,7-trisubstituted indazoles containing C5 aryl sulfonamides were synthesized. Several compounds were discovered with nanomolar K_i values, with 3',4'-dichloro-biphenyl-3-sulfonic acid (3-chloro-7-isobutylamino-1H-indazol-5-yl)-amide (Figure 6D) having the highest potency. Very recently, femtomolar K_i compounds have been synthesized that are analogues of the transition state, rather than of the substrate or products[116]. The most potent inhibitor from this study is (3R,4S)-4-(4-chlorophenyl-thiomethyl)-1-[(9-deazaadenin-9-yl)methyl]-3-hydroxypyrrolidine (Figure 6E). Another recent study discusses the synthesis of a SAH/MTA nucleosidase inhibitor with a K_i of 1.7 nM[117]. This compound, 2-amino-4-[5-(4-amino-5H-pyrrolo[3,2-*d*]pyrimidin-7-yl)-3,4-dihydroxypyrrolidin-2-ylmethylsulfanyl]-butyric acid (Figure 6F), is nearly identical to one of the proposed inhibitors from Guillerm et al., with the exception of containing an adenine ligand. No reports have been published concerning the effect of any Pfs inhibitor against bacteria.

4.2.2. Inhibitors of S-ribosylhomocysteinase

Far fewer studies have targetted S-ribosylhomocysteinase (LuxS) for the development of inhibitors. The only known functions of this enzyme are the synthesis of DPD, SAH detoxification, and possibly a minor role in the sulfur recycling pathway. Thus it serves as a less broad-spectrum target for antimicrobial drug development than Pfs. However, inhibition of LuxS offers a unique opportunity to primarily attenuate only AI-2 quorum

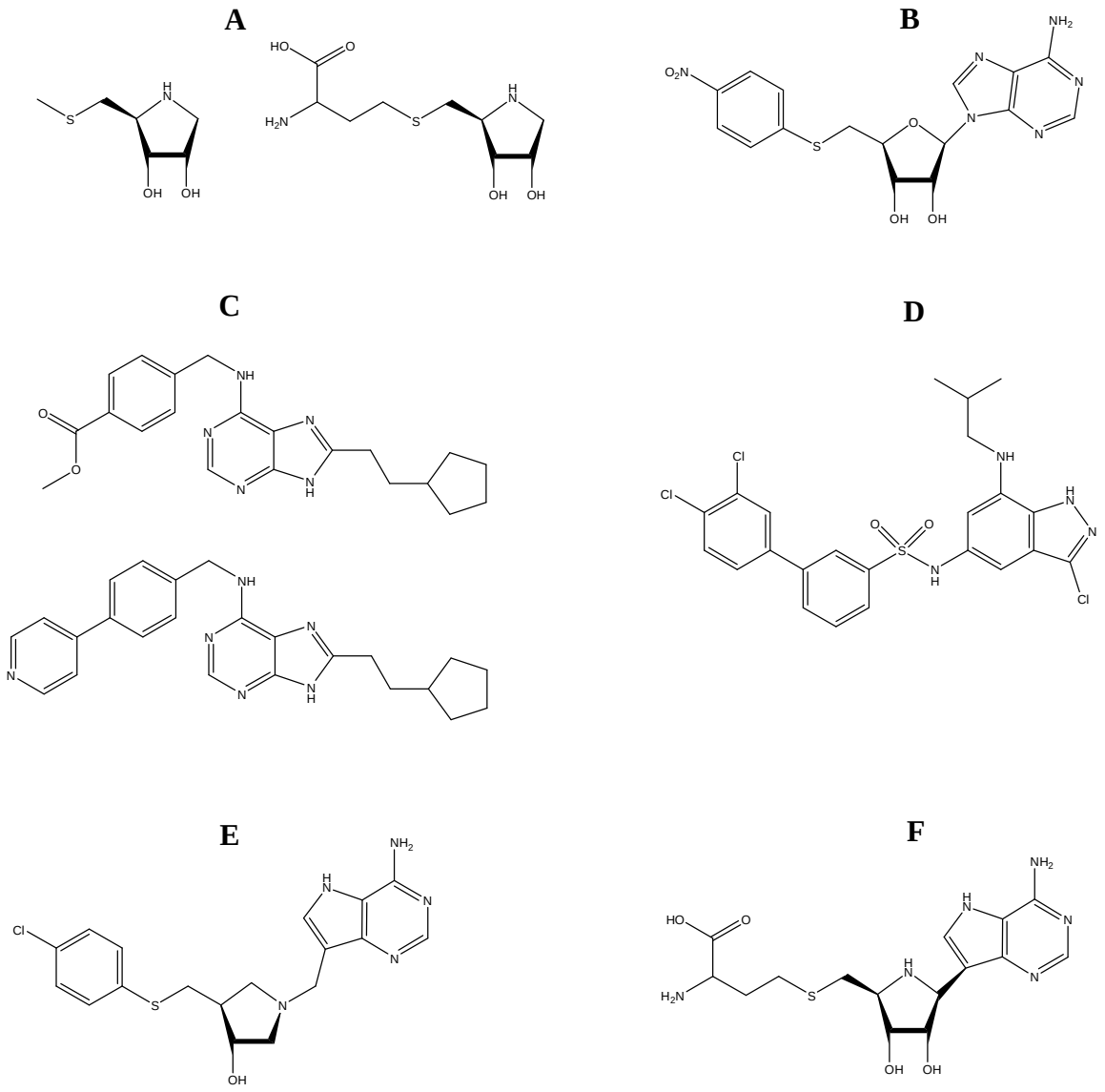

Figure 6: Chemical structures of inhibitors of SAH/MTA nucleosidase. (A) hydroxylated pyrollidines speculated to be enzyme inhibitors[110]; (B) 5'-(p-nitrophenyl)thioadenosine with a K_i of 0.02 µM[111]; (C) purine benzylamine derivatives with K_i of 0.043 µM (top) and 0.0028 µM (bottom)[114]; (D) indazole sulfonamide derivative with K_i of 0.0016 µM[115]; (E) transition state analogue with K_i of 47 fM[116]; (F) SAH derivative with K_i of 0.0017 µM[117].

sensing, likely without a significant effect on bacterial growth. This could be of particular interest in controlling gene expression in industrial fermentation processes. For example, it could be desirable to prevent a culture from sensing that it has reached a high density in order to prolong the transition to the stationary phase. Additionally,

recombinant protein fusions could be designed as part of an artificial AI-2 quorum sensing circuit[118] that exhibit tunable expression through the use of inhibitors of LuxS.

Zhao et al. tested SRH analogues for inhibitory activity against S-ribosylhomocysteinase, including S-ribosylthiobutyric acid, 5-methylthioribose, 5-(trifluoromethyl)thioribose, and 5-(4-nitrophenyl)thioribose[119]. All of these compounds introduced ligands to the sulfur atom, and resembled earlier discovered inhibitors of Pfs without the adenine group. It was found that none of these compounds had any activity against S-ribosylhomocysteinase, and it was postulated that the amine in the homocysteine residue on SRH is critical for binding to the active site. The catalytic mechanism of the enzyme was determined by Zhu et al.[120]. It was found that S-ribosylhomocysteinase catalyzes three distinct reactions, and knowledge of the mechanism enabled subsequent rational inhibitor design. Alfaro et al. developed two inhibitors, S-anhydroribosyl-L-homocysteine, and S-homoribosyl-L-cysteine (Figure 7A)[121]. S-anhydroribosyl-L-homocysteine (SARH) was shown to be a very weak inhibitor of LuxS. The addition of 100 µM of S-homoribosyl-L-cysteine nearly completely quenched the reaction of either 0.34 µM LuxS or 3.4 µM LuxS with 100 µM of SRH. The K_i was not determined, but it is likely in the high µM to mM range for this compound. The most recent study reporting inhibitors of S-ribosylhomocysteinase involved the synthesis of analogues of an intermediate during the catalyzed reaction[122]. Two diastereomeric compounds (Figure 7B), (2S)-2-amino-4-[(2R,3S)-2,3-dihydroxy-3-N-hydroxycarbamoylpropylmercapto]butyric acid (Pei compound **10**), and (2S)-2-amino-4-[(2R,3R)-2,3-dihydroxy-3-N-hydroxycarbamoyl-propylmercapto]butyric acid (Pei compound **11**) were found to have sub-micromolar K_i values against certain forms of

LuxS. The K_i values of Pei compounds **10** and **11** are shown in Table 1 against LuxS from *Bacillus subtilus*, *Escherichia coli*, and *Vibrio harveyi* with the stated center metal ions. Lineweaver-Burke plots verified that these compounds inhibit LuxS competitively.

Despite all of this work to synthesize and characterize the *in vitro* activity of inhibitors of Pfs and LuxS, there are no published results on the *in vivo* effects of these inhibitors in bacteria.

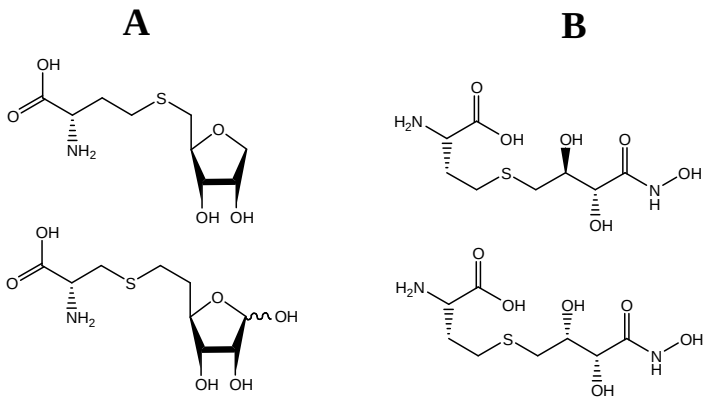

Figure 7: Chemical structures of inhibitors of S-ribosylhomocysteinase. (A) S-anhydroribosyl-L-homocysteine (top) and S-homoribosyl-L-cysteine (bottom)[121]; (B) transition state analogue inhibitors, Pei compound **10** (top), and Pei compound **11** (bottom)[122].

Table 1: Inhibition constants of Pei compounds **10** and **11** against LuxS from different bacterial species with the stated coordinated metal ions[46].

Enzyme	**Coordinated metal ion**	**K_i (μM)** Pei **10**	Pei **11**
E. coli LuxS	Co^{2+}	3.2 ± 0.3	12.7 ± 0.4
V. harveyi LuxS	Co^{2+}	9.7 ± 0.4	12.8 ± 0.3
B. subtilis LuxS	Co^{2+}	0.72 ± 0.02	0.37 ± 0.04
	Fe^{2+}	0.72 ± 0.03	0.43 ± 0.02
	Zn^{2+}	19.6 ± 1.1	10.6 ± 0.4

4.2.3. Brominated furanones

In addition to direct inhibitors of enzymes in the AI-2 biosynthesis pathway, another possible class of inhibitors are the halogenated furanones first isolated from *Delisea pulchra*, a red alga which was observed to have a biofilm-free surface[123]. These compounds have structural similarity to AHLs, and arguably also have a similarity to certain equilibrium forms of AI-2. Many studies have been conducted that demonstrate interference with AHL quorum sensing on addition of brominated furanones (most studies utilize (5Z)-4-bromo-5-(bromomethylene)-3-butyl-2(5H)-furanone, Figure 8) from *Delisea pulchra*, including: inhibition of swarming motility in *Proteus mirabilis*[124]; reduced binding of tritiated N-3-(oxohexanoyl)-L-homoserine lactone to LuxR in *E. coli*[125]; reduced bioluminescence and toxin production by *Vibrio harveyi*[126]; and repression of *lasB* expression, reduced virulence factor production, decreased biofilm antibiotic resistance, and altered biofilm architecture leading to increased biofilm detachment in *Pseudomonas aeruginosa*[127,128]. The brominated furanone in Figure 8 has also been shown to repress siderophore synthesis in *Pseudomonas putida* and to induce siderophore synthesis in *P. aeruginosa*[129].

Brominated furanones derived from *Delisea pulchra* have also been found to directly inhibit AI-2 quorum sensing independently from AI-1 quorum sensing in *Vibrio harveyi*, as well as inhibit biofilm formation and swarming in *E. coli*, which is only known to

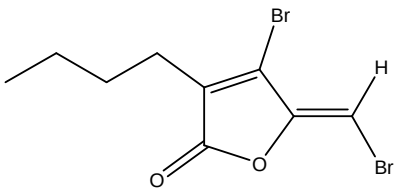

Figure 8: Brominated furanone, (5Z)-4-bromo-5-(bromomethylene)-3-butyl-2(5H)-furanone.

possess an AI-2 quorum sensing system[130]. A microarray study of *E. coli* grown in the presence or absence of 60 μg mL^{-1} of brominated furanone or *in vitro* synthesized AI-2 showed that the brominated furanone repressed 79% of the genes induced by addition of *in vitro* AI-2, although only a handful of genes repressed by AI-2 were induced by the brominated furanone[76]. The repressed genes were primarily related to chemotaxis, flagella synthesis, and motility. Brominated furanones also have broad-spectrum antimicrobial activity against many Gram-positive bacteria which lack AHL quorum sensing systems. Brominated furanones have been found to quench growth in a concentration-dependent manner in *Bacillus subtilis* and *Bacillus anthracis*, reduce swarming and biofilm formation in *Bacillus subtilis*, and reduce expression of three different virulence genes in *Bacillus anthracis*[131,132]. In *Staphylococcus aureus* and *Staphylococcus epidermis*, they have been demonstrated to quench growth while having no effect on cultured mouse cells[133]. To date, no direct evidence has been published that definitively links the activity of brominated furanones to AI-2 quorum sensing in Gram-positive bacteria.

Despite the murky connection to quorum sensing, brominated furanones have proven to be surface active compounds capable of directly preventing biofilm formation on substrates. Various polymer surfaces with physically adsorbed furanone were shown to have reduced bacterial loading and slime production in *Staphylococcus epidermis*[134]. Another study incorporated furanone into polystyrene disks, and also used crosslinking procedures to covalently bind the furanone onto catheters[135]. Bacterial load of *Staphylococcus epidermis* was decreased on the polystyrene-furanone disks. Furanone-coated catheters exhibited lower bacterial counts, and those implanted into sheep resulted

in lower-grade infections than control catheters for up to 65 days. None of these studies has speculated on the mechanism of action of surface-bound furanones, however it is possible that all studies conducted to date are actually testing furanone in a surface active state. Brominated furanones are not soluble in aqueous solution, and quickly precipitate as visible particles when a small amount of dissolved furanone in a non-aqueous solution is added to bacterial media. These furanone particles can also be observed to spontaneously coat the polystyrene used in most biofilm formation assays. One possibility is that the furanones act on receptor proteins on the cell membrane, including quorum sensing molecule receptor sites, and do not need to enter the cell.

Chapter 5: Experimental

5.1. Materials

The bacterial strains used in this study and their sources are listed in Table 2. Luria broth base, brain heart infusion, marine broth, nutrient broth, and vitamin assay casamino acids were obtained from Becton Dickinson (Cockeysville, MD). Tryptic soy broth, thiamine (hydrochloride), riboflavin, L-arginine, D-(+)-glucose (anhydrous, mixed anomers), imidazole (approximately 99%), isopropyl β-D-1-thiogalactopyranoside, adenine, S-adenosyl-L-homocysteine, and Dulbecco's phosphate buffered saline (modified, without $CaCl_2$ and $MgCl_2$) were purchased from Sigma (St. Louis, MO). Crystal violet (high purity biological stain) and glycerol (99+%) were purchased from Acros Organics (Geel, Belgium). Magnesium sulfate (anhydrous), potassium chloride (ACS reagent), potassium phosphate dibasic (anhydrous, ACS reagent), potassium phosphate monobasic (ACS reagent), sodium citrate, zinc acetate, Tris (crystallized free base, molecular biology grade), ampicillin sodium salt (biotech grade), HPLC grade water, and chloroform (ACS reagent) were purchased from Fisher Scientific (Fair Lawn, NJ). Sodium chloride, sodium hydroxide (pellets, ACS reagent), concentrated hydrochloric acid, and acetonitrile (Baker analyzed HPLC solvent) were purchased from J. T. Baker (Phillipsburg, NJ). Absolute ethanol (anhydrous, USP grade, ACS reagent), 95% ethanol (USP grade, ACS reagent), and acetone (ACS reagent) were purchased from Pharmco-Aaper (Brookfield, CT). DL-homocysteine (purum, >95.0%) was purchased from Fluka (Buchs, Switzerland). Phosphate buffered saline (PBS) was prepared by dissolving 8 g NaCl, 0.2 g KCl, 1.44 g Na_2HPO_4, and 0.24 g KH_2PO_4 in deionized water to a final volume of 1 L, adjusting to pH 7.4 with 5 N HCl, and autoclaving at 121°C for

25 minutes. S-anhydroribosyl-L-homocysteine (SARH) was obtained from Dr. Sunny Zhaohui Zhou at Washington State University. A 10 mM stock solution of SARH was prepared in PBS. Pei compounds **10** and **11** were obtained from Dr. Dehua Pei at Ohio State University. Stock solutions were prepared containing 1 mM of each inhibitor in PBS. The brominated furanone in Figure 8 was obtained from Dr. Thomas Wood at Texas A&M University at a concentration of 32.25 mg/mL in 95% ethanol. Inhibitor stock solutions were 0.22 µm filter-sterilized and stored at either 4˚C (brominated furanone), -20˚C (SARH), or -80˚C (Pei compounds **10** and **11**).

5.2. Bacterial cell culture

The bacterial strains and plasmids used in this study are listed in Table 2. *Escherichia coli* DH5α stock was originally obtained from Dr. Thomas Wood at Texas A&M University. Strains obtained as freeze-dried cultures from American Type Culture Collection (ATCC) were revived overnight according to the provided instructions. The following day, the overnight culture was used to inoculate 50 mL of fresh medium in 250 mL flasks, and cultures were grown to the exponential growth phase (OD_{600} of 0.3 to 0.6) at 250 rpm and the appropriate temperature on a Certomat BS-1 air shaker (B. Braun Biotech, Edgewood, NY). The culture was then aliquoted into cryogenic tubes and a filter-sterilized 40% (v/v) aqueous glycerol solution was added to bring the glycerol concentration up to 25% (v/v).

Luria-Bertani (LB) medium contained 10 g/L tryptone, 5 g/L yeast extract, and 5 g/L sodium chloride, and was prepared according to the manufacturer's instructions from Luria broth base. Brain heart infusion (BHI) medium contained 37 g/L of brain heart infusion. Tryptic soy broth medium (TSB) was prepared with 30 g/L of tryptic soy broth.

LB, BHI, and TSB media containing 0.2% (w/v) D-glucose, and two-fold diluted and ten-fold diluted LB (12.5 g/L, 2.5 g/L) and TSB (15 g/L, 3 g/L) with and without 0.2% (w/v) D-glucose were also prepared. Autoinducer bioassay (AB) medium was prepared by dissolving 17.5 g NaCl, 6.0 g $MgSO_4$, and 2.0 g vitamin assay casamino acids per 1 L of deionized water, autoclaving for 30 minutes at 121˚C, and allowing to cool. To 500 mL of this solution, 5 mL of filter-sterilized 1 M potassium phosphate solution, 5 mL of filter-sterilized 0.1 M L-arginine, 10 mL of autoclaved glycerol, 0.5 mL of filter-sterilized 10 µg/mL riboflavin, and 0.5 mL of filter-sterilized 1 mg/mL thiamine were added. Marine broth was prepared according to the provided instructions.

Table 2: Bacterial strains and plasmids used in this study.

Strain/plasmid	Relevant genotype and property	Source or reference
Strains		
Escherichia coli		
W3110	Wild-type	Laboratory stock
DH5α	*luxS*$^-$ strain	Laboratory stock
K-12	Wild-type	ATCC 25404
NC13	RK4353Δ*pfs*(8-226)::Kan^r	Laboratory stock
Vibrio harveyi		
BB170	BB120 *luxN*::Tn5 (sensor 1$^-$, sensor 2$^+$)	Laboratory stock
MM30	BB120 *luxS*::Tn5	ATCC BAA-1120
Bacillus cereus	Biofilm-forming strain (isolated from spoiled cheese)	ATCC 10987
Listeria innocua	Isolated from cabbage	ATCC 51742
Pseudomonas fluorescens	Isolated from lactate-enriched water	ATCC 17552
Plasmids		
pTrcHis-Pfs-Tyr	pTrcHisB derivative, W3110 *pfs*$^+$, Amp^r	Ref. 136
pTrcHis-LuxS-Tyr	pTrcHisC derivative, W3110 *luxS*$^+$Amp^r	Ref. 136

5.3. Recombinant enzyme purification

E. coli DH5α containing the p6His-Pfs-5Tyr plasmid constructed from pTrcHisB (Invitrogen), and *E. coli pfs* null-mutant strain NC13 (genotype RK4353Δ*pfs(8-226)*::Kan^r) containing the p6His-LuxS-5Tyr plasmid constructed from pTrcHisC

(Invitrogen) were originally constructed in this laboratory as described by Fernandes et al.[136]. For each strain, 10 mL culture tubes containing 2 mL of LB medium and 5 µL of 20 µg/mL ampicillin were inoculated with a scrape of cryogenically frozen stock, and grown overnight at 37˚C and 250 rpm in an air shaker. The next day, cultures were scaled up by adding 5 mL of the overnight culture to 95 mL of LB medium with 100 µL ampicillin in a 500 mL flask. The following day, the culture was scaled up again by adding 100 mL of the prior culture to 1400 mL of LB medium with 1.5 mL of ampicillin in a 3 L flask. The scaled-up culture was grown to an OD of 0.4 to 0.7 and induced with 1.5 mL of 1 M IPTG. After induction, the cultures were grown for another 4-6 hours at 37˚C and 250 rpm. The cells were centrifuged at 4500 rpm at 4˚C into pellets and frozen at -20˚C after discarding the supernatant.

To purify the histidine-tagged enzymes, the frozen cell pellets were resuspended in 30 mL of PBS with 10 mM imidazole, pH 7.4, and aliquoted into tubes containing no more than 10 mL of suspension each. Each tube was sonicated for 10 min using a sonic dismembrator (Fisher Scientific 550) at a power setting of 4.5, with 0.5 s on/off pulses, to lyse the cells. The cell lysate was removed by centrifuging each tube for 15 minutes at 10000 g and 10˚C, and again for 10 minutes at 14000 g and room temperature after aliquoting into 1.5 mL centrifuge tubes. The cell lysate was collected, and the cell pellets were combined and resuspended in 10 mL of PBS with 10 mM imidazole. The suspension was sonicated and centrifuged as before, with the cell lysate collected. The cell pellet was then resuspended in 5 mL of PBS with 10 mM imidazole, sonicated, and centrifuged, with the cell lysate collected again. All clarified cell lysates were combined and filtered through a 0.22 µM PES filter (low protein binding, Corning).

A HiTrap Chelating IMAC column (5 mL volume, GE Healthcare, Piscataway, NJ) chelated with Ni^{2+} was equilibrated with 3 column volumes of dilute washing buffer (20 mM potassium phosphate, 250 mM sodium chloride, 10 mM imidazole, pH 7.4) at a flow rate of 4 mL/min with a peristaltic pump (Watson Marlow 505Du), before loading the cell lysate at 2 mL/min. The column was then washed consecutively with three column volumes of dilute washing buffer at 2 mL/min, and three column volumes of a second washing buffer (20 mM potassium phosphate, 250 mM sodium chloride, 50 mM imidazole, pH 7.4). Next, three columns of elution buffer (20 mM potassium phosphate, 250 mM sodium chloride, 350 mM imidazole, pH 7.4) was loaded at 2 mL/min. Only the first 8 mL of eluant was collected, and dialyzed (SpectraPor 2 membrane, 12 to 14 kDa MWCO, Spectrum Laboratories, Rancho Dominguez, CA) overnight at 4°C into 2 L of Dulbecco's modified PBS. The dialysate was aliquoted and frozen with 33% glycerol at -80˚C.

To determine the concentration of each enzyme, the absorbance was measured at 280 nm in a quartz cuvette. Molar absorption coefficients for His-Pfs-Tyr and His-LuxS-Tyr were approximately calculated from a weighted sum of the number of tyrosine, tryptophan, and cysteine amino acid residues present in each enzyme, and were found to be 0.708 mL mg^{-1} cm^{-1} and 1.00 mL mg^{-1} cm^{-1} for His-Pfs-Tyr and His-LuxS-Tyr, respectively. The concentration of enzyme in mg/mL was taken to be the absorbance at 280 nm divided by the extinction coefficient in mL mg^{-1} cm^{-1}.

5.4. *In vitro* synthesis of AI-2 and SRH

Using the calculated enzyme concentrations, His-Pfs-Tyr and His-LuxS-Tyr (for AI-2), or only His-Pfs-Tyr (for SRH) were added to tubes to bring the final concentration to

100 µg/mL of each in 0.5 mL final volume. Enough PBS was added to bring the volume to 0.5 mL. The enzyme reaction was started with the addition of 0.5 mL of 1 mM S-adenosyl-L-homocysteine in 50 mM Tris buffer at pH 7.8. Tubes were shaken at 37˚C, 250 rpm for 4 hours. The reaction was terminated by the addition of 0.75 mL of chloroform. After vortexing, tubes were centrifuged at 5000 g for 5 minutes. Approximately 0.75 mL of the top water layer in each tube was pipetted into a new tube, and 0.22 µm filter-sterilized. Solutions were used in the biofilm formation assay immediately after synthesis, without freezing. Samples were stored at -20˚C for later analysis to verify activity with the autoinducer-2 activity assay, and conversion by HPLC.

5.5. High performance liquid chromatography

To verify conversion of SAH to SRH and ultimately to DPD, all *in vitro* AI-2 and SRH samples were analyzed by normal phase HPLC on a silica column (Waters Spherisorb, 5 µm particle size, 15 cm x 3.2 mm) with either 0.5 mL/min or 1.0 mL/min of 30% water and 70% acetonitrile. The injected loop volume was 5 µL. A UV detector at the column outlet recorded intensity at 210 nm (at which only SAH and adenine are UV-active) and 260 nm (at which SAH, SRH, and adenine are UV-active). Samples containing only SAH, adenine, or SRH and adenine were included in each run due to drifts in retention time with this method.

5.6. Autoinducer-2 activity assay

V. harveyi BB170 (a reporter strain for AI-2 that lacks the AI-1 sensor) was inoculated with one loop from a cryogenic tube into 2 mL of AB medium and shaken overnight in an air shaker at 30˚C, 250 rpm in dark conditions. The next day, the culture was diluted 5000:1 in AB medium. To each 20 µL sample volume, 180 µL of diluted BB170 culture

was added. AB medium was used as a negative control, and for appropriate experiments, *in vitro* synthesized AI-2 was used as a positive control. In experiments where cell-free supernatants were samples, negative controls also included autoclaved medium or nutrient-depleted medium. Samples inoculated with BB170 were shaken at 250 rpm in an air shaker, and luminescence measurements were taken every half hour to hour in a luminometer (EG&G Berthold Junior). Nutrient-depleted media were prepared by growing *Vibrio harveyi* MM30 in AB medium overnight at 30˚C with agitation (250 rpm). The culture was aliquoted into 1.5 mL centrifuge tubes and centrifuged for 10 minutes at 4500 g. The supernatant from each tube was decanted, and cells were resuspended in the cell free supernatant plus the addition of a 1:3 ratio by volume of medium containing 50 g/L NaCl, 24 g/L $MgSO_4$, 40 mM potassium phosphate, and 10 mL per L of 0.4 M L-arginine. This addition of this media supplement served to mimic salt concentrations and L-arginine content in AB medium. Cells were incubated at 30˚C for 16 h with agitation (250 rpm). *V. harveyi* MM30 (*luxS* deletion mutant of BB120) was removed by centrifuging for 10 minutes at 13800 g, followed by 0.22 µm filter-sterilizing of the supernatant. Samples were frozen at -20˚C until thawing for analysis as described above.

5.7. Biofilm formation assay

Culture tubes containing 3 mL of the appropriate medium were inoculated with one loop from cryogenic tubes, and grown overnight at the appropriate temperature in an air shaker at 250 rpm. The next day, the OD of the overnight culture was taken and the number obtained was used to dilute to an OD of 0.05. The OD 0.05 cultures were aliquoted into 5 mL culture tubes, to which *in vitro* AI-2 or different concentrations of

inhibitors were added. In experiments involving the addition of *in vitro* AI-2, the amount of buffer added (1:1 PBS/50 mM Tris) was the same for all tubes (except where noted). Negative controls for these experiments were the addition of buffer alone, and the addition of adenine and DL-homocysteine to a final concentration of 50 µM adenine and 100 µM DL-homocysteine (only L-homocysteine is present in *in vitro* AI-2 samples). In experiments involving the addition of quorum sensing inhibitors, equivalent amounts of PBS or 95% ethanol were added to all tubes, and negative controls contained only PBS or 95% ethanol. The contents of each tube was aliquoted into wells in non-treated polystyrene 96 well plates (Corning Costar 3370), with 300 µL added to each well (only 200 µL was used for *Pseudomonas fluorescens*). Plates were incubated without shaking at specified temperatures for specified times. Prior to analyzing the plates for biofilm, the optical density of non-disturbed wells was taken as a measure of bulk growth. The plates were then rinsed in a gentle stream of deionized water three times and blotted on paper towels. Each well was stained by the addition of 300 µL of 0.1% (w/v) crystal violet solution. After 20 minutes, plates were rinsed three times in a gentle stream of deionized water and blotted dry. Biofilm-associated crystal violet was solubilized with 95% ethanol, or 80% ethanol/20% acetone for *Bacillus cereus*. The OD_{595} of each well was measured using a plate reader (Dynex MRX, Chantilly, VA).

5.8. Statistics

Sample standard deviations were calculated for all sets of replicate data about the mean value. When one set of data with an average value of x and a standard deviation Δx was normalized with another set of data with an average value of y and a standard

deviation of Δy, the following formulas were used to propagate the normalized standard deviation, Δz.

$$z + \Delta z = \frac{(x + \Delta x)}{(y + \Delta y)}$$

$$\Delta z = z\sqrt{\left(\frac{\Delta x}{x}\right)^2 + \left(\frac{\Delta y}{y}\right)^2}$$

Chapter 6: Results and Discussion

6.1. Optimization of conditions for biofilm formation

Because the ultimate goal of this work was to identify quorum sensing inhibitors that reduce biofilm formation, an initial screening was performed to quantify the effect of the addition of *in vitro* synthesized AI-2 on biofilm formation in all bacterial species and strains investigated in this study. However, in order to obtain meaningful results from the 96-well biofilm assay, growth conditions first needed to be established that promoted biofilm growth significant enough to detect colorimetric differences from crystal violet staining. Due to previous experiments performed in our laboratory, it was known that LB medium was suitable for biofilm growth in *Escherichia coli*. Additionally, it has been previously reported that LB medium supplemented with 0.2% glucose resulted in the most biofilm formation in *E. coli* JM109[76]. However, little to no information existed on optimal conditions for biofilm formation in *Listeria innocua* and *Bacillus cereus*. A series of dilutions of different rich media, supplementation with glucose and yeast extract, and different temperatures were tested (Figures 9 and 10). For *Listeria innocua*, it was found that biofilm formation was greatest when grown at 23°C in BHI medium supplemented with 0.2% glucose. For *Bacillus cereus*, it was clear that nutrient depletion was favorable for biofilm formation, with two-fold diluted LB medium resulting in the most biofilm formation. Therefore for all subsequent biofilm formation assays of *L. innocua* and *B. cereus* were conducted with BHI supplemented with 0.2% glucose at room temperature, and two-fold diluted LB medium at 30-32°C, respectively. Additionally, because the effect of glucose was of interest, BHI medium without added

glucose and two-fold diluted LB medium supplemented with 0.2% glucose were also tested for *L. innocua* and *B. cereus*, respectively.

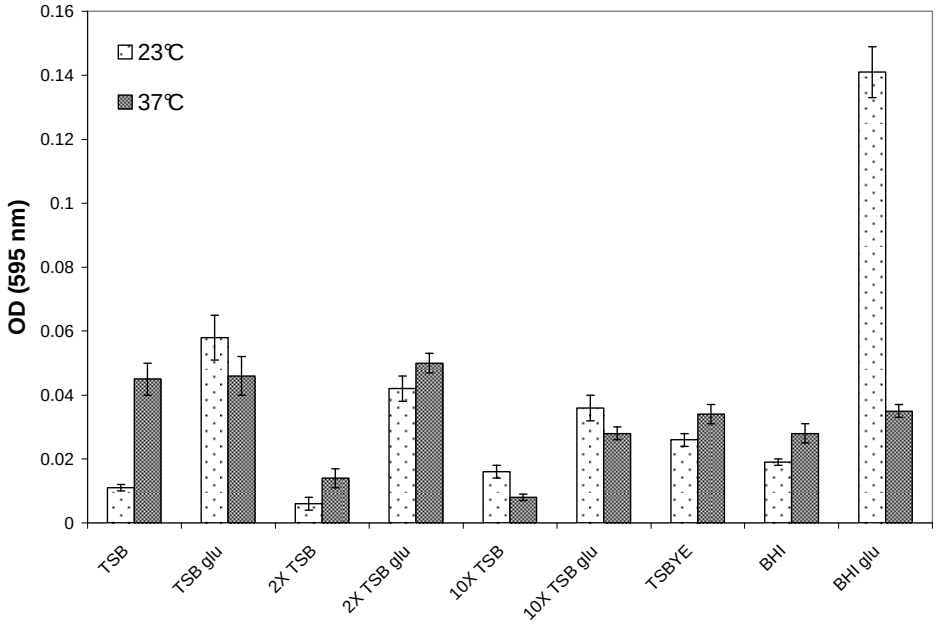

Figure 9: *Listeria innocua* biofilm formation after 48 h growth at 23°C and 37°C (TSB, tryptic soy broth; TSBYE, TSB supp. with 0.6% yeast extract; BHI, brain heart infusion medium; 2X, two-fold diluted; 10X, ten-fold diluted; glu, supplemented with 0.2% glucose). Error bars represent standard deviations about the mean of five to six replicate wells.

6.2. *In vitro* synthesis of AI-2

In vitro synthesis of all AI-2 used in biofilm formation assays was performed on the day that plates were inoculated. All batches of AI-2 used for biofilm formation assays were characterized by HPLC to determine the conversions of SAH to SRH and adenine. Although SRH is detectable by HPLC at 260 nm, the peak area varies considerably due to its small size and baseline interference, making quantitation of SRH conversion difficult. Examples of HPLC chromatograms obtained are shown in Figure 11. Additionally, each batch was tested for its ability to induce bioluminescence in *Vibrio harveyi* BB170. Table 3 lists the fold induction of bioluminescence, defined as the relative light units (RLU) of the sample divided by the RLU of the negative control without added AI-2, and

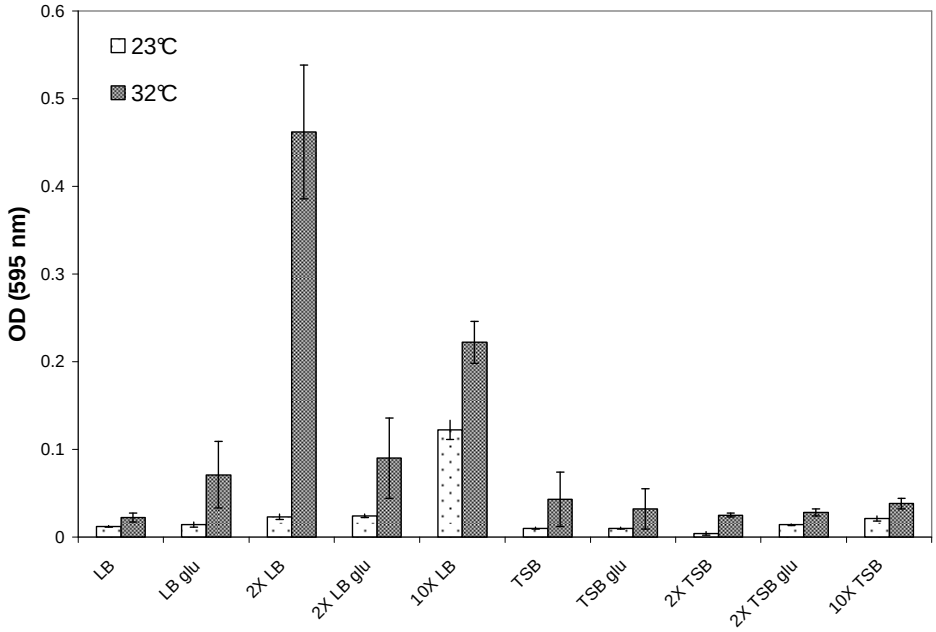

Figure 10: *Bacillus cereus* biofilm formation after 48 h growth at 23°C and 32°C (LB, Luria-Bertani medium; TSB, tryptic soy broth; 2X, two-fold diluted; 10X, ten-fold diluted; glu, supplemented with 0.2% glucose). Error bars represent standard deviations about the mean of five to six replicate wells.

the conversions of SAH and SRH based on the respective peak areas. All biofilm formation assay results involving the addition of AI-2 are annotated with a letter representing the sample used from Table 3. Although there was insufficient quantity of sample 'C' for analysis, it was synthesized identically to other samples in Table 3.

Table 3: Characterization of *in vitro* synthesized AI-2 samples used in biofilm formation assays. Fold induction of *V. harveyi* bioluminescence are the relative light units (RLU) of the sample divided by the RLU of the negative control at the time of their maximum difference (5 h). Percent conversion of SAH was determined by HPLC from the adenine peak area.

AI-2 Sample	Fold induction of *V. harveyi* bioluminescence	Percent conversion SAH to SRH
A	1266	100%
B	4216	100%
C	Not analyzed	Not analyzed
D	1152	100%
E	706	100%
F	17012	82%
G	12279	80%
H	2971	100%
I	7622	75%

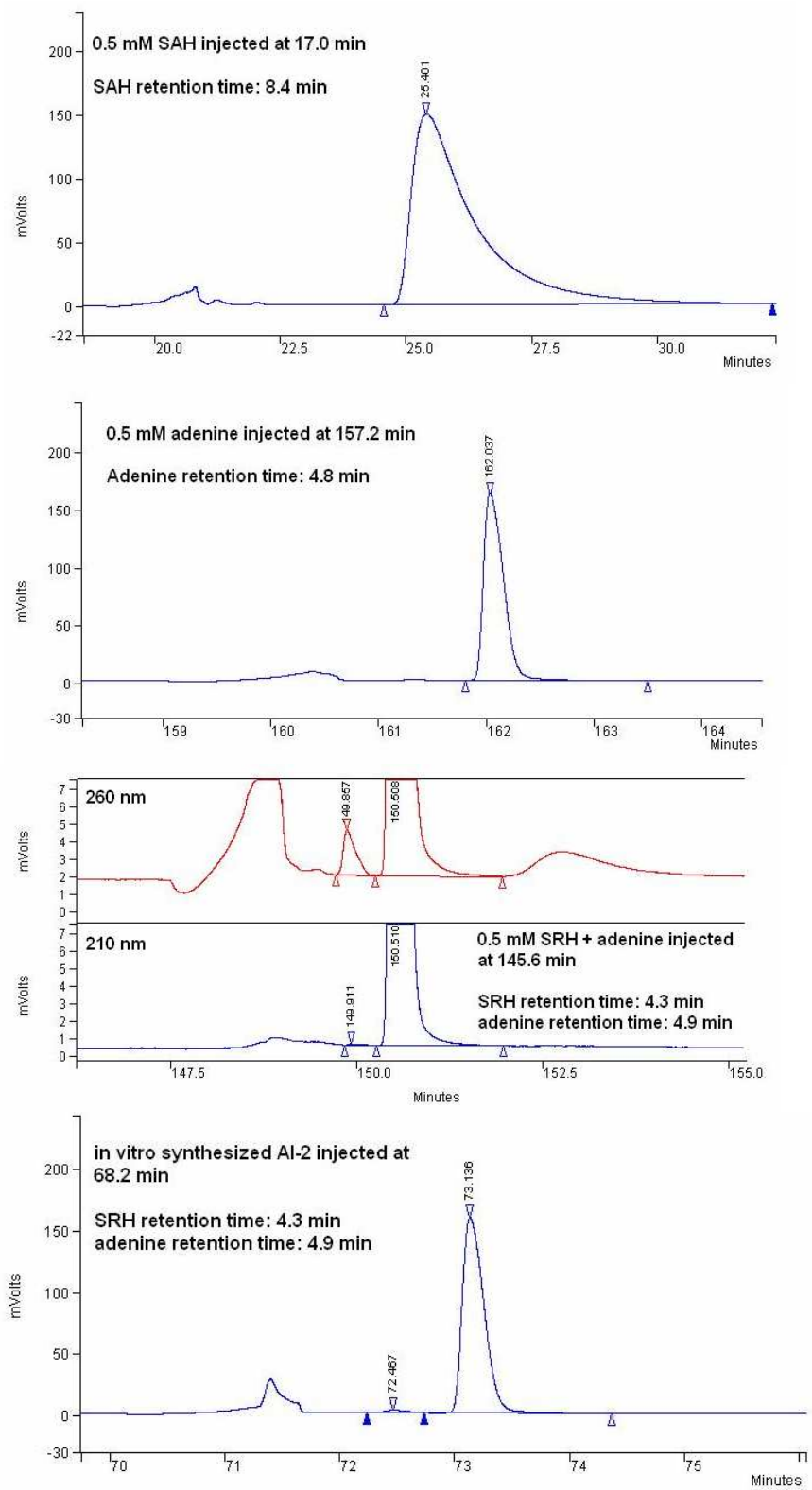

Figure 11: HPLC chromatograms of 0.5 mM SAH at 260 nm (top); 0.5 mM adenine at 260 nm (second from top); 0.5 mM *in vitro* synthesized SRH at 210 nm and 260 nm, which contains adenine as a reaction product (third from top); and 0.5 mM of *in vitro* synthesized AI-2 at 260 nm, which also contains adenine and homocysteine as reaction products (bottom).

6.3. Effect of *in vitro* synthesized AI-2 on biofilm formation

In order to understand the results obtained from screening AI-2 quorum sensing inhibitors, it is useful to characterize how AI-2 affects biofilm formation under the selected sets of growth conditions.

The effect of *in vitro* AI-2 on biofilm formation in *E. coli* was tested to verify that the 96 well format of the biofilm assay produced similar results to those obtained previously in this group using culture tubes (unpublished data). Results of independent experiments are shown for W3110, DH5α, and K-12 in Figure 12, and for W3110 and DH5α in Figure 13 (with improved controls and glucose supplementation). An AI-2 concentration-dependent increase in biofilm is observed for *E. coli* W3110 and *E. coli* K-12. For *E. coli* W3110 grown in LB medium, AI-2 stimulates a 1.8-fold increase in biofilm over the negative control containing a similar concentration of adenine and homocysteine, and a 2.4-fold increase in biofilm over the control when grown in LB medium supplemented with 0.2% glucose. Similarly, for *E. coli* DH5α, a 1.6-fold increase in biofilm is observed in LB medium, and a 2.3-fold increase in LB medium supplemented with 0.2% glucose. Glucose increases AI-2 production in *E. coli* through indirect stimulation of *luxS* expression[95]. Meanwhile, cAMP-CRP represses transcription of the *lsr* operon in the presence of glucose, delaying import of AI-2 until glucose is depleted upon reaching the stationary phase. This may account for the magnified effect of glucose on biofilm formation with the addition of AI-2 that is observed in W3110, as the level of extracellular AI-2 is expected to be heightened. In DH5α, which lacks *luxS*, additional glucose reduces biofilm formation relative to LB medium alone. This is possibly due solely to delayed importation of AI-2 from not reaching the stationary phase (the optical

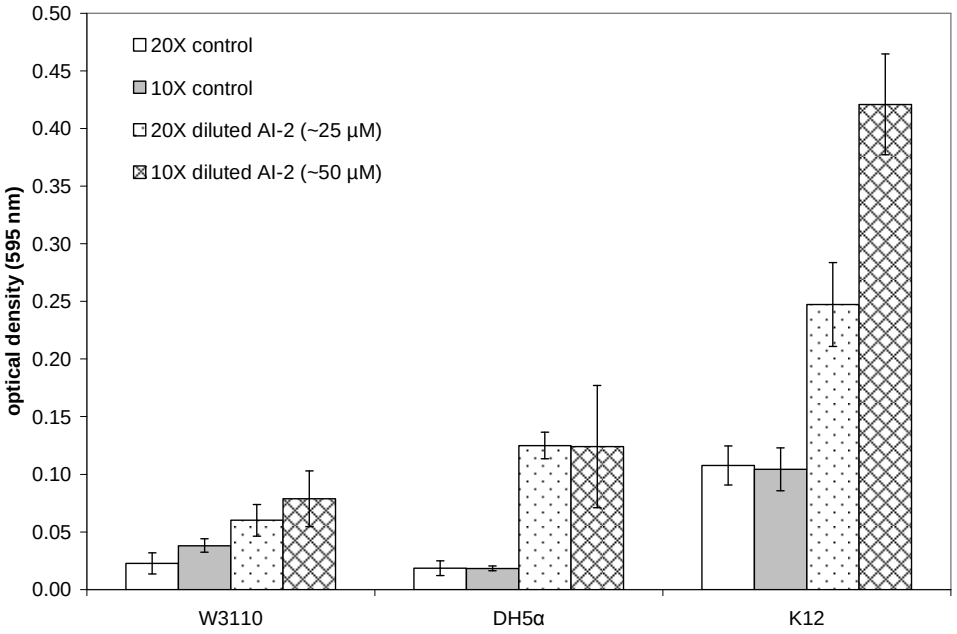

Figure 12: Effect of AI-2 on biofilm formation of *E. coli* strains W3110, DH5α, and K-12 after 48 h growth in LB medium in 96 well plates at 37°C. Control wells contained the same quantity of buffer as wells containing AI-2, but did not contain adenine or homocysteine. AI-2 was sample "A" in Table 3. Error bars represent standard deviations about the mean of six replicate wells.

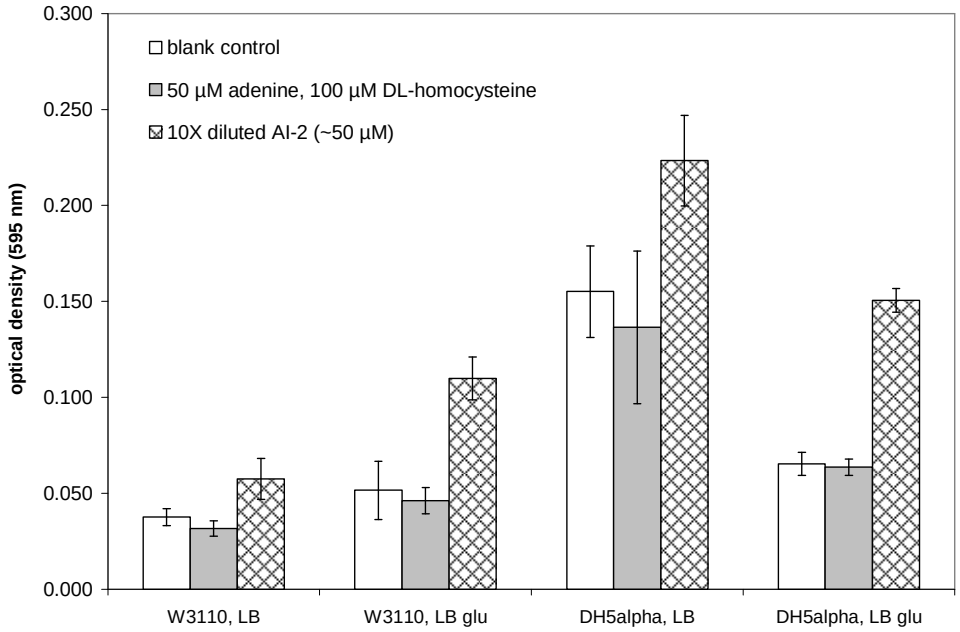

Figure 13: Effect of AI-2 on biofilm formation of *E. coli* strains W3110 and DH5α after 50 h of growth at 37°C in LB medium and LB supplemented with 0.2% glucose. AI-2 was sample "B" in Table 3. Error bars represent standard deviations about the mean of six replicate wells (four for blank control and 10X diluted AI-2 columns of DH5α grown in LB medium).

density of DH5α in LB medium with 0.2% glucose is only 0.7, compared to 1.4 in LB medium). AI-2 had no effect on the optical density of non-disturbed wells, relative to the negative controls (data not shown). AI-2 is known to stimulate biofilm formation in *E. coli* by increasing motility through MotA, a proton conductor for flagellum motion, and MqsR, an uncharacterized protein that stimulates the two-component motility regulatory system QseBC.[81]

The effect of AI-2 on biofilm formation in *Bacillus cereus* is shown in Figure 14. After 23.5 h growth, a drastic reduction (four-fold to seven-fold) in biofilm is seen in two-fold diluted LB medium with added AI-2, and after 45.5 h growth, a similar reduction is seen in two-fold diluted LB medium supplemented with 0.2% glucose (three-fold to seven-fold). However, the negative control containing 50 µM adenine and 100 µM DL-homocysteine reproduces this effect. Auger et al. performed a similar experiment, testing various lower concentrations of AI-2 and their effect on biofilm formation in *B. cereus* grown in LB medium[52]. A concentration-dependent inhibition of biofilm formation was observed. They state that SAH, adenine, and homocysteine did not affect biofilm formation in their experiment up to concentrations of 10 µM, although whether they used L-homocysteine or DL-homocysteine is not stated. L-homocysteine is not readily available commercially, although it can be prepared from L-homocysteine thiolactone by treatment with concentrated NaOH, followed by neutralization with KH_2PO_4 is available[137]. Unfortunately this procedure generates a solution of L-homocysteine with enormous concentrations of sodium and potassium ions, and homocysteine tends to dimerize and precipitate out of solution in the absence of a reducing agent. Thus it was not possible to prepare L-homocysteine for the purpose of

this work. To further investigate whether adenine or DL-homocysteine was responsible for the decrease in biofilm, each was tested at different concentrations in separate biofilm assays (data not shown). DL-homocysteine appeared to reduce biofilm formation at high concentrations, while adenine had no effect. Interestingly, it has been shown that in *B. cereus*, the genes encoding YrhA (an O-acetylserine thiol lyase) and YrhB (a cystathionine γ-synthase) form an operon with *luxS*[138], implicating the possibility of co-regulation. YrhA and YrhB are required for methionine to cysteine conversion through homocysteine as an intermediate[139]. High concentrations of homocysteine, present either alone or in the *in vitro* synthesized AI-2, may be repressing *luxS*. Additionally, *B. cereus* possesses an Lsr-like system[52], so it is possible that glucose represses *lsr* transcription, thereby delaying importation of AI-2 until glucose is depleted. As shown in Figure 14, biofilm growth in glucose-supplemented medium is very low after 23.5 hours but is markedly increased after 45.5 hours. AI-2 also appears to induce a slight growth inhibitory effect in *B. cereus*, independent from addition of adenine and homocysteine, as shown in Figure 15.

The effect of AI-2 on biofilm formation in *Listeria innocua* is shown in Figure 16. It was discovered late in this work that *L. innocua* unexpectedly always forms more biofilm in the fifth column of wells from the edge of the microplate in BHI medium. Therefore all biofilm assay data for *L. innocua* was normalized column-wise against averaged optical densities from a control biofilm assay where *L. innocua* was grown in BHI and BHI supplemented with 0.2% glucose. No statistically significant effect of AI-2 on biofilm formation in *L. innocua* is observed. Although no reports exist in the literature on the effect of AI-2 on *Listeria innocua* biofilm formation, two studies have been

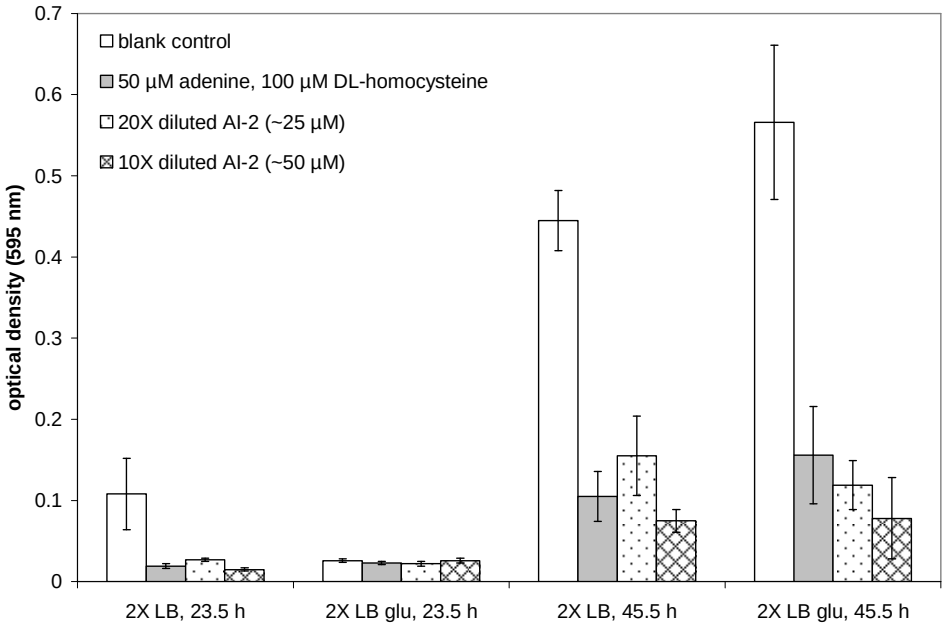

Figure 14: Effect of AI-2 on biofilm formation of *Bacillus cereus* after 23.5 h and 45.5 h of growth at 32°C in two-fold diluted LB medium (2X LB) and 2X LB supplemented with 0.2% glucose (2X LB glu). AI-2 was sample "C" in Table 3. Error bars represent standard deviations about the mean of six replicate wells.

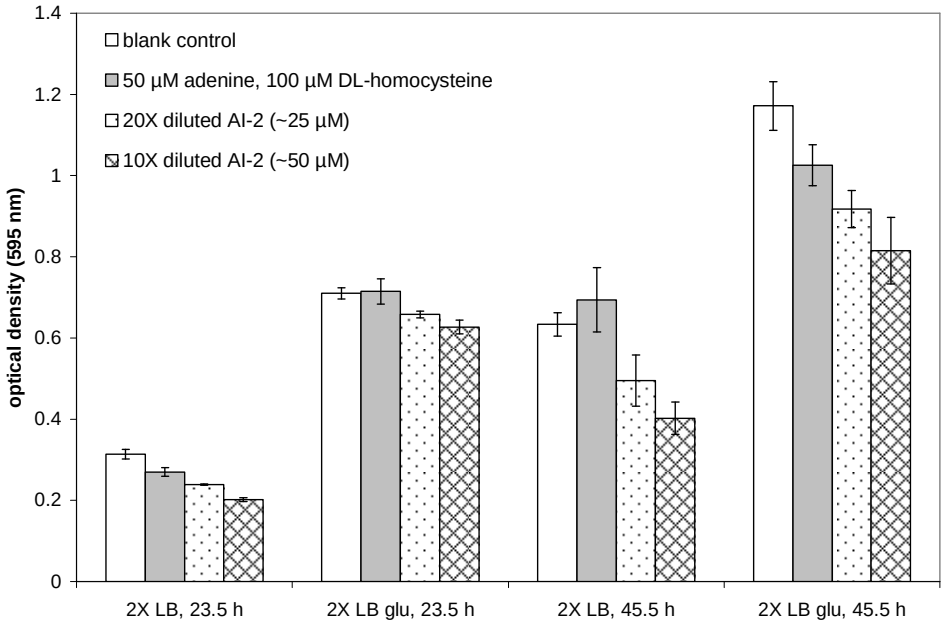

Figure 15: Effect of AI-2 on bulk growth of *Bacillus cereus* after 23.5 h and 45.5 h of growth at 32°C in two-fold diluted LB medium (2X LB) and 2X LB supplemented with 0.2% glucose (2X LB glu). AI-2 was sample "C" in Table 3. Error bars represent standard deviations about the mean of six replicate wells.

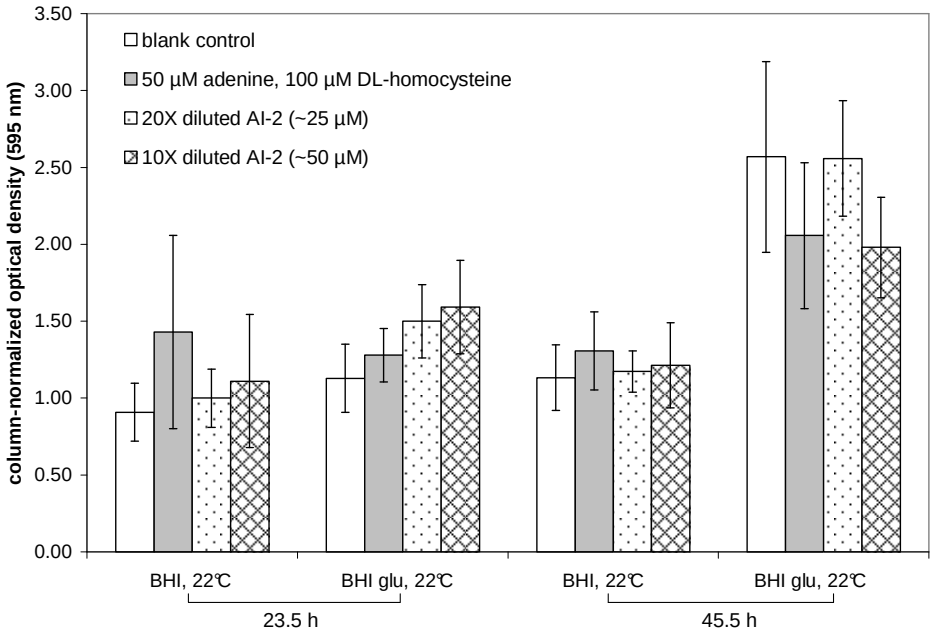

Figure 16: Effect of AI-2 on biofilm formation of *Listeria innocua* after 23.5 h and 45.5 h growth at 22°C in BHI medium and BHI medium supplemented with 0.2% glucose. Optical densities are normalized as described in the text. AI-2 was sample "C" in Table 3. Error bars represent propagated standard deviations about the mean of six replicate wells.

conducted on *Listeria monocytogenes*, a closely related species. Belval et al. found that the addition of AI-2 to 42 h old biofilms of *L. monocytogenes* EGD-e and a *luxS* mutant strain grown in TSB had a statistically insignificant effect, however they found that the addition of SRH resulted in a statistically significant increase in biofilm.[8] Their *luxS* mutant strain formed denser biofilms containing more than 10 times as many attached cells as EGD-e, but only after 48 h growth. Similar results were also reported by Sela et al.[9]. A *luxS* mutant would be expected to experience an intercellular and/or extracellular accumulation of SRH. To examine whether *Listeria innocua* would exhibit a similar increase in biofilm on addition of SRH, *in vitro* synthesized SRH was added in the same manner as *in vitro* AI-2 (Figure 17). The *in vitro* SRH induced an eleven-fold increase in bioluminescence in *Vibrio harveyi* BB170 over the control, and conversion was

determined by HPLC to be 82.5%. No statistically significant effect of SRH addition was observed on biofilm formation.

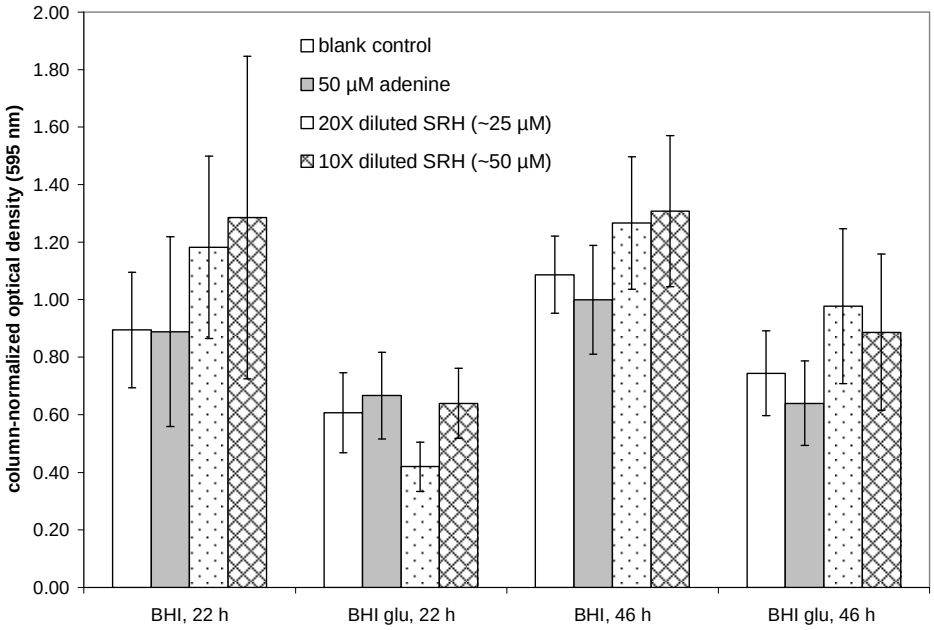

Figure 17: Effect of SRH on biofilm formation of *Listeria innocua* after 22 h and 46 h growth at 22°C in BHI medium and BHI medium supplemented with 0.2% glucose. Optical densities are normalized as described in the text. Error bars represent propagated standard deviations about the mean of six replicate wells.

6.4. Effect of LuxS inhibitors on biofilm formation

6.4.1. S-anhydroribosyl-L-homocysteine (SARH)

SARH, a relatively weak inhibitor of LuxS obtained from Alfaro et al., was screened against *E. coli*, *B. cereus*, and *L. innocua* at concentrations ranging from 50 µM to 2 mM. This compound, when added at a concentration of 2 mM to 0.34 µM of LuxS *in vitro*, reduced the concentration of homocysteine formed by 60-70% over a period of a few minutes[121]. Figures 18, 19, 20, and 21 show the effect of SARH on biofilm formation in *E. coli*. DH5α, *E. coli* K-12, *B. cereus*, and *L. innocua*, respectively. No effect on growth was observed at any concentration of SARH, as measured by the optical density of

undisturbed cells in the 96 well plates prior to analyzing for biofilm. As expected, SARH has no statistically significant effect at any concentration on *E. coli* DH5α, which is a *luxS* deficient strain. In *E. coli* K-12, no clear concentration-dependent effect was observed. However, after growth in LB medium for 47 h, it appeared that low concentrations of SARH actually increased biofilm formation, followed by a reduction back to control levels at 0.5 mM and above. This trend does not appear to be solely due to 'edge effects' on the 96 well plate (which could result from spatial variations in aeration, evaporation, and forces applied to the adhering biofilm during plate processing), because the column of wells containing 0.1 mM SARH was closest to the edge, with increasing distance in columns containing 0.5 mM, 0 mM, 2 mM, and 0.05 mM.

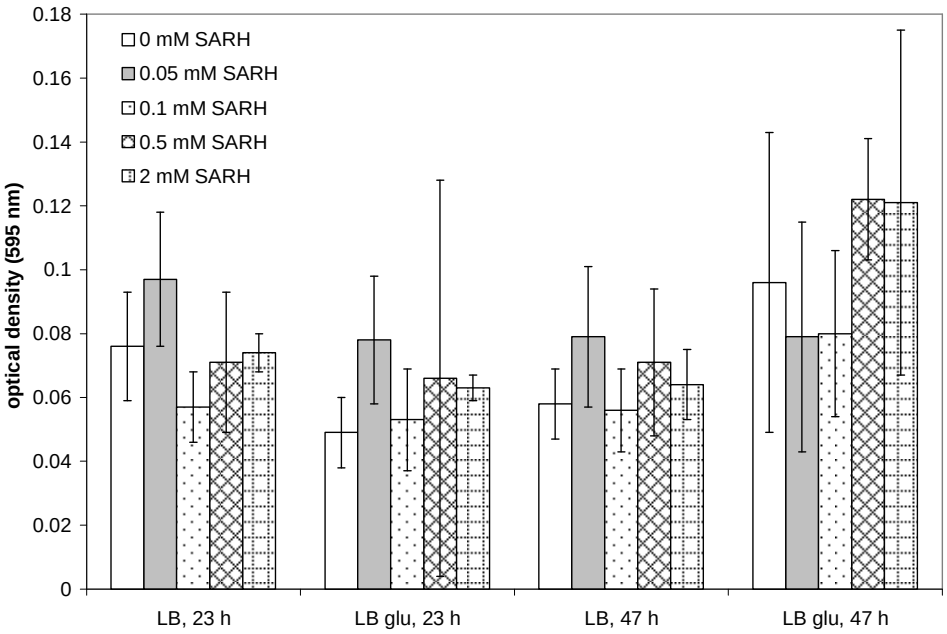

Figure 18: Effect of SARH addition to biofilm formation of *Escherichia coli* DH5α, a *luxS* deficient strain, after 23 h and 47 h growth at 37°C in LB medium and LB supplemented with 0.2% glucose. Error bars represent standard deviations about the mean of five to six replicate wells.

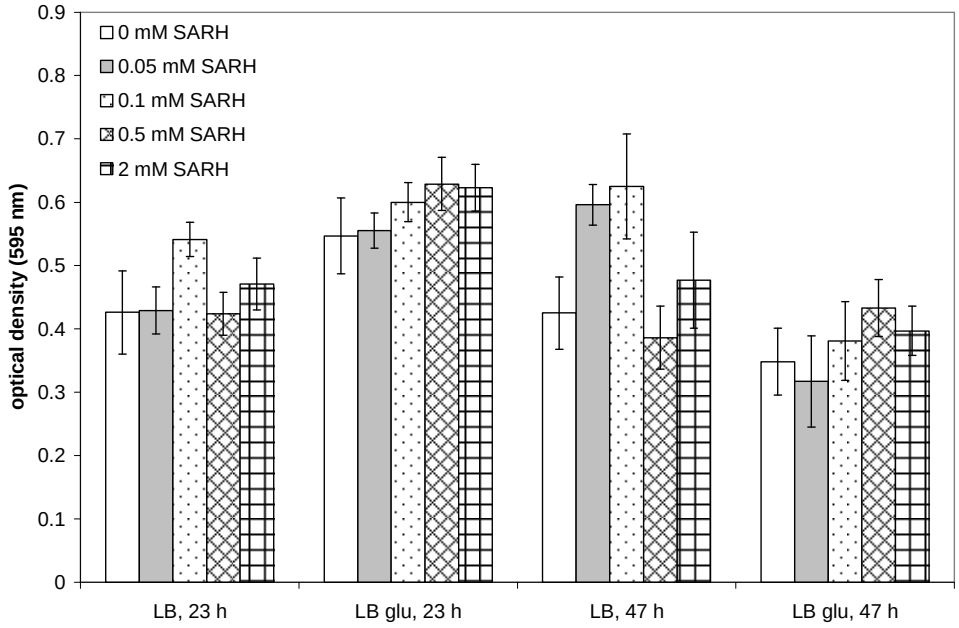

Figure 19: Effect of SARH addition on biofilm formation of *Escherichia coli* K-12 after 23 h and 47 h growth at 37°C in LB medium and LB supplemented with 0.2% glucose. Error bars represent standard deviations about the mean of six replicate wells.

SARH had no effect on biofilm formation in *Bacillus cereus* after 26 h growth, however after 50.5 h growth in 2X LB, a reduction in biofilm is seen at all concentrations of SARH. The same effect is not seen in 2X LB supplemented with 0.2% glucose. This appears to be due to 96 well plate 'edge effects,' with more biofilm often being observed in only the sixth column of wells. This was where the control wells (0 mM SARH) were located. Furthermore, the reduction of biofilm seen in 2X LB after 50.5 h was also not able to be replicated in another similar experiment conducted several months later (data not shown)

As seen in Figure 21, SARH also had no statistically significant effect on biofilm formation in *Listeria innocua*.

Because SARH is such a weak *in vitro* inhibitor, its action inside a bacterial cell is particularly difficult to predict, therefore the results obtained are not surprising.

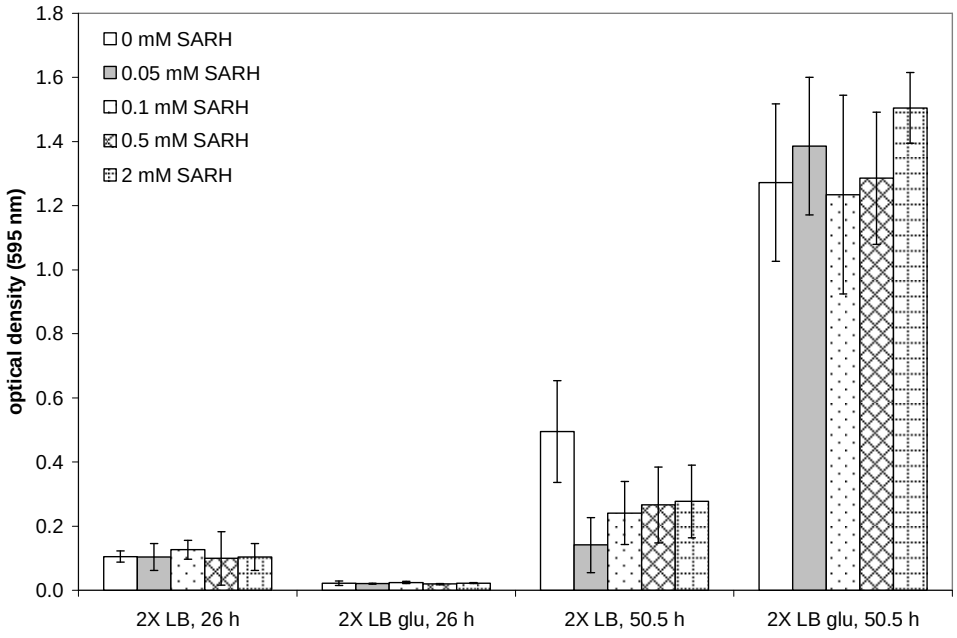

Figure 20: Effect of SARH addition on biofilm formation of *Bacillus cereus* after 26 h and 50.5 h growth at 32°C in two-fold diluted LB medium (2X LB) and 2X LB supplemented with 0.2% glucose. Error bars represent standard deviations about the mean of six replicate wells.

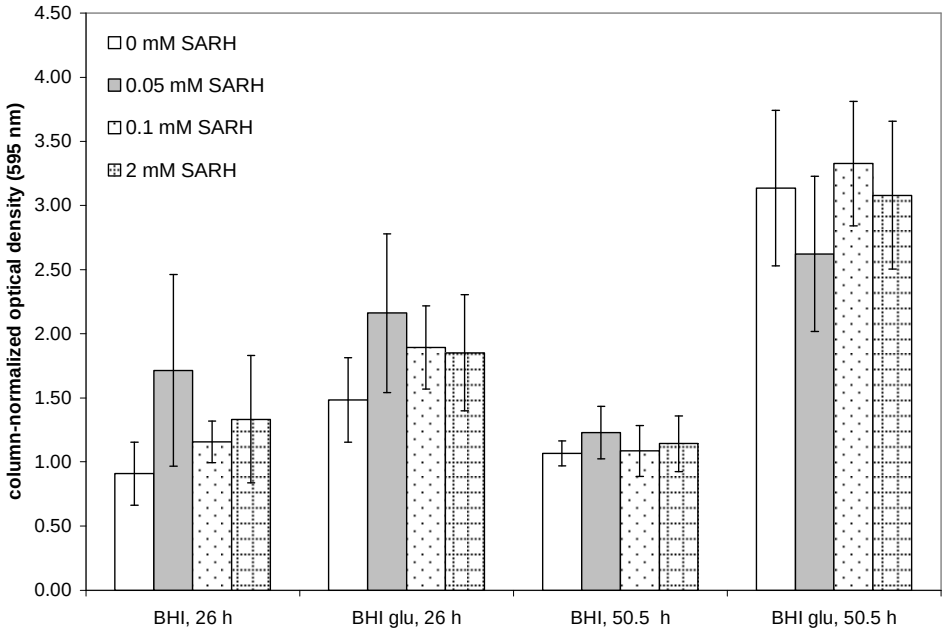

Figure 21: Effect of SARH addition on biofilm formation of *Listeria innocua* after 26 h and 50.5 h growth at 22°C in BHI medium and BHI supplemented with 0.2% glucose. Optical densities are normalized as described in the text. Error bars represent propagated standard deviations about the mean of six replicate wells.

Additionally, SARH is a medium sized and highly hydrophobic ribose moiety that may require a specific transporter protein for it to pass across the cell membrane.

6.4.2. Pei compounds 10 and 11

The LuxS inhibitors from Shen et al.[122], herein referred to as Pei **10** and **11**, are the most potent synthesized to date. These compounds were screened individually against *E. coli*, *B. cereus*, and *L. innocua* at concentrations between 2 µM to 50 µM. Figures 22, 23, 24, 25, and 26 show the effect of Pei **10** and **11** on *E. coli* W3110, *E. coli* DH5α, *E. coli* K-12, *B. cereus*, and *L. innocua*, respectively.

In *E. coli* W3110 (Figure 22), a large increase in biofilm is evident from the addition of 50 µM of Pei **10** over the negative control when grown in LB supplemented with 0.2% glucose for 23 hours. This increase may be due to increased bulk growth, with the undisturbed wells containing 50 µM Pei **10** having an averaged optical density of 1.2, whereas the wells containing 0 µM, 2 µM, and 10 µMhad optical densities of 0.96, 0.78, and 0.76, respectively. For all other sets of data in Figure 22, there were no significant variations in bulk growth (data not shown). In LB supplemented with 0.2% glucose, both Pei **10** and Pei **11**, at the highest tested concentration of 50 µM, appear to slightly decrease biofilm formation after about 48 hours growth. In *E. coli* DH5α (Figure 23), Pei **10** and **11** have no effect on biofilm formation at any tested concentration. This is expected because DH5α does not possess *luxS*. For *E. coli* K-12 (Figure 24), a small edge effect is observed in many sets of data, with the columns containing the control (0 µM), 2 µM, 5 µM, and 10 µM of either Pei**10** or **11** being located in the columns that are third, second, first, and fourth closest from the edge, respectively. The inhibitors appear to have no effect on biofilm formation at any tested concentration.

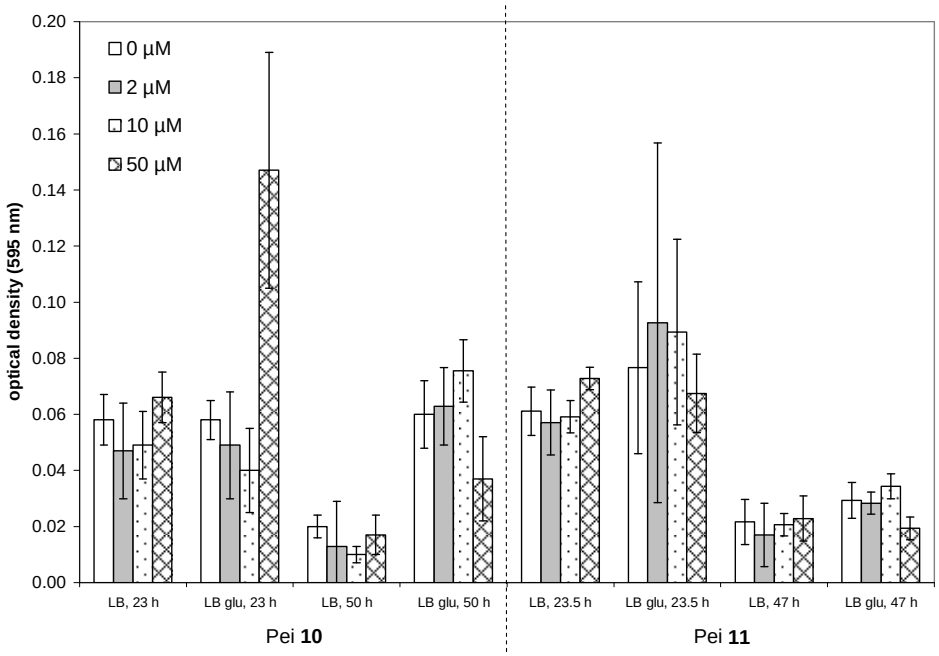

Figure 22: Effect of addition of Pei compounds **10** (left) and **11** (right) on biofilm formation of *Escherichia coli* W3110 after 23 h and 50 h growth, and 23.5 h and 47 h growth, respectively, at 37°C in LB medium and LB supplemented with 0.2% glucose. Error bars represent standard deviations about the mean of six replicate wells.

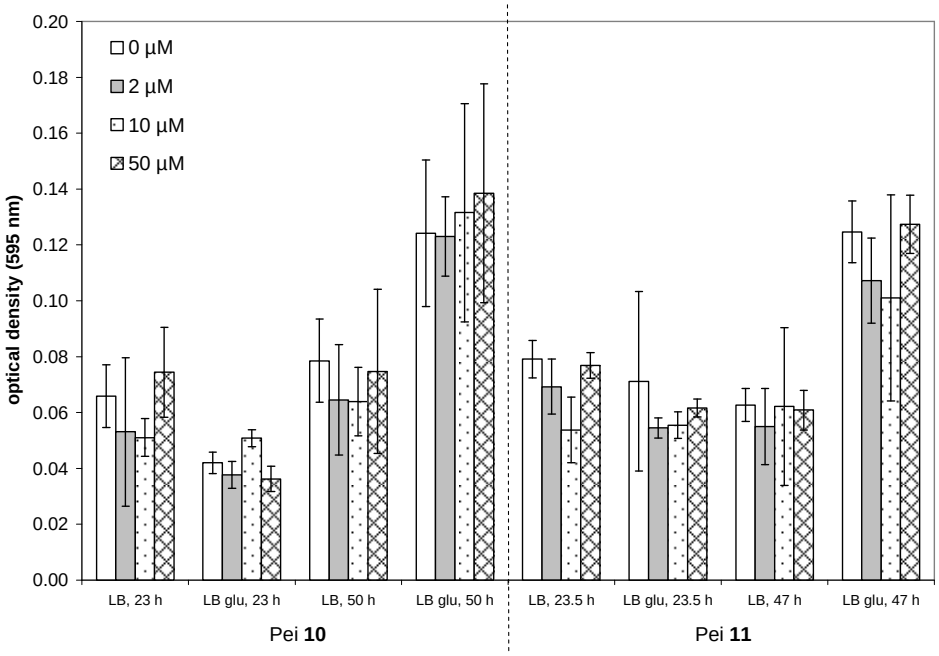

Figure 23: Effect of addition of Pei compounds **10** (left) and **11** (right) on biofilm formation of *Escherichia coli* DH5α after 23 h and 50 h growth, and 23.5 h and 47 h growth, respectively, at 37°C in LB medium and LB supplemented with 0.2% glucose. Error bars represent standard deviations about the mean of six replicate wells.

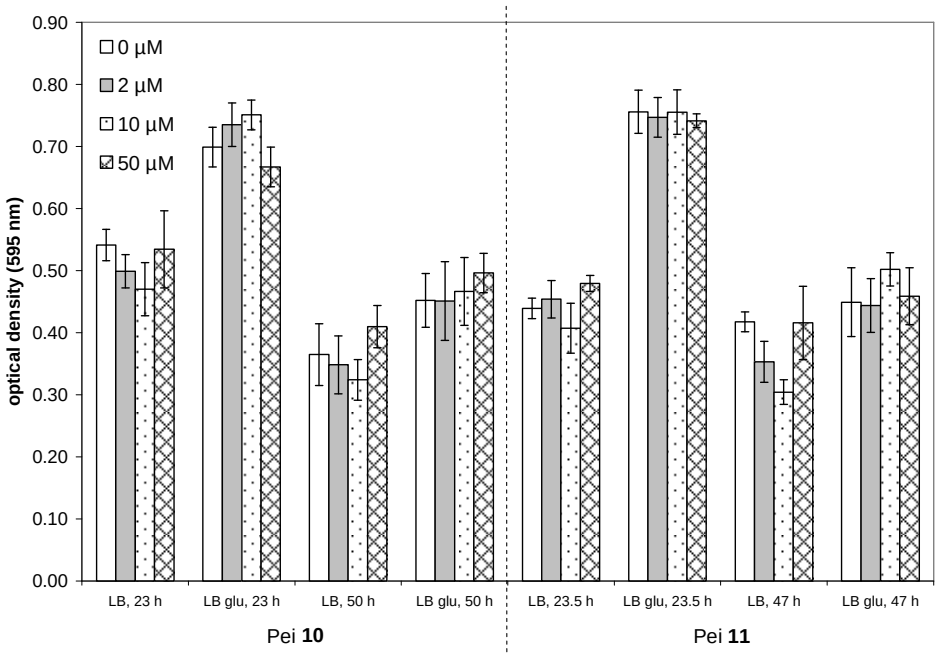

Figure 24: Effect of addition of Pei compounds **10** (left) and **11** (right) on biofilm formation of *Escherichia coli* K-12 after 23 h and 50 h growth, and 23.5 h and 47 h growth, respectively, at 37°C in LB medium and LB supplemented with 0.2% glucose. Error bars represent standard deviations about the mean of six replicate wells.

In *B. cereus* (Figure 25), the addition of Pei **10** and **11** result in statistically insignificant changes in biofilm quantity. The large variations in biofilm quantity observed amongst different added concentrations of Pei **11** in 2X LB medium supplemented with 0.2% glucose after 47 hours growth appears to be due to edge effects, with wells containing 0 µM, 2 µM, 10 µM, and 50 µMof Pei **11** located in columns third, second, first, and fourth furthest from the edge of the plate, respectively.

In *L. innocua* (Figure 26), the addition of Pei **10** and **11** also resulted in no stastically significant effect on biofilm formation. There appears to be a slight reduction at all concentrations of both Pei **10** and **11** in BHI medium supplemented with 0.2% glucose after approximately 48 hours growth, but the average optical densities are not significant due to the size of the error bars.

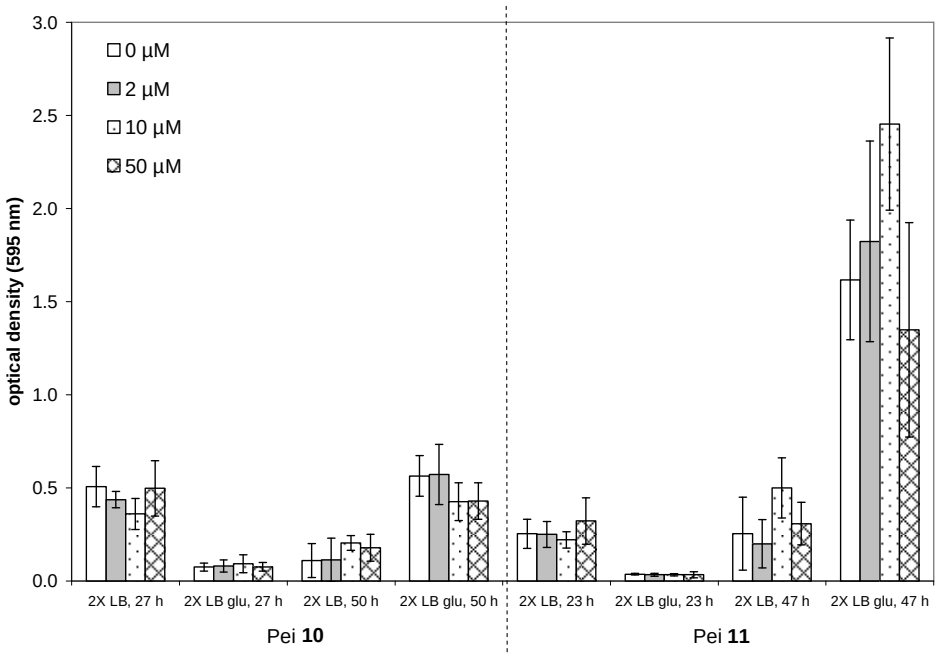

Figure 25: Effect of addition of Pei compounds **10** (left) and **11** (right) on biofilm growth of *Bacillus cereus* after 27 h and 50 h growth, and 23 h and 47 h growth, respectively, at 32˚C in two-fold diluted LB medium (2X LB) and 2X LB supplemented with 0.2% glucose. Error bars represent standard deviations about the mean of five or six replicate wells.

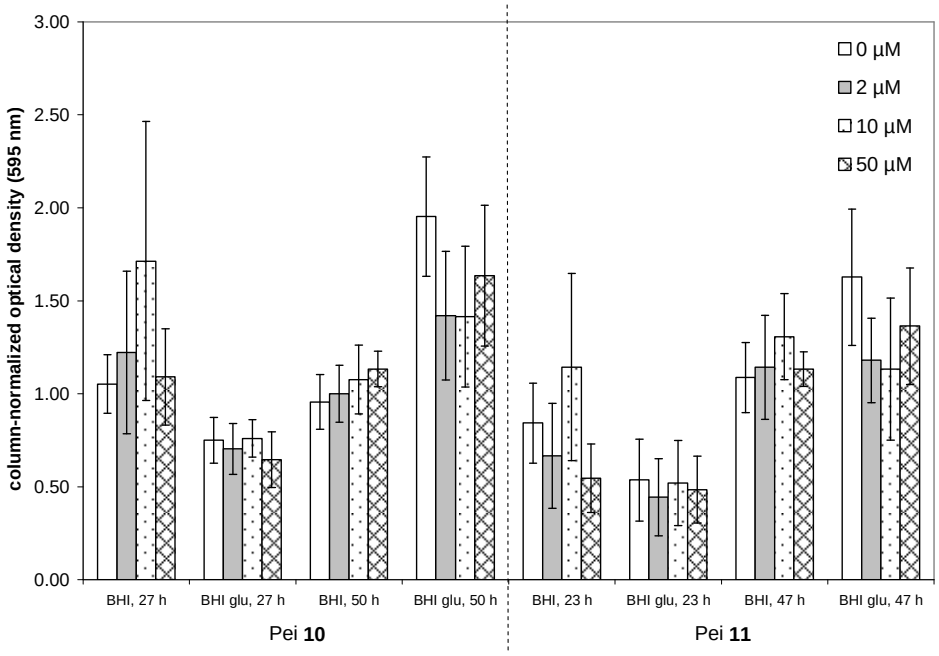

Figure 26: Effect of addition of Pei compounds **10** (left) and **11** (right) on biofilm growth of *Listeria innocua* after 27 h and 50 h growth, and 23 h and 47 h growth, respectively, at 22˚C in BHI medium and BHI supplemented with 0.2% glucose. Optical densities are normalized as described in the text. Error bars represent propagated standard deviations about the mean of six replicate wells.

6.5. Effect of brominated furanone on biofilm formation and growth

The brominated furanone, (5Z)-4-bromo-5-(bromomethylene)-3-butyl-2(5H)-furanone, was obtained from Dr. Thomas Wood as a solution in 95% ethanol. The furanone was screened against *B. cereus*, *L. innocua*, *Pseudomonas fluorescens*, and three strains of *E. coli* at concentrations ranging from 25 to 100 µg/mL. The same amount of 95% ethanol was added to all test wells in each experiment.

In *E. coli* W3110, the addition of brominated furanone was found to increase biofilm formation up to 1.5-fold in LB medium (Figure 27). Conversely, the addition of 100 µg/mL reduced biofilm formation by nearly 50% in LB medium supplemented with 0.2% glucose after 23 hours of growth. Significant decreases in bulk growth (measured by taking the optical density of the wells) due to the addition of 100 µg/mL brominated furanone were observed after 23 hours and 47 hours (Figure 28). An increase in biofilm formation was seen despite a decrease in bulk growth in LB medium after both 23 h and 47 h.

Similarly to W3110, the addition of 50-100 µg/mL of brominated furanone to *E. coli* DH5α (Figure 29) increased biofilm formation in LB medium, however the addition of only 25 µg/mL resulted in a small reduction in biofilm formation. The addition of brominated furanone only caused a significant decrease in bulk growth (32% lower optical density) in LB supplemented with glucose after 47 hours.

The effect of addition of brominated furanone on *E. coli* K-12 biofilm formation is shown in Figure 30. In LB supplemented with glucose, a concentration-dependent reduction in biofilm is observed. The addition of 100 µg/mL of brominated furanone resulted in a 55% reduction in biofilm after 23 hours growth, and a 64% reduction in

biofilm after 47 hours growth. These results are very similar to those previously reported for *E. coli* JM109, which exhibited a 51% decrease in biofilm formation on the addition of 100 µg/mL furanone, when grown in LB supplemented with 0.2% glucose[76]. Because glucose supplementation stimulates AI-2 synthesis in *E. coli* by indirectly upregulating *luxS*, the decreases in biofilm formation seen in *E. coli* W3110 and K-12 (DH5α is a *luxS* negative strain) when grown in LB medium supplemented with 0.2% glucose indicate that the brominated furanone may be attenuating AI-2 quorum sensing. The mechanism by which the brominated furanone influences DH5α is not known.

The addition of brominated furanone to *Listeria innocua* strongly quenches biofilm formation, with minimum biofilm evident with the addition of 50 µg/mL (Figure 31). At a concentration of 100 µg/mL furanone, biofilm formation in BHI medium increases over that seen with 50 µg/mL furanone, but is still decreased relative to the negative control.

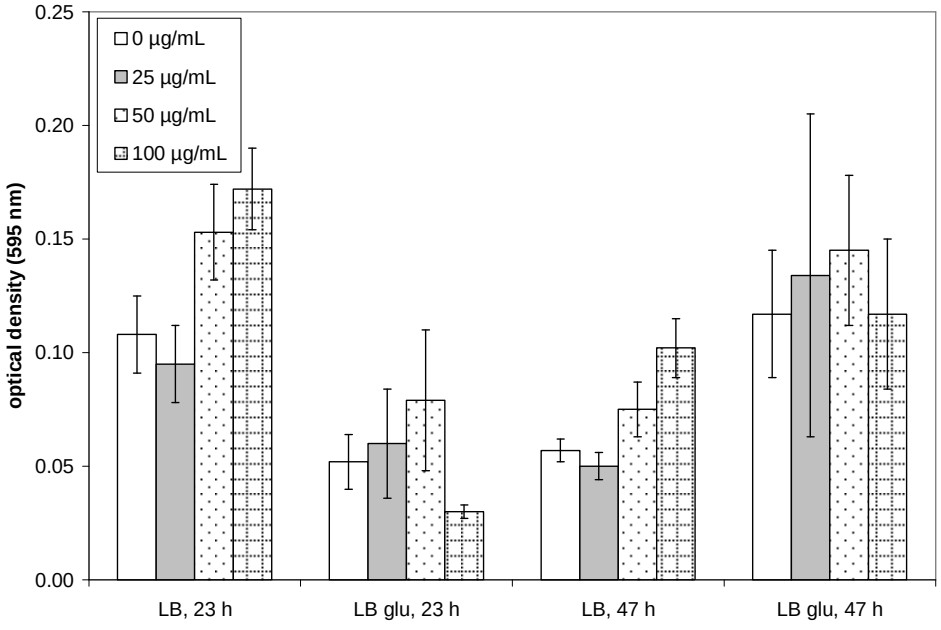

Figure 27: Effect of addition of brominated furanone on biofilm growth of *Escherichia coli* W3110 after 23 h and 47 h growth at 37˚C in LB medium and LB supplemented with 0.2% glucose. Error bars represent standard deviations about the mean of six replicate wells.

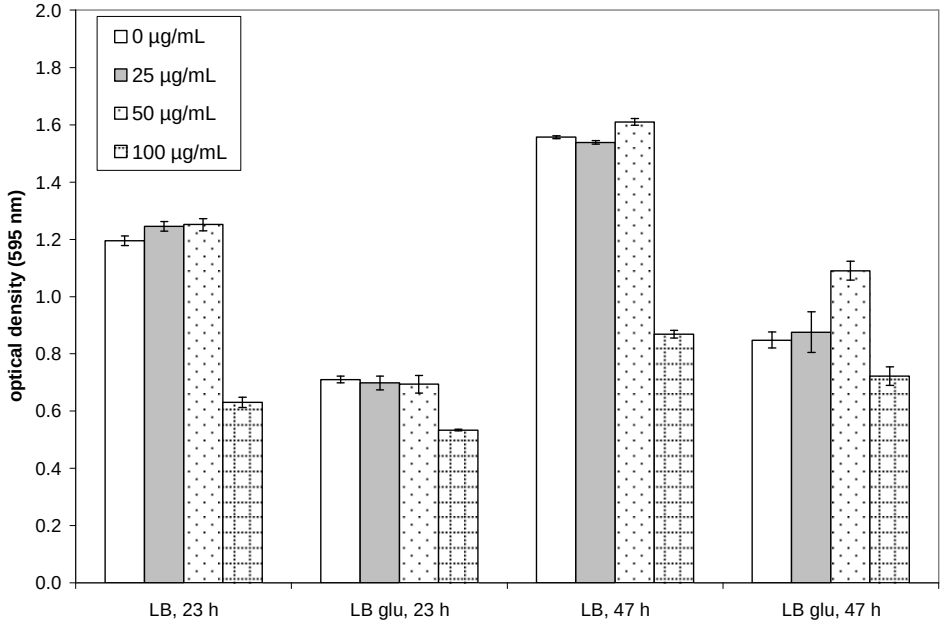

Figure 28: Effect of addition of brominated furanone on bulk growth of *Escherichia coli* W3110 after 23 h and 47 h growth at 37˚C in LB medium and LB supplemented with 0.2% glucose. These readings are optical densities of non-disturbed wells. Error bars represent standard deviations about the mean of six replicate wells.

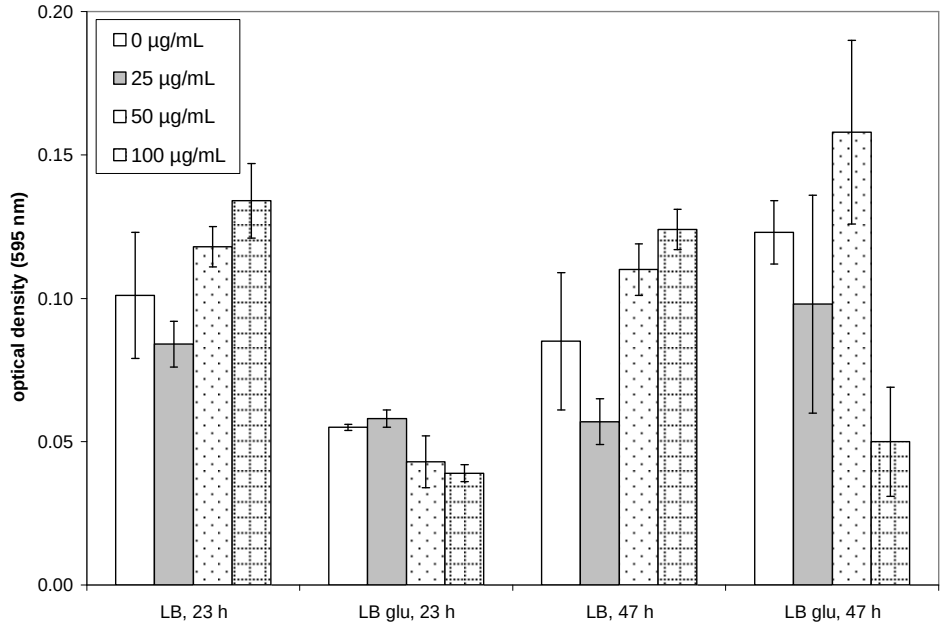

Figure 29: Effect of addition of brominated furanone on biofilm growth of *Escherichia coli* DH5α after 23 h and 47 h growth at 37˚C in LB medium and LB supplemented with 0.2% glucose. Error bars represent standard deviations about the mean of five or six replicate wells.

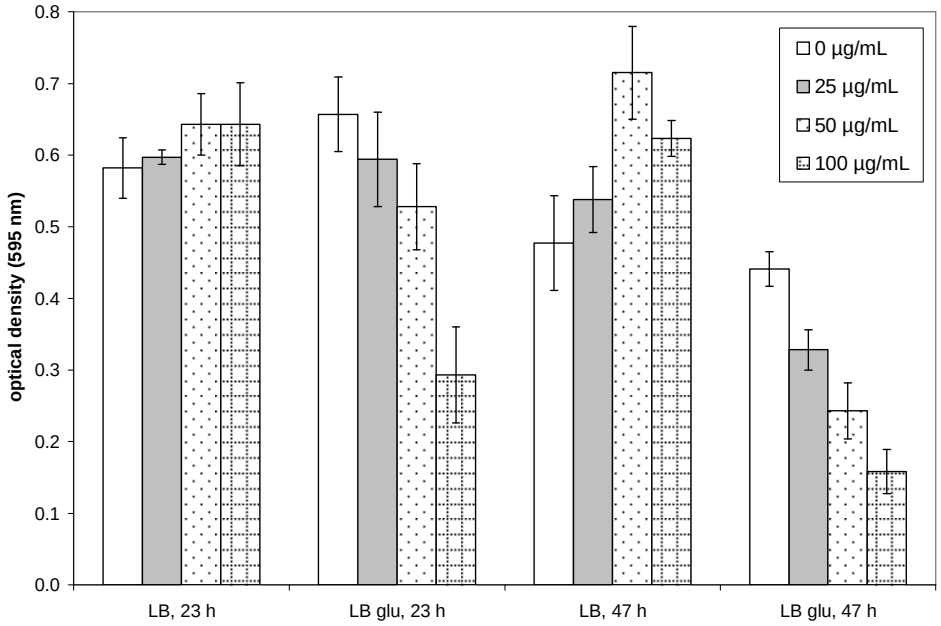

Figure 30: Effect of addition of brominated furanone on biofilm growth of *Escherichia coli* K-12 after 23 h and 47 h growth at 37˚C in LB medium and LB supplemented with 0.2% glucose. Error bars represent standard deviations about the mean of five or six replicate wells.

In BHI medium supplemented with 0.2% glucose, the addition of 100 µg/mL furanone results in less biofilm formation than the addition of 25 µg/mL furanone, with 50 µg/mL remaining the optimal tested concentration. It is immediately apparent from Figure 32 that the addition of furanone also strongly quenches bulk growth in *Listeria innocua*. To determine whether biofilm growth was reduced relative to bulk growth, the ratio of optical densities in Figure 31 to Figure 32 is plotted in Figure 33. At a concentration of 100 µg/mL furanone, although less biofilm is formed than in the control, more biofilm is formed relative to the bulk growth in medium. At a concentration of 25 µg/mL furanone, biofilm is reduced relative to bulk growth over the control. Thus the brominated furanone preferentially targets biofilm formation of *Listeria innocua* at lower concentrations. Considering that the addition of *in vitro* synthesized AI-2 did not affect

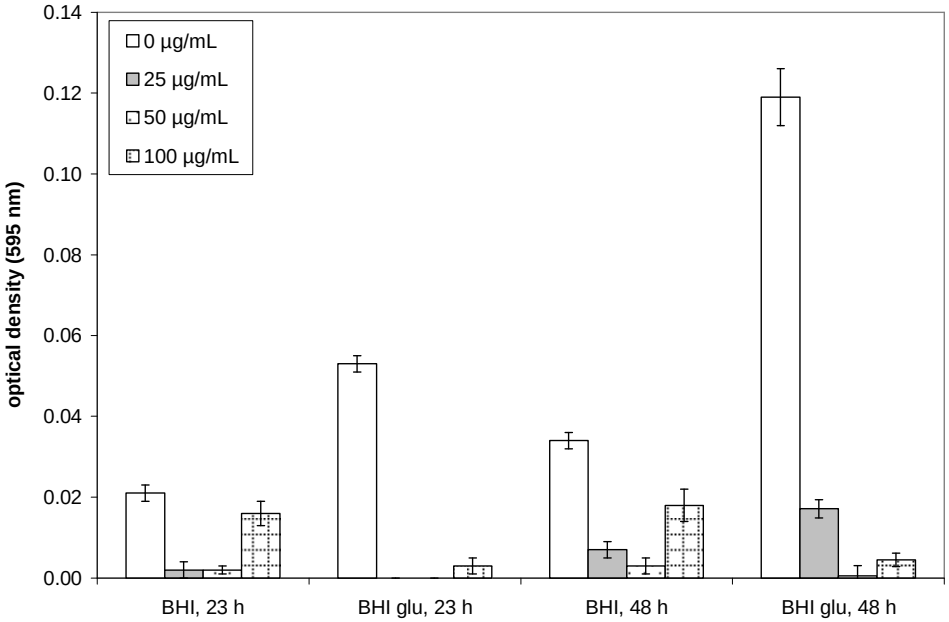

Figure 31: Effect of addition of brominated furanone on biofilm growth of *Listeria innocua* after 23 h and 48 h growth at 22˚C in BHI medium and BHI supplemented with 0.2% glucose. Error bars represent standard deviations about the mean of six replicate wells.

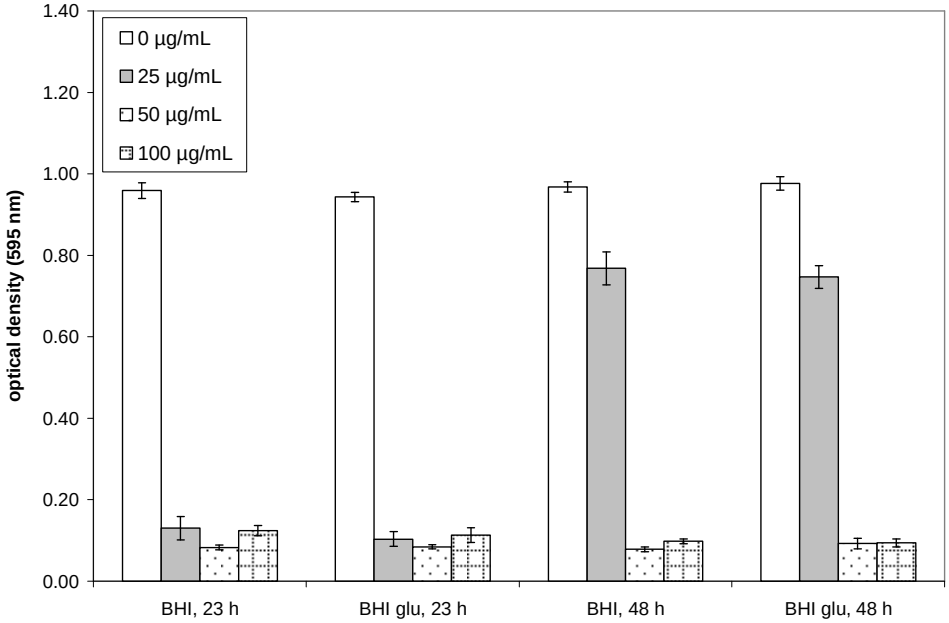

Figure 32: Effect of addition of brominated furanone on bulk growth of *Listeria innocua* after 23 h and 48 h growth at 22˚C in BHI medium and BHI supplemented with 0.2% glucose. These readings are optical densities of non-disturbed wells. Error bars represent standard deviations about the mean of six replicate wells.

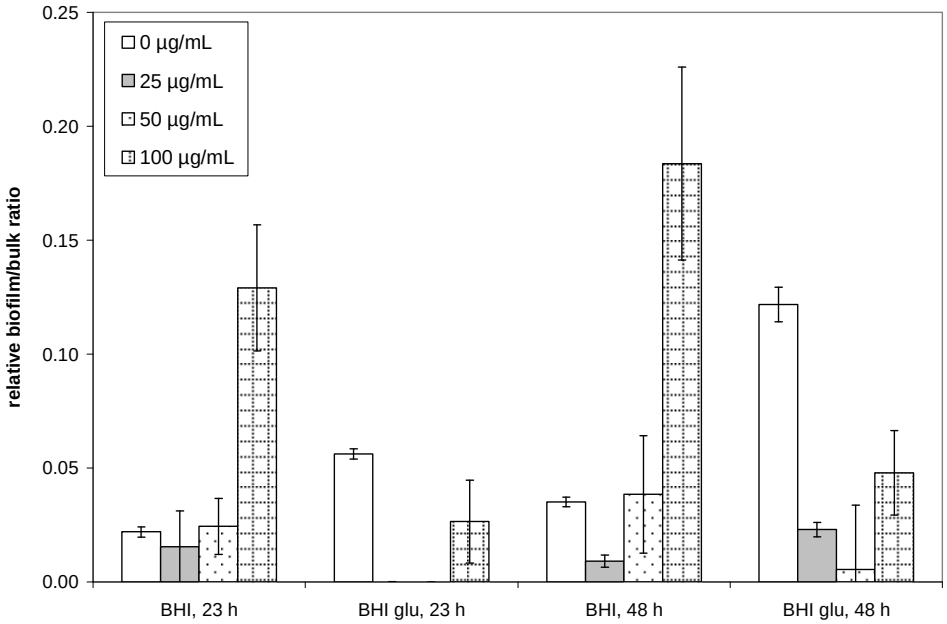

Figure 33: Effect of brominated furanone on biofilm growth in *Listeria innocua* normalized to the non-disturbed optical densities. The ratio of destained crystal violet optical densities at 595 nm in Figure 31 were divided by the optical densities in Figure 32. Error bars represent propagated standard deviations about the mean of six replicate wells.

L. innocua, the mechanism by which the furanone quenches biofilm formation and growth is not understood.

In *Bacillus cereus*, high concentrations of brominated furanone increase biofilm formation in two-fold diluted LB medium and greatly decrease biofilm formation in two-fold diluted LB medium supplemented with 0.2% glucose (Figure 34). Minimum biofilm formation results from the addition of 25 µg/mL furanone after 23 h growth, and from the addition of 50 µg/mL furanone after 48 hours growth. Bulk growth in media is also quenched by the addition of furanone (Figure 35), similarly to *L. innocua*. The addition of 25 µg/mL furanone almost completely eliminates growth for at least 23 hours in medium with or without supplemental glucose. After 48 hours, cell density recovers in glucose-supplemented medium with 25 µg/mL furanone. However, at 50 µg/mL

furanone, growth remains minimal after 48 hours. The ratio of optical density in Figure 34 to Figure 35 is plotted in Figure 36. The brominated furanone only preferentially targets biofilm formation of *Bacillus cereus* over bulk growth at a concentration of 25 µg/mL in a glucose-supplemented medium at the 48 hour time point. Ren et al. observed that 20 µg/mL furanone significantly extended the lag phase of growth in *Bacillus subtilis*, and 40 µg/mL completely inhibited growth in shake flasks but did not completely inhibit biofilm formation[131]. The results presented here on *B. cereus* are in close agreement with these observations. Ren et al. also observed that 40 µg/mL furanone decreased the percentage of live cells (determined by live/dead staining) in *B. subtilis* biofilms compared to the control. Because crystal violet interacts with many negatively-charged cell components, dead cells in the biofilm may contribute to the destained optical densities seen in Figure 34. These results extend the list of Gram-positive species known to exhibit inhibited growth and biofilm formation due to the addition of brominated furanone. They also provide evidence that under certain conditions, biofilm growth is preferentially inhibited relative to bulk growth. It is not clear how these results could be related to AI-2 quorum sensing in either *B. cereus* or *L. innocua*. The furanone has been shown to induce several heat shock and ribose transport and metabolism genes in *B. subtilis*, alluding no connection to quorum sensing[140].

Because the brominated furanone also has been shown to interfere with AHL quorum sensing, it was also screened against *Pseudomonas fluorescens*, a species lacking LuxS. Although *P. fluorescens* cannot produce AI-2, it is possible that it can detect or uptake it from the environment, as is the case with *P. aeruginosa*[141]. *P. fluorescens* produces several different AHLs, including N-hexanoylhomoserine lactone, N-(3-hydroxy-7-*cis*-

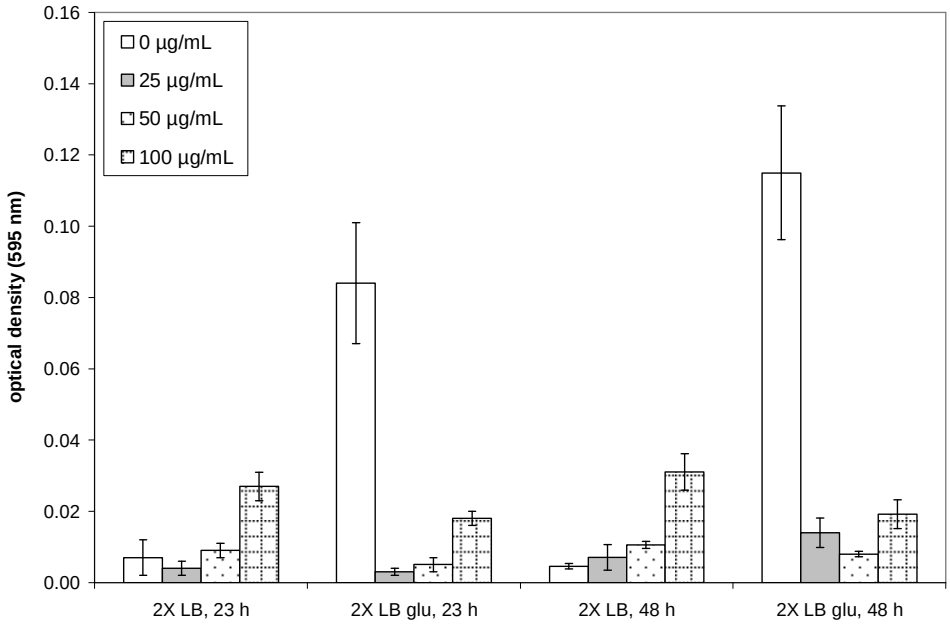

Figure 34: Effect of addition of brominated furanone on biofilm growth of *Bacillus cereus* after 23 h and 48 h growth at 22˚C in two-fold diluted LB (2X LB) medium and 2X LB supplemented with 0.2% glucose. Error bars represent standard deviations about the mean of six replicate wells.

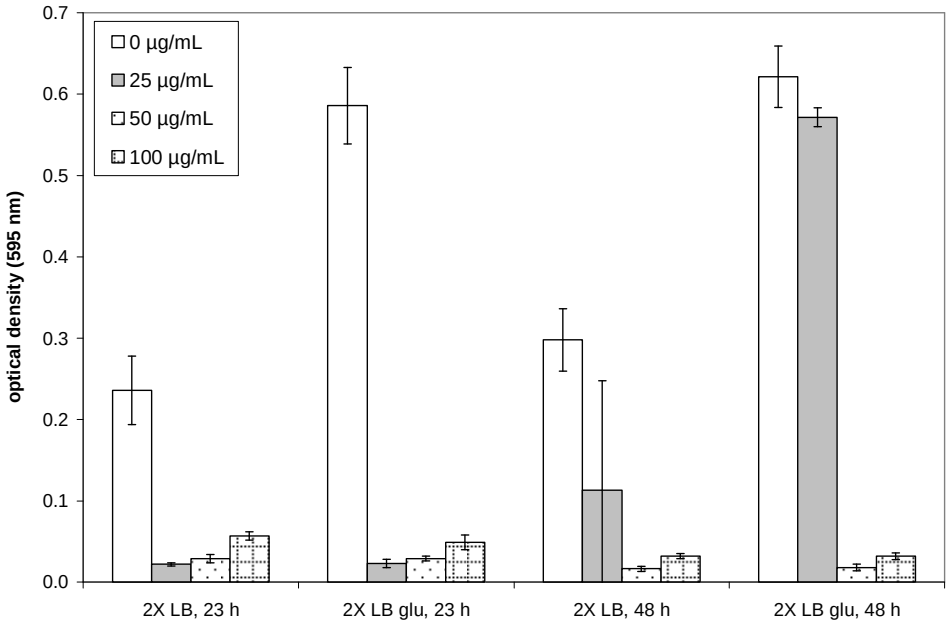

Figure 35: Effect of addition of brominated furanone on bulk growth of *Bacillus cereus* after 23 h and 48 h growth at 32˚C in two-fold diluted LB (2X LB) medium and 2X LB supplemented with 0.2% glucose. These readings are optical densities of non-disturbed wells. Error bars represent standard deviations about the mean of six replicate wells.

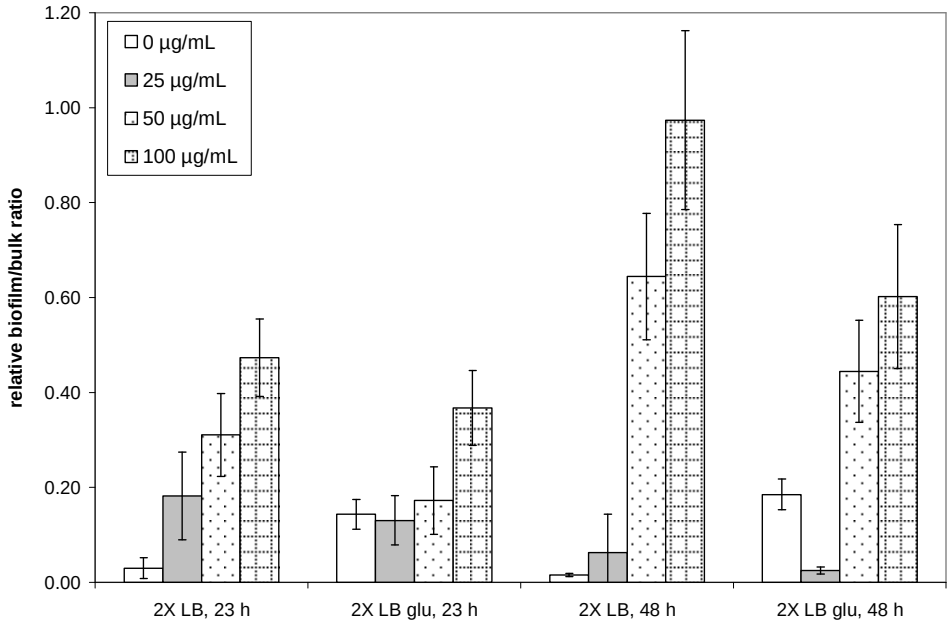

Figure 36: Effect of brominated furanone on biofilm growth in *Bacillus cereus* normalized to the non-disturbed optical densities. The ratio of destained crystal violet optical densities at 595 nm in Figure 34 were divided by the optical densities in Figure 35. Error bars represent propagated standard deviations about the mean of six replicate wells.

tetradecanoyl)homoserine lactone, N-tetradecanoylhomo-serine lactone, N-(3-hydroxydecanoyl)homoserine lactone, and N-(3-oxodecanoyl)-homoserine lactone[37]. The brominated furanone had virtually no effect on biofilm formation in nutrient broth or LB supplemented with 1.0% sodium citrate (citrate supplementation promotes biofilm formation in *P. fluorescens*[141]), with only a slight decrease observed after 48 hours in nutrient broth (Figure 37). However, a concentration-dependent decrease in bulk growth (39% reduction in optical density with the addition of 100 µg/mL furanone over the control) is observed in LB supplemented with 1.0% sodium citrate after 23 hours (Figure 38). No reports in the literature have observed a brominated furanone dependent growth limitation in any *Pseudomonas* species. One possibility is that a larger iron limitation exists in LB medium than in nutrient broth, which contains beef extract. Although iron limitation does not affect the growth rate, it has been shown to decrease the stationary

phase cell density in *P. aeruginosa*[143]. Bacteria produce siderophores to chelate iron in iron-limited environments. If the addition of brominated furanone represses siderophore synthesis, as it does in *P. putida* in a concentration-dependent manner[129], it is possible that *P. fluorescens* has a reduced ability to uptake iron and therefore reaches a lower stationary phase cell density. It is not clear why reduced cell density due to brominated furanone is not observed in LB medium supplemented with 1.0% sodium citrate after 48 hours.

E. coli also synthesizes numerous siderophores, with one of the best studied being enterochelin (enterobactin). Enterochelin-mediated iron transport is essential for growth under iron-deficient conditions[144]. However, genes encoding enzymes involved in enterochelin synthesis (entB, entE) are neither repressed nor induced by the addition of

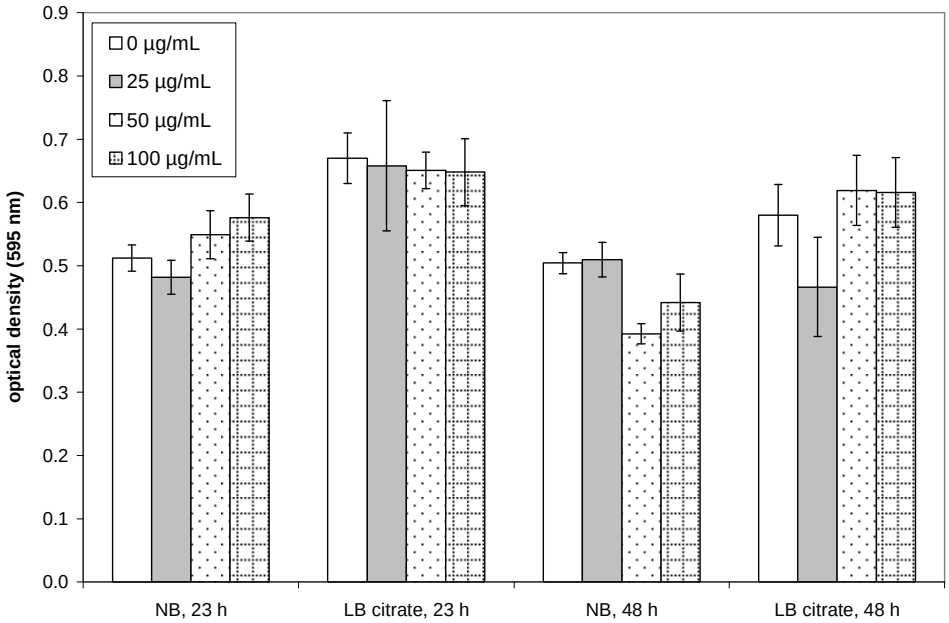

Figure 37: Effect of addition of brominated furanone on biofilm growth of *Pseudomonas fluorescens* after 23 h and 48 h growth at 22˚C in nutrient broth and LB supplemented with 1.0% sodium citrate. Error bars represent standard deviations about the mean of six replicate wells.

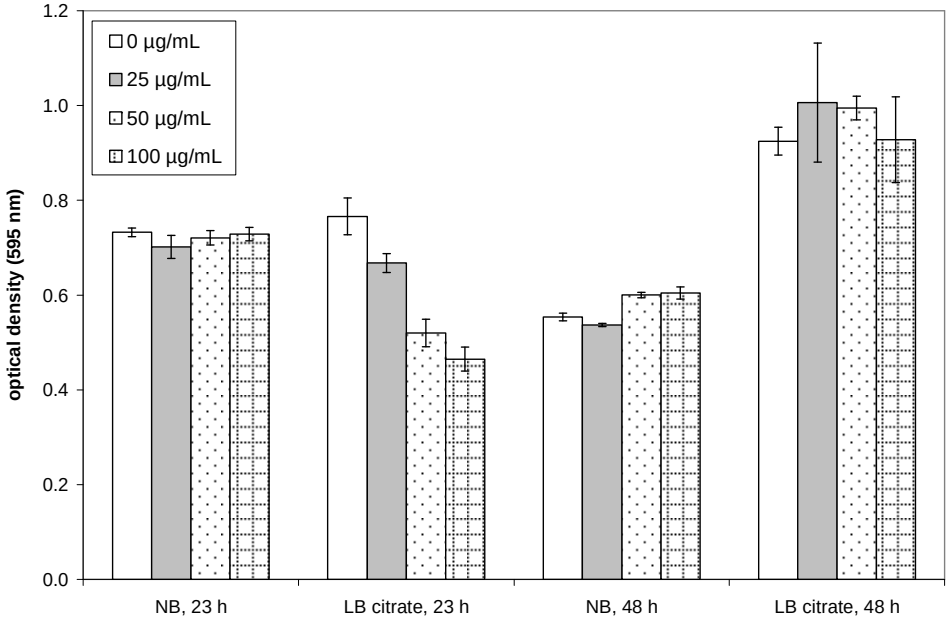

Figure 38: Effect of addition of brominated furanone on bulk growth of *Pseudomonas fluorescens* after 23 h and 48 h growth at 22˚C in nutrient broth and LB supplemented with 1.0% sodium citrate. Error bars represent standard deviations about the mean of six replicate wells.

brominated furanone, and are repressed by growth in glucose-supplemented medium, which increases AI-2 synthesis[76]. Thus the proposed mechanism by which growth is inhibited by brominated furanone in *P. fluorescens* is likely not the case for *E. coli*.

6.6. Effect of LuxS inhibitors on AI-2 production in *Listeria innocua*

As shown in Figure 39, Pei **10** and **11** have no effect on growth rate in *L. innocua* cultures grown at 22˚C on an air shaker at 250 rpm. The growth constants calculated for the control (no added inhibitor), Pei **10**, and Pei **11** are 0.57 h^{-1}, 0.58 h^{-1}, and 0.58 h^{-1}, respectively. To determine whether Pei **10** and **11** actually reduce the level of autoinducer-2 activity in the supernatant, cell-free supernatants were collected at various time points directly from the samples removed to take the optical density measurements in Figure 39. It was found that components in non-diluted BHI medium repressed bioluminescence in *Vibrio harveyi*, whereas ten-fold diluted BHI medium induced

bioluminescence after 4 hours, thereby mimicking the autoinducer-2 response. Catabolite repression of luciferase biosynthesis in *Vibrio harveyi* due to high levels of glucose is well known[145]. It is possible that other nutrients can also act as catabolite repressors. Turovskiy and Chikindas report that a modified BHI medium completely quenches the bioluminescent response of *V. harveyi*, as does the addition of 0.5 to 2.0 g/L of glucose to samples[145]. Furthermore, the presence of 0.03 to 0.13 g/L of glucose was shown to nonlinearly induce bioluminescence. Therefore the collected cell-free supernatants from *L. innocua* were depleted by inoculating with *V. harveyi* MM30, a *luxS* deletion mutant of *V. harveyi* BB120, following a procedure similar to that employed by Turovskiy and Chikindas[146]. The depleted cell-free supernatants were then analyzed for their ability to induce bioluminescence in *V. harveyi* BB170. Because the effects of Pei **10** and **11** on the reporter strain are unknown, negative control samples were incorporated that contained *V. harveyi* MM30 depleted fresh medium with 50 µM of each inhibitor or only PBS. The bioluminescence measured from each *L. innocua* cell-free supernatant was then divided by the bioluminescence measured from the appropriate control. The normalized bioluminescence measurements for each collected time point after 4 hours incubation are shown in Figure 40. Four hours was selected because it was the final measurement time before the bioluminescence of control samples began increasing. It is likely that the depletion by *V. harveyi* MM30 was not complete, and very small levels of glucose or other media components were still interfering with the activity assay. Surprisingly, normalized bioluminescent measurements from samples containing either Pei **10** or **11** inhibitors were lower than the negative control containing only PBS at *L. innocua* growth times between 2.5 to 5.25 hours. This is indicative of lower levels of

extracellular AI-2, which would be expected if the inhibitors were being internalized by the cells and competitively inhibiting LuxS. At 8.25 hours and 24 hours, samples containing Pei **10** and **11** no longer have reduced bioluminescence relative to the control. The effect of the inhibitors on AI-2 production therefore appears to be transient on a time-scale well below that required for significant initiation of biofilm formation. Simulations on competitive and uncompetitive inhibitors in a model open system (having constant input of substrates and removal of products) have shown that competitive inhibitors result in very mild and transient responses in situations where the accumulating intermediate cannot be degraded in a rapid alternative pathway[147]. SRH can only be degraded by LuxS, so its accumulation would be self-limiting as mass action overcomes inhibition. Another factor that would reduce the effectiveness of all of the studied LuxS inhibitors is their extreme hydrophilicity. An ability to bind to specific transporters in order to pass through the inner cell membrane would likely be required. Pei **10** and **11** both closely resemble methionine on one end, leaving open the possibility that methionine transporters can import these molecules. *E. coli* possesses both a high-affinity and a low-affinity methionine transporter and can import L-methionine, D-methionine, N-acetylmethionine, and methionine sulfoxide.[148,149] The *metNPQ* operon in *B. subtilis* encodes an ABC transporter that can import D-methionine, L-methionine, and methionine sulfoxide, with an unidentified transporter also able to uptake L-methionine and methionine sulfoxide.[150] The KEGG Pathway Database (http://www.genome.jp/kegg/pathway.html) lists orthologues of *metNPQ* in *B. cereus* and *L. innocua*. More studies need to be conducted to determine if Pei **10** and **11** can pass through the inner cell membrane, and if so, by what means they are able to do this.

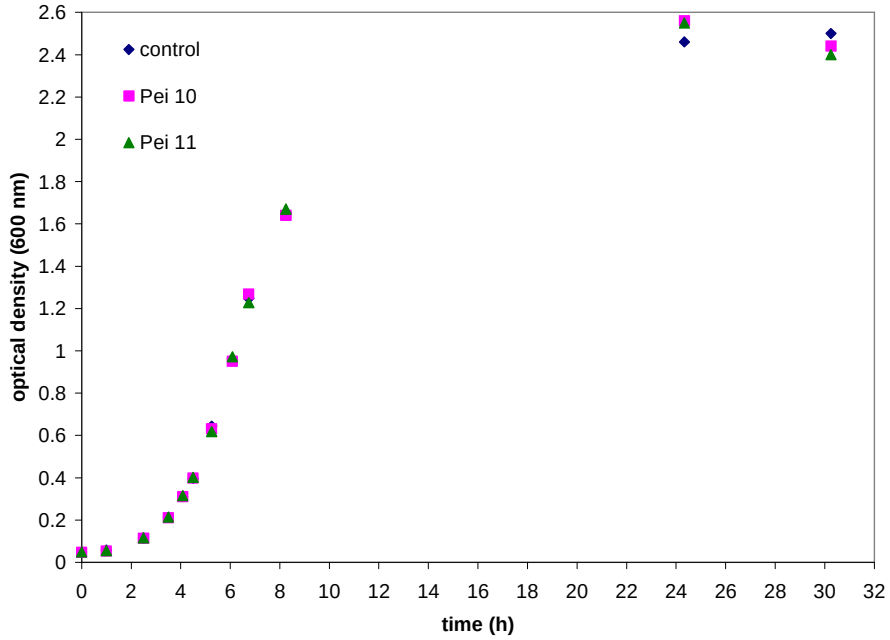

Figure 39: Growth of *Listeria innocua* in the presence of 50 µM Pei **10** (squares), 50 µM Pei **11** (triangles), and a negative control containing the same quantity of PBS (diamonds) in BHI medium at 22˚C. The inhibitors have no effect on growth rate.

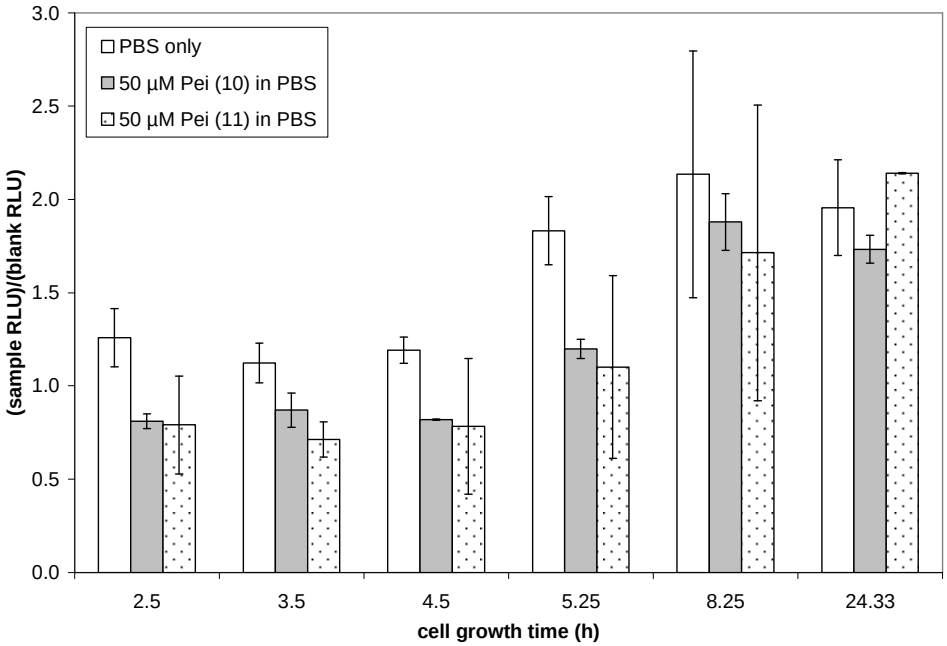

Figure 40: Autoinducer-2 activity assay of *Listeria innocua* cell-free supernatants taken at different growth times in the presence of 50 µM of Pei **10** or Pei **11** dissolved in PBS, or a control containing the same amount of PBS. Relative light units (RLU) of each sample were normalized to RLUs from a control containing depleted fresh medium with the same concentration of inhibitors dissolved in PBS, or only PBS for the negative control.

Chapter 7: Conclusions

This work investigated the effect of *in vitro* synthesized AI-2, three LuxS inhibitors and a brominated furanone inhibitor on biofilm formation in *Escherichia coli*, *Bacillus cereus*, and *Listeria innocua*. Additionally, autoinducer-2 activity was characterized in *L. innocua* cell-free supernatants grown in the presence of two potent LuxS inhibitors.

In vitro synthesized AI-2 results in increased biofilm formation in *E. coli*. A depletable level of glucose supplementation accentuates the increase in biofilm due to AI-2 in *E. coli* W3110, likely through stimulation of *luxS* expression via cAMP-CRP. In *B. cereus*, addition of *in vitro* synthesized AI-2 results in large reductions of biofilm that appears to be due to the addition of large concentrations of homocysteine present as a reaction product. The addition of glucose greatly decreases biofilm formation in *B. cereus*, possibly due to repression of *lsr* transcription in a manner similar to *E. coli*. The addition of AI-2 to *L. innocua* had no effect on biofilm formation, nor did the addition of *in vitro* synthesized SRH.

The LuxS inhibitor SARH had no clear effect on any of the tested bacteria, which was an expected result due to its lack of potency and very hydrophilic nature. Pei compounds **10** and **11** appear to have decreased biofilm formation in *E. coli* W3110 by 38% and 34%, respectively, in LB medium supplemented with 0.2% glucose after 50 hours growth. Glucose would be expected to magnify the effect of LuxS inhibitors by initially stimulating *luxS* expression while inhibiting AI-2 uptake. Pei **10** and **11** had no effect on biofilm formation in *B. cereus* and *L. innocua*.

The brominated furanone (5Z)-4-bromo-5-(bromomethylene)-3-butyl-2(5H)-furanone was found to increase biofilm formation in *E. coli* W3110 in LB medium, while 100

µg/mL furanone sharply decreased bulk growth in LB medium with and without added glucose. The furanone also generally increased biofilm formation in *E. coli* DH5α in LB medium, without an effect on bulk growth. A concentration-dependent reduction in biofilm formation was observed in *E. coli* K-12, but only in glucose-supplemented medium. In *L. innocua* and *B. cereus*, which are both Gram-positive, bulk growth and biofilm formation were strongly quenched. Normalized to bulk growth, biofilm development in *L. innocua* is preferentially inhibited by furanone in glucose-supplemented medium. In *B. cereus*, bulk growth is preferentially quenched relative to biofilm development in a concentration-dependent manner. The brominated furanone appears to reduce bulk growth of *Pseudomonas fluorescens* in LB medium supplemented with 1.0% sodium citrate at 23 hours, possibly through repression of siderophore synthesis.

L. innocua was grown in the presence of LuxS inhibitors Pei **10** and **11**, and nutrient-depleted cell-free supernatants were analyzed for AI-2 activity based on their ability to induce bioluminescence in *Vibrio harveyi* BB170. Transient reductions in AI-2 production of 20 to 40 percent were observed during the exponential growth phase. It is postulated that the level of inhibition may be too low and too transient to induce changes in biofilm phenotype under most circumstances. Pei **10** and **11** may be transported into the cell via methionine transporters.

A plethora of future work can be suggested based on the results of this study. Analysis of AI-2 activity in cell-free supernatants from *B. cereus* and *E. coli* grown in the presence of Pei **10** and **11** LuxS inhibitors would provide valuable additional information (this study was limited by the quantity of inhibitors available). Microscopy of biofilms

grown in the presence of inhibitors and AI-2 would allow biofilm morphology to be determined. The transport of inhibitors into bacterial cells needs to be better understood, and attempts should be made to deliver inhibitors into the cell (eg. through the use of vesicles). The development of *in vivo* models of enzyme inhibition coupled with metabolic networks should be pursued for making predictions on the effects of quorum sensing inhibitors prior to exhaustive screening studies. Finally, the precise mechanism of action of brominated furanones, particularly against growth and biofilm formation in Gram-positive bacteria, needs to be determined.

References

1. Costerton, J. W.; A short history of the development of the biofilm concept. in *Microbial Biofilms*, eds. M. Ghannoum and G. A. O'Toole. ASM Press: Washington, DC. pp. 4-19. 2004.
2. Davies, D. Understanding biofilm resistance to antimicrobial agents. *Nat. Rev. Drug Discov.*, **2**, 114-122 (2003).
3. Ehrlich, G. D., Hu, F. Z., and Post, J. C. Role for biofilms in infectious disease. in *Microbial Biofilms*. eds. M. Ghannoum and G. A. O'Toole. ASM Press: Washington, DC. pp. 332-358. 2004.
4. Donlan, R. M. Biofilms and device-associated infections. *Emerging Infect. Dis.*, **7**, 277-281 (2001).
5. Lyczak, J. B., Cannon, C. L., and Pier, G. B. Lung infections associated with cystic fibrosis. *Clin. Microbiol. Rev.*, **15**, 194-222 (2002).
6. Characklis, W. G. Microbial fouling. in *Biofilms*, eds. W. G. Characklis and K. C. Marshall. John Wiley & Sons, Inc.: New York. pp. 523-584. 1990.
7. Mittelman, M. W. "Bacterial biofilms and biofouling: translational research in marine biotechnology." Proc. of Workshop for Opportunities for Environmental Applications of Marine Biotechnology, Oct. 1999.
8. Characklis, W. G., McFeters, G. A., and Marshall, K. C. Physiological ecology in biofilm systems. in *Biofilms*, eds. W. G. Characklis and K. C. Marshall. John Wiley & Sons, Inc.: New York. pp. 341-394. 1990.
9. Little, B. J., Wagner, P. A., Characklis, W. G., and Lee, W. Microbial corrosion. in *Biofilms*, eds. W. G. Characklis and K. C. Marshall. John Wiley & Sons, Inc.: New York, pp. 635-670. 1990.
10. Musk, D. J., Jr. and Hergenrother, P. J. Chemical countermeasures for the control of bacterial biofilms: Effective compounds and promising targets. *Curr. Med. Chem.*, **13**, 2163-2177 (2006).
11. Passmore, M. and Costerton, J. W. Biofilms, bacterial signaling, and their ties to marine biology. *J. Ind. Microbiol. Biotechnol.*, **30**, 407-413 (2003).
12. Stewart, P. S., Mukherjee, P. K., and Ghannoum, M. A. Biofilm Antimicrobial Resistance. in *Microbial Biofilms*, eds. M. Ghannoum and G. A. O'Toole. ASM Press: Washington, DC. pp. 250-268. 2004.
13. Characklis, W. G. Microbial biofouling control. in *Biofilms*, eds. W. G. Characklis and K. C. Marshall. John Wiley & Sons, Inc.: New York. pp. 585-633. 1990.
14. Brizzolara, R. A., Nordham, D. J., Walch, M., Lennen, R. M., Simmons, R., Burnett, E., and Mazzola, M. S. Non-chemical biofouling control in heat exchangers and seawater piping systems using acoustic pulses generated by an electrical discharge. *Biofouling*, **19**, 19-35 (2003).
15. "Organotin Antifouling Paints," EPA (Australia) Information Bulletin, Pub. 703, Jun. 2000.
16. "Discharge Assessment Report: Hull Coating Leachate (Draft)," EPA-842-D-06-002, Aug. 2003.

17. Xavier, J. B., Picioreanu, C., Abdul Rani, S., van Loosdrecht, M. C. M., and Stewart, P. S. Biofilm-control strategies based on enzymic disruption of the extracellular polymeric substance matrix - a modelling study. *Microbiol.*, **151**, 3817-3832 (2005).
18. Gottenbos, B., van der Mei, H. C., Klatter, F., Nieuwenhuis, P., and Busscher, H. J. In vitro and in vivo antimicrobial activity of covalently coupled quaternary ammonium silane coatings on silicone rubber. *Biomaterials*, **23**, 1414-1423 (2002).
19. Oosterhof, J. J. H., Buisjssen, K. J. D. A., Busscher, H. J., van der Laan, B. F. A. M., and van der Mei, H. C. Effects of quaternary ammonium silane coatings on mixed fungal and bacterial biofilms on tracheoesophageal shunt prostheses. *Appl. Environ. Microbiol.*, **72**, 3673-3677 (2006).
20. Tiller, J. C., Liao, C.-J., Lewis, K., and Klibanov, A. M. Designing surfaces that kill bacteria on contact. *Proc. Natl. Acad. Sci.*, **98**, 5981-5985 (2001).
21. Kingshott, P., Wei, J., Bagge-Ravn, D., Gadegaard, N., and Gram, L. Covalent attachment of poly(ethylene glycol) to surfaces, critical for reducing bacterial adhesion. *Langmuir*, **19**, 6912-6921 (2003).
22. Ki, D. P., Young, S. K., Dong, K. H., Young, H. K., Eun, H. B. L., Hwal, S., and Kyu, S. C. Bacterial adhesion on PEG modified polyurethane surfaces. *Biomaterials*, **19**, 851-859 (1998).
23. Gudipati, C. S., Finlay, J. A., Callow, J. A., Callow, M. E., and Wooley, K. L. The antifouling and fouling-release performance of hyperbranched fluoropolymer (HBFP)-poly(ethylene glycol) (PEG) composite coatings evaluated by adsorption of biomacromolecules and the green fouling alga *Ulva*. *Langmuir*, **21**, 3044-3053 (2005).
24. Valle, J., Da Re, S., Henry, N., Fontaine, T., Balestrino, D., Latour-Lambert, P., and Ghigo, J.-M. Broad-spectrum biofilm inhibition by a secreted bacterial polysaccharide. *Proc. Natl. Acad. Sci.*, **103**, 12558-12563 (2006).
25. Musk, D. J., Banko, D. A., and Hergenrother, P. J. Iron salts perturb biofilm formation and disrupt existing biofilms of *Pseudomonas aeruginosa*. *Chem. Biol.*, **12**, 789-796 (2005).
26. Johnson, M., Cockayne, A., Williams, P. H., and Morrissey, J. A. Iron-responsive regulation of biofilm formation in *Staphylococcus aureus* involves Fur-dependent and Fur-independent mechanisms. *J. Bacteriol.*, **187**, 8211-8215 (2005).
27. Gillis, R. J. and Iglewski, B. H. Azithromycin retards *Pseudomonas aeruginosa* biofilm formation. *J. Clin. Microbiol.*, **42**, 5842-5845 (2004).
28. Carter, G., Young, L. S., and Bermudez, L. E. A subinhibitory concentration of clarithromycin inhibits *Mycobacterium avium* biofilm formation. *Antimicrob. Agents Chemother.*, **48**, 4907-4910 (2004).
29. Ren, D., Zuo, R., González Barrios, A. F., Bedzyk, L. A., Eldridge, G. R., Pasmore, M. E., and Wood, T. K. Differential gene expression for investigation of *Escherichia coli* biofilm inhibition by plant extract ursolic acid. *Appl. Environ. Microbiol.*, **71**, 4022-4034 (2005).

30. Hu, J.-F., Garo, E., Goering, M. G., Pasmore, M., Yoo, H.-D., Esser, T., Sestrich, J., Cremin, P. A., Hough, G. W., Perrone, P., Lee, Y.-S. L., Le, N.-T., O'Neil-Johnson, M., Costerton, J. W., and Eldridge, G. R. Bacterial biofilm inhibitors from *Diospyros dendo*. *J. Nat. Prod.*, **69**, 118-120 (2006).
31. Olofsson, A.-C., Hermansson, M., and Elwing, H. N-acetyl-L-cysteine affects growth, extracellular polysaccharide production, and bacterial biofilm formation on solid surfaces. *Appl. Environ. Microbiol.*, **69**, 4814-4822 (2003).
32. Nealson, K. H., Platt, T., and Hastings, J. W. Cellular control of the synthesis and activity of the bacterial luminescent system. *J. Bacteriol.*, **104**, 313-322 (1970).
33. Eberhard, A., Burlingame, A. L., Eberhard, C., Kenyon, G. L., Nealson, K. H., and Oppenheimer, N. J. Structural identification of autoinducer of *Photobacterium fischeri* luciferase. *Biochem.*, **20**, 2444-2449 (1981).
34. Fuqua, C. and Greenberg, E. P. Listening in on bacteria: Acyl-homoserine lactone signalling. *Nat. Rev. Molec. Cell Biol.*, **3**, 685-695 (2002).
35. Fuqua, C., Parsek, M. R., and Greenberg, E. P. Regulation of gene expression by cell-to-cell communication: Acyl-homoserine lactone quorum sensing. *Annu. Rev. Genet.*, **35**, 439-468 (2001).
36. Gilson, L., Kuo, A., and Dunlap, P. V. AinS and a new family of autoinducer synthesis proteins. *J. Bacteriol.*, **177**, 6946-6951 (1995).
37. Laue, B. E., Jiang, Y., Chhabra, S. R., Jacob, S., Stewart, G. S. A. B., Hardman, A., Downie, J. A., O'Gara, F., and Williams, P. The biocontrol strain *Pseudomonas fluorescens* F113 produces the *Rhizobium small* bacteriocin, N-(3-hydroxy-7-cis-tetradecenoyl)homoserine lactone, via HdtS, a putative novel N-acylhomoserine lactone synthase. *Microbiol.*, **146**, 2469-2480 (2000).
38. Venturi, V. Regulation of quorum sensing in *Pseudomonas*. *FEMS Microbiol. Rev.*, **30**, 274-291 (2006).
39. Marketon, M. M., Glenn, S. A., Eberhard, A., and González, J. E. Quorum sensing controls exopolysaccharide production in *Sinorhizobium meliloti*. *J. Bacteriol.*, **185**, 325-331 (2003).
40. von Bodman, S. B., Majerczak, D. R., and Coplin, D. L. A negative regulator mediates quorum-sensing control of exopolysaccharide production in *Pantoea stewartii* subsp. s*tewartii*. *Proc. Natl. Acad. Sci.*, **95**, 7687-7692 (1998).
41. Pirhonen, M., Flego, D., Heikinheimo, R., and Palva, E. T. A small diffusible signal molecule is responsible for the global control of virulence and exoenzyme production in the plant pathogen *Erwinia carotovora*. *EMBO J.*, **12**, 2467-2476 (1993).
42. Piper, K. R., von Bodman, S. B., and Farrand, S. K. Conjugation factor of *Agrobacterium tumefaciens* regulates Ti plasmid transfer by autoinduction. *Nature*, **362**, 448-450 (1993).
43. Federle, M. J. and Bassler, B. L. Interspecies communication in bacteria. *J. Clin. Invest.*, **112**, 1291-1299 (2003).
44. Wolf-Rainer, A. Controlling biofilms of Gram-positive pathogenic bacteria. *Curr. Med. Chem.*, **13**, 1509-1524 (2006).

45. Nakayama, J., Cao, Y., Horii, T., Sakuda, S., Akkermans, A. D. L., de Vos, W. M., and Nagasawa, H. Gelatinase biosynthesis-activating pheromone: a peptide lactone that mediates quorum sensing in *Enterococcus faecalis*. *Molec. Microbiol.*, **41**, 145-154 (2001).
46. Lazazzera, B. A. and Grossman, A. D. The ins and outs of peptide signaling. *Trends Microbiol.*, **6**, 288-294 (1998).
47. Bassler, B. L., Wright, M., Showalter, R. E., and Silverman, M. R. Intercellular signalling in *Vibrio harveyi*: sequence and function of genes regulating expression of luminescence. *Molec. Microbiol.*, **9**, 773-786 (1993).
48. Bassler, B. L., Wright, M., and Silverman, M. R. Multiple signalling systems controlling expression of luminescence in *Vibrio harveyi*: sequence and function of genes encoding a second sensory pathway. *Molec. Microbiol.*, **13**, 273-286 (1994).
49. Surette, M. G. and Bassler, B. L. Quorum sensing in *Escherichia coli* and *Salmonella typhimurium*. *Proc. Natl. Acad. Sci. USA*, **95**, 7046-7050 (1998).
50. Surette, M. G., Miller, M. B., and Bassler, B. L. Quorum sensing in *Escherichia coli, Salmonella typhimurium*, and *Vibrio harveyi*: A new family of genes responsible for autoinducer production. *Proc. Natl. Acad. Sci USA*, **96**, 1639-1644 (1999).
51. Lombardía, E., Rovetto, A. J., Arabolaza, A. L., and Grau, R. R. A LuxS-dependent cell-to-cell language regulates social behavior and development in *Bacillus subtilis*. *J. Bacteriol.*, **188**, 4442-4452 (2006).
52. Auger, S., Krin, E., Aymerich, S., and Gohar, M. Autoinducer 2 affects biofilm formation by *Bacillus cereus*. *Appl. Environ. Microbiol.*, **72**, 937-941 (2006).
53. Jones, M. B. and Blaser, M. J. Detection of a *luxS*-signaling molecule in *Bacillus anthracis*. *Infect. Immun.*, **71**, 3914-3919 (2003).
54. Belval, S. C., Gal, L., Margiewes, S., Garmyn, D., Piveteau, P., and Guzzo, J. Assessment of the roles of LuxS, S-ribosylhomocysteine, and autoinducer 2 in cell attachment during biofilm formation by *Listeria monocytogenes* EGD-e. *Appl. Environ. Microbiol.*, **72**, 2644-2650 (2006).
55. Sela, S., Frank, S., Belausov, E., and Pinto, R. A mutation in the *luxS* gene influences *Listeria monocytogenes* biofilm formation. *Appl. Environ. Microbiol.*, **72**, 5653-5658 (2006).
56. Yang, L., Portugal, F., and Bentley, W. E. Conditioned medium from *Listeria innocua* stimulates emergence from a resting state: Not a response to *E. coli* quorum sensing autoinducer AI-2. *Biotechnol. Prog.*, **22**, 387-393 (2006).
57. Merritt, J., Qi, F., Goodman, S. D., Anderson, M. H., and Shi, W. Mutation of *luxS* affects biofilm formation in *Streptococcus mutans*. *Infect. Immun.*, **71**, 1972-1979 (2003).
58. Fong, K. P., Chung, W. O., Lamont, R. J., and Demuth, D. R. Intra- and interspecies regulation of gene expression by *Actinobacillus actinomycetemcomitans* LuxS. *Infect. Immun.*, **69**, 7625-7634 (2001).
59. McNab, R., Ford, S. K., El-Sabaeny, A., Barbieri, B., Cook, G. S., and Lamont, R. J. LuxS-based signaling in *Streptococcus gordonii*: Autoinducer-2 controls carbohydrate metabolism and biofilm formation with *Porphyromonas gingivalis*. *J. Bacteriol.*, **185**, 274-284 (2003).

60. Frias, J., Olle, E., and Alsina, M. Periodontal pathogens produce quorum sensing signal molecules. *Infect. Immun.*, **69**, 3431-3434 (2001).
61. Johnson, M. R. Ph.D. Dissertation. Intercellular communication in hyperthermophilic microorganisms. North Carolina State University, Aug. 2005.
62. Schauder, S., Shokat, K., Surette, M. G., and Bassler, B. L. The LuxS family of bacterial autoinducers: Biosynthesis of a novel quorum-sensing signal molecule. *Molec. Microbiol.*, **41**, 463-476 (2001).
63. Guranowski, A. B., Chiang, P. K., and Cantoni, G. L. 5'-Methylthioadenosine nucleosidase: Purification and characterization of the enzyme from *Lupinus luteus* seeds. *Eur. J. Biochem.*, **114**, 293-299 (1981).
64. Miller, C. H. and Duerre, J. A. S-ribosylhomocysteine cleavage enzyme from *Escherichia coli*. *J. Biol. Chem.*, **243**, 92-97 (1968).
65. LaMonte, B. L. and Hughes, J. A. *In vivo* hydrolysis of S-adenosylmethionine induces the *met* regulon of *Escherichia coli*. *Microbiol.*, **152**, 1451-1459 (2006).
66. Sun, J., Daniel, R., Wagner-Döbler, I., and Zeng, A.-P. Is autoinducer-2 a universal signal for interspecies communication: A comparative genomic and phylogenetic analysis of the synthesis and signal transduction pathways. *BMC Evol. Biol.*, **4**, 36 (2004).
67. Xavier, K. B. and Bassler, B. L. LuxS quorum sensing: more than just a numbers game. *Curr. Opin. Microbiol.*, **6**, 191-197 (2003).
68. Vendeville, A., Winzer, K., Heurlier, K., Tang, C. M., and Hardie, K. R. Making 'sense' of metabolism: autoinducer-2, LuxS, and pathogenic bacteria. *Nature Rev. Microbiol.*, **3**, 383-396 (2005).
69. Hofmann, T. and Schieberle, P. Quantitative model studies on the effectiveness of different precursor systems in the formation of the intense food odorants 2-furfurylthiol and 2-methyl-3-furanthiol. *J. Agric. Food Chem.*, **46**, 235-241 (1998).
70. Chen, X., Schauder, S., Potier, N., Van Dorsselaer, A., Pelczer, I., Bassler, B. L., and Hughson, F. M. Structural identification of a bacterial quorum-sensing signal containing boron. *Nature*, **415**, 545-549 (2002).
71. Winzer, K., Hardie, K. R., Burgess, N., Doherty, N., Kirke, D., Holden, M. T. G., Linforth, R., Cornell, K. A., Taylor, A. J., Hill, P. J., and Williams, W. LuxS: its role in central metabolism and the *in vitro* synthesis of 4-hydroxy-5-methyl-3(2H)-furanone. *Microbiology*, **148**, 909-922 (2002).
72. Miller, S. T., Xavier, K. B., Campagna, S. R., Taga, M. E., Semmelhack, M. F., Bassler, B. L., and Hughson, F. M. *Salmonella typhimurium* recognizes a chemically distinct form of the bacterial quorum-sensing signal AI-2. *Molec. Cell*, **15**, 677-687 (2004).
73. Li, J., Wang, L., Hashimoto, Y., Tsao, C.-Y., Wood, T. K., Valdes, J. J., Zafiriou, E., and Bentley, W. E. A stochastic model of *Escherichia coli* AI-2 quorum signal circuit reveals alternative synthesis pathways. *Molec. Sys. Biol.*, Article no. 67 (2006).

74. Hauck, T., Hübner, Y., Brühlmann, F., and Schwab, W. Alternative pathway for the formation of 4,5-dihydroxy-2,3-pentanedione, the proposed precursor of 4-hydroxy-5-methyl-3(2H)-furanone as well as autoinducer-2, and its detection as natural constituent of tomato fruit. *Biochim. Biophys. Acta*, **1623**, 109-119 (2003).
75. DeLisa, M. P., Wu, C.-F., Wang, L., Valdes, J. J., and Bentley, W. E. DNA microarray-based identification of genes controlled by autoinducer 2-stimulated quorum sensing in *Escherichia coli*. *J. Bacteriol.*, **183**, 5239-5247 (2001).
76. Ren, D., Bedzyk, L. A., Ye, R. W., Thomas, S. M., and Wood, T. K. Differential gene expression shows natural brominated furanones interfere with the autoinducer-2 bacterial signaling system of *Escherichia coli*. *Biotechnol. Bioeng.*, **88**, 630-642 (2004).
77. Yuan, L., Hillman, J. D., and Progulske-Fox, A. Microarray analysis of quorum-sensing-regulated genes in *Porphyromonas gingivalis*. *Infect. Immun.*, **73**, 4146-4154 (2005).
78. Widmer, K. W., Jesudhasan, P. R., Dowd, S. E., and Pillai, S. D. Differential gene expression of virulence-related genes in a *Salmonella enterica* serotype typhimurium *luxS* mutant in response to autoinducer AI-2 and poultry meat-derived AI-2 inhibitor. *Foodborne Pathogens Dis.*, **4**, 5-15 (2007).
79. Dove, J. E., Yasukawa, K., Tinsley, C. R., and Nassif, X. Production of the signalling molecule, autoinducer-2, by *Neisseria meningitidis*: lack of evidence for a concerted transcriptional response. *Microbiol.*, **149**, 1859-1869 (2003).
80. Schauder, S., Penna, L., Ritton, A., Manin, C., Parker, F., and Renauld-Mongénie, G. Proteomics analysis by two-dimensional differential gel electrophoresis reveals the lack of a broad response of *Neisseria meningitidis* to in vitro-produced AI-2. *J. Bacteriol.*, **187**, 392-395 (2005).
81. González Barrios, A. F., Zuo, R., Hashimoto, Y., Yang, L., Bentley, W. E., and Wood, T. K. Autoinducer 2 controls biofilm formation in *Escherichia coli* through a novel motility quorum-sensing regulator (MqsR, B3022). *J. Bacteriol.*, **188**, 305-316 (2006).
82. Ohtani, K., Hayashi, H., and Shimizu, T. The *luxS* gene is involved in cell-cell signalling for toxin production in *Clostridium perfringens*. *Molec. Microbiol.*, **44**, 171-179 (2002).
83. Coulthurst, S. J., Kurz, C. L., and Salmond, G. P. C. *luxS* mutants of *Serratia* defective in autoinducer-2-dependent 'quorum sensing' show strain-dependent impacts on virulence and production of carbapenem and prodigiosin. *Microbiol.*, **150**, 1901-1910 (2004).
84. Blehert, D. S., Palmer, R. J., Jr., Xavier, J. B., Almeida, J. S., and Kolenbrander, P. E. Autoinducer 2 production by *Streptococcus gordonii* DL1 and the biofilm phenotype of a *luxS* mutant are influenced by nutritional conditions. *J. Bacteriol.*, **185**, 4851-4860 (2003).
85. Cole, S. P., Harwood, J., Lee, R., She, R., and Guiney, D. G. Characterization of monospecies biofilm formation by *Helicobacter pylori*. *J. Bacteriol.*, **186**, 3124-3132 (2004).

86. Egland, P. G., Palmer, R. J., Jr., and Kolenbrander, P. E. Interspecies communication in *Streptococcus gordonii-Veillonella atypica* biofilms: Signaling in flow conditions requires juxtaposition. *Proc. Natl. Acad. Sci.*, **101**, 16917-16922 (2004).
87. Freeman, J. A. and Bassler, B. L. Sequence and function of LuxU: A two-component phosphorelay protein that regulates quorum sensing in *Vibrio harveyi*. *J. Bacteriol.*, **181**, 899-906 (1999).
88. Lilley, B. N. and Bassler, B. L. Regulation of quorum sensing in *Vibrio harveyi* by LuxO and Sigma-54. *Molec. Microbiol.*, **36**, 940-954 (2000).
89. Lenz, D. H., Mok, K. C., Lilley, B. N., Kulkarni, R. V., Wingreen, N. S., and Bassler, B. L. The small RNA chaperone Hfq and multiple small RNAs control quorum sensing in *Vibrio harveyi* and *Vibrio cholerae*. *Cell*, **118**, 69-82 (2004).
90. DeLisa, M. P., Valdes, J. J., and Bentley, W. E. Mapping stress-induced changes in autoinducer AI-2 production in chemostat-cultivated *Escherichia coli* K-12. *J. Bacteriol.*, **183**, 2918-2928 (2001).
91. Taga, M. E., Miller, S. T., and Bassler, B. L. Lsr-mediated transport and processing of AI-2 in *Salmonella typhimurium*. *Molec. Microbiol.*, **50**, 1411-1427 (2003).
92. Xavier, K. B. and Bassler, B. L. Regulation of uptake and processing of the quorum sensing autoinducer AI-2 in *Escherichia coli*. *J. Bacteriol.*, **187**, 238-248 (2005).
93. Iida, A., Harayama, S., Iino, T., and Hazelbauer, G. L. Molecular cloning and characterization of genes required for ribose transport and utilization in *Escherichia coli* K-12. *J. Bacteriol.*, **158**, 674-682 (1984).
94. Taga, M. E., Semmelhack, J. L., and Bassler, B. L. The LuxS-dependent autoinducer AI-2 controls the expression of an ABC transporter that functions in AI-2 uptake in *Salmonella typhimurium*. *Molec. Microbiol.*, **42**, 777-793 (2001).
95. Wang, L., Hashimoto, Y., Tsao, C.-Y., Valdes, J. J., and Bentley, W. E. Cyclic AMP (cAMP) and cAMP receptor protein influence both synthesis and uptake of extracellular autoinducer 2 in *Escherichia coli*. *J. Bacteriol.*, **187**, 2066-2076 (2005).
96. Warner, J. B. and Lolkema, J. S. CcpA-dependent carbon catabolite repression in bacteria. *Microbiol. Molec. Biol. Rev.*, **67**, 475 (2003).
97. Wen, Z. T. and Burne, R. A. Functional genomics approach to identifying genes required for biofilm development by *Streptococcus mutans*. *Appl. Environ. Microbiol.*, **68**, 1196-1203 (2002).
98. Pesci, E. C., Milbank, J. B. J., Pearson, J. P., McKnight, S., Kende, A. S., Greenberg, E. P., and Iglewski, B. H. Quinolone signaling in the cell-to-cell communication system of *Pseudomonas aeruginosa*. *Proc. Natl. Acad. Sci.*, **96**, 11229-11234 (1999).
99. Diggle, S. P., Lumjiaktase, P., Dipilato, F., Winzer, K., Kunakorn, M., Barrett, D. A., Chhabra, S. R., Cámara, M., and Williams, P. Functional genetic analysis reveals a 2-alkyl-4-quinolone signaling system in the human pathogen *Burkholderia pseudomallei* and related bacteria. *Chem. Biol.*, **13**, 701-710 (2006).

100. Wang, D., Ding, X., and Rather, P. N. Indole can act as an extracellular signal in *Escherichia coli*. *J. Bacteriol.*, **183**, 4210-4216 (2001).
101. Sperandio, V., Torres, A. G., Jarvis, B., Nataro, J. P., and Kaper, J. B. Bacteria-host communication: The language of hormones. *Proc. Natl. Acad. Sci.*, **100**, 8951-8956 (2003).
102. Walters, M., Sircili, M. P., and Sperandio, V. AI-3 synthesis is not dependent on *luxS* in *Escherichia coli*. *J. Bacteriol.*, **188**, 5668-5681 (2006).
103. Hentzer, M. and Givskov, M., Pharmacological inhibition of quorum sensing for the treatment of chronic bacterial infections. *J. Clinical Investigation*, **112**, 1300-1307 (2003).
104. Smith, K. M., Bu, Y., and Suga, H. Induction and inhibition of *Pseudomonas aeruginosa* quorum sensing by synthetic autoinducer analogs. *Chemistry and Biology*, **10**, 81-89 (2003).
105. Geske, G. D., Wezeman, R. J., Siegel, A. P., and Blackwell, H. E. Small molecule inhibitors of bacterial quorum sensing and biofilm formation. *J. Am. Chem. Soc.*, **127**, 12762-12763 (2005).
106. Pajula, R. L. and Raina, A. Methylthioadenosine, a potent inhibitor of spermine synthase from bovine brain. *FEBS Letters*, **99**, 343-345 (1979).
107. Lee, J. E., Settembre, E. C., Cornell, K. A., Riscoe, M. K., Sufrin, J. R., Ealick, S. E., and Howell, P. L. Structural comparison of MTA phosphorylase and MTA/AdoHcy nucleosidase explains substrate preferences and identifies regions exploitable for inhibitor design. *Biochemistry*, **43**, 5159-5169 (2004).
108. Sufrin, J. R., Meshnick, S. R., Spiess, A. J., Garofalo-Hannan, J., Pan, X. Q., and Bacchi, C. J. Methionine recycling pathways and antimalarial drug design. *Antimicrob. Agents Chemother.*, **39**, 2511-2515 (1995).
109. de la Haba, G. and Cantoni, G. The enzymatic synthesis of S-adenosyl-L-homocysteine from adenosine and homocysteine. *J. Biol. Chem.*, **234**, 603-608 (1959).
110. Guillerm, G., Varkados, M., Auvin, S., and Le Goffic, F. Synthesis of hydroxylated pyrrolidine derivatives as potential inhibitors of SAH/MTA nucleosidase. *Tetrahedron Lett.*, **28**, 535-538 (1987).
111. Cornell, K. A., Swarts, W. E., Barry, R. D., and Riscoe, M. K. Characterization of recombinant *Escherichia coli* 5'-methylthioadenosine/S-adenosyl-homocysteine nucleosidase: analysis of enzymatic activity and substrate specificity. *Biochem. Biophys. Res. Comm.*, **228**, 724-732 (1996).
112. Gatel, M., Muzard, M., Guillerm, D., and Guillerm, G. Kinetic properties of fluorinated substrate analogues on 5'-methylthioadenosine nucleosidase from *Escherichia coli*. *Eur. J. Med. Chem.*, **31**, 37-41 (1996).
113. Lee, J. E., Cornell, K. A., Riscoe, M. K., and Howell, P. L. Structure of *Escherichia coli* 5'-methylthioadenosine/S-adenosylhomocysteine nucleosidase inhibitor complexes provide insight into the conformational changes required for substrate binding and catalysis. *J. Biol. Chem.*, **278**, 8761-8770 (2003).
114. Tedder, M. E., Nie, Z., Margosiak, S., Chu, S., Feher, V. A., Almassy, R., Appelt, K., and Yager, K. M. Structure-based design, synthesis, and antimicrobial activity of purine derived SAH/MTA nucleosidase inhibitors. *Bioorg. Med. Chem. Lett.*, **14**, 3165-3168 (2004).

115. Li, X., Chu, S., Feher, V. A., Khalili, M., Nie, Z., Margosiak, S., Nikulin, V., Levin, J., Sprankle, K. G., Tedder, M. E., Almassy, R., Appelt, K., and Yager, K. M. Structure-based design, synthesis, and antimicrobial activity of indazole-derived SAH/MTA nucleosidase inhibitors. *J. Med. Chem.*, **46**, 5663-5673 (2003).
116. Singh, V., Evans, G. B., Lenz, D. H., Mason, J. M., Clinch, K., Mee, S., Painter, G. F., Tyler, P. C., Furneaux, R. H., Lee, J. E., Howell, P. L., and Schramm, V. L. Femtomolar transistion state analogue inhibitors of 5'-methylthioadenosine/ S-adenosylhomocysteine nucleosidase from *Escherichia coli*. *J. Biol. Chem.*, **280**, 18265-18273 (2005).
117. Kamath, V. P., Zhang, J., Morris, P. E., and Babu, Y. S. Synthesis of a potent 5'-methylthioadenosine/S-adenosylhomocysteine (MTAN) inhibitor. *Bioorg. Med. Chem. Lett.*, **16**, 2662-2665 (2006).
118. March, J. C. and Bentley, W. E. Quorum sensing and bacterial cross-talk in biotechnology. *Curr. Opin. Biotechnol.*, **15**, 495-502 (2004).
119. Zhao, G., Wan, W., Mansouri, S., Alfaro, J. F., Bassler, B. L., Cornell, K. A., and Zhou, Z. S. Chemical synthesis of S-ribosyl-L-homocysteine and activity assay as a LuxS substrate. *Bioorg. Med. Chem. Lett.*, **13**, 3897-3900 (2003).
120. Zhu, J., Hu, X., Dizin, E., and Pei, D. Catalytic mechanism of S-ribosylhomocysteinase (LuxS): direct observation of ketone intermediates by ^{13}C NMR spectroscopy. *J. Am. Chem. Soc.*, **125**, 13379-13381 (2003).
121. Alfaro, J. F., Zhang, T., Wynn, D. P., Karschner, E. L., and Zhou, Z. S. Synthesis of LuxS inhibitors targeting bacterial cell-cell communication. *Org. Lett.*, **6**, 3043-3046 (2004).
122. Shen, G., Rajan, R., Zhu, J., Bell, C. E., and Pei, D. Design and synthesis of substrate and intermediate analogue inhibitors of S-ribosylhomocysteinase. *J. Med. Chem.*, **49**, 3003-3011 (2006).
123. de Nys, R., Wright, A. D., Konig, G. M., and Sticher, O. New halogenated furanones from the marine alga *Delisea pulchra* (cf. *fimbriata*). *Tetrahedron*, **49**, 11213-11220 (1993).
124. Gram, L., de Nys, R., Maximilien, R., Givskov, M., Steinberg, P., and Kjelleberg, S. Eukaryotic interference with homoserine lactone-mediated prokaryotic signalling. *Appl. Environ. Microbiol.*, **62**, 4284-4287 (1996).
125. Manefield, M., de Nys, R., Kumar, N., Read, R., Givskov, M., Steinberg, P., and Kjelleberg, S. Evidence that halogenated furanones from *Delisea pulchra* inhibit acylated homoserine lactone (AHL)-mediated gene expression by displacing the AHL signal from its receptor protein. *Microbiology*, **145**, 283-291 (1999).
126. Manefield, M., Harris, L., Rice, S. A., de Nys, R., and Kjelleberg, S. Inhibition of luminescence and virulence in the black tiger prawn (*Penaeus monodon*) pathogen *Vibrio harveyi* by intercellular signal antagonists. *Appl. Environ. Microbiol.*, **66**, 2079-2084 (2000).

127. Hentzer, M., Riedel, K., Rasmussen, T. B., Heydorn, A., Anderson, J. B., Parsek, M. R., Rice, S. A., Eberl, L., Molin, S., Høiby, N., Kjelleberg, S., and Givskov, M. Inhibition of quorum sensing in *Pseudomonas aeruginosa* biofilm bacteria by a halogenated furanone compound. *Microbiology*, **148**, 87-102 (2002).
128. Hentzer, M., Wu, H., Anderson, J. B., Riedel, K., Rasmussen, T. B., Bagge, N., Kumar, N., Schembri, M. A., Song, Z., Kristoffersen, P., Manefield, M., Costerton, J. W., Molin, S., Eberl, L., Steinberg, P., Kjelleberg, S., Høiby, N., and Givskov, M. Attenuation of *Pseudomonas aeruginosa* virulence by quorum sensing inhibitors. *EMBO J.*, **22**, 3803-3815 (2003).
129. Ren, D., Zuo, R., and Wood, T. K. Quorum-sensing antagonist (5Z)-4-bromo-5-(bromomethylene)-3-butyl-2(5H)-furanone influences siderophore synthesis in *Pseudomonas putida* and *Pseudomonas aeruginosa*. *Appl. Microbiol. Biotechnol.*, **66**, 689-695 (2005).
130. Ren, D., Sims, J. J., and Wood, T. K. Inhibition of biofilm formation and swarming of *Escherichia coli* by (5Z)-4-bromo-5-(bromomethylene)-3-butyl-2(5H)-furanone. *Environ. Microbiol.*, **3**, 731-736 (2001).
131. Ren, D.; Sims, J. J.; Wood, T. K.; Inhibition of biofilm formation and swarming of *Bacillus subtilis* by (5Z)-4-bromo-5-(bromomethylene)-3-butyl-2(5H)-furanone. *Lett. Appl. Microbiol.*, **34**, 293-299 (2002).
132. Jones, M. B., Jani, R., Ren, D., Wood, T. K., and Blaser, M. J. Inhibition of *Bacillus anthracis* growth and virulence-gene expression by inhibitors of quorum sensing. *J. Infect. Dis.*, **191**, 1881-1888 (2005).
133. Kjelleberg, S., Steinberg, P. D., Holmstrom, C., and Back, A. "Inhibition of Gram-positive bacteria." U. S. Patent 7,026,353.
134. Baveja, J. K., Willcox, M. D. P., Hume, E. B. H., Kumar, N., Odell, R., and Poole-Warren, L. A. Furanones as potential anti-bacterial coatings on biomaterials. *Biomaterials*, **25**, 5003-5012 (2004).
135. Hume, E. B. H., Baveja, J., Muir, B., Schubert, T. L., Kumar, N., Kjelleberg, S., Griesser, H. J., Thissen, H., Read, R., Poole-Warren, L. A., Schindhelm, K., and Willcox, M. D. P. The control of *Staphylococcus epidermis* biofilm formation and in vivo infection rates by covalently bound furanones. *Biomaterials*, **25**, 5023-5030 (2004).
136. Fernandes, R., Tsao, C.-Y., Hashimoto, Y., Wang, L., Wood, T. K., Payne, G. F., and Bentley, W. E. Magnetic nanofactories: localized synthesis and delivery of quorum-sensing signaling molecule autoinducer-2 to bacterial cell surfaces. *Metab. Eng.*, **9**, 228-239 (2007).
137. Duerre, J. A. and Miller, C. H. Preparation of L-homocysteine from L-homocysteine thiolactone. *Anal. Biochem.*, **17**, 310-315 (1966).
138. Rodionov, D. A., Vitreschak, A. G., Mironov, A. A., and Gelfand, M. S. Comparative genomics of the methionine metabolism in Gram-positive bacteria: a variety of regulatory systems. *Nucleic Acids Res.*, **32**, 3340-3353 (2004).
139. Hullo, M.-F., Auger, S., Soutourina, O., Barzu, O., Yvon, M., Danchin, A., and Martin-Verstraete, I. Conversion of methionine to cysteine in *Bacillus subtilis* and its regulation. *J. Bacteriol.*, **189**, 187-197 (2007).

140. Ren, D., Bedzyk, L. A., Setlow, P., England, D. F., Kjelleberg, S., Thomas, S. M., Ye, R. W., and Wood, T. K. Differential gene expression to investigate the effect of (5*Z*)-4-bromo-5-(bromomethylene)-3-butyl-2(5*H*)-furanone on *Bacillus subtilis*. *Appl. Environ. Microbiol.*, **70**, 4941-4949 (2004).
141. Duan, K., Dammel, C., Stein, J., Rabin, H., and Surette, M. G. Modulation of *Pseudomonas aeruginosa* gene expression by host microflora through interspecies communication. *Molec. Microbiol.*, **50**, 1477-1491 (2003).
142. Hinsa, S. M., and O'Toole, G. A. Biofilm formation by *Pseudomonas fluorescens* WCS365: a role for LapD. *Microbiol.*, **152**, 1375-1383 (2006).
143. Somerville, G., Mikoryak, C. A., and Reitzer, L. Physiological characterization of *Pseudomonas aeruginosa* during exotoxin A synthesis: Glutamate, iron limitation, and aconitase activity. *J. Bacteriol.*, **181**, 1072-1078 (1999).
144. Langman, L., Young, I. G., Frost, G. E., Rosenberg, H., and Gibson, F. Enterochelin system of iron transport in *Escherichia coli*: mutations affecting ferric-enterochelin esterase. *J. Bacteriol.*, **112**, 1142-1149 (1972).
145. Nealson, K. H., Eberhard, A., and Hastings, J. W. Catabolite repression of bacterial bioluminescence: functional implications. *Proc. Natl. Acad. Sci.*, **69**, 1073-1076 (1972).
146. Turovskiy, Y. and Chikindas, M. L. Autoinducer-2 bioassay is a qualitative, not quantitative method influenced by glucose. *J. Microbiol. Methods*, **66**, 497-503 (2006).
147. Westley, A. M. and Westley, J. Enzyme inhibition in open systems. *J. Biol. Chem.*, **271**, 5347-5352 (1996).
148. Kadner, R. J. and Watson, W. J. Methionine transport in *Escherichia coli*: physiological and genetic evidence for two uptake systems. *J. Bacteriol.*, **119**, 401-409 (1974).
149. Kadner, R. J. Transport and utilization of D-methionine and other methionine sources in *Escherichia coli*. *J. Bacteriol.*, **129**, 207-216 (1977).
150. Hullo, M.-F., Auger, S., Dassa, E., Danchin, A., and Martin-Verstraete, I. The *metNPQ* operon of *Bacillus subtilis* encodes an ABC permease transporting methionine sulfoxide, D- and L-methionine. *Res. Microbiol.*, **155**, 80-86 (2004).